Lie group analysis of an internal flow and heat transfer inside a combustion chamber of a solid rocket motor

K Modise

orcid.org 0000-0002-1867-4092

Dissertation accepted in partial fulfilment of the requirements for the degree *Master of Science in Applied Mathematics* at the North-West University

Supervisor: Dr G Magalakwe

Graduation May 2020

25245317

Lie group analysis of an internal flow and heat transfer inside a combustion chamber of a solid rocket motor

by

Karabo Modise (25245317)

A research project submitted in partial fulfilment of the requirements for a Masters degree in Applied Mathematics at the North-West University, Potchefstroom Campus.

Department of Mathematics and Applied Mathematics

Faculty of Natural and Agricultural Sciences

November 2019

Supervision by Dr. Gabriel Magalakwe

The financial assistance of CSIR-DST Interbursary Support Programme towards this research is hereby acknowledged. Opinions expressed and conclusions arrived at, are those of the author and are not necessarily to be attributed to the CSIR-DST Interbursary Support Programme.

Declaration

I declare that the mini-dissertation for the degree of Masters of Science at North-West University, Potchefstroom Campus, hereby submitted, has not previously been submitted by me for a degree at this or any other university, that this is my own work in design and execution and that all material contained herein has been duly acknowledged.

Signed: .....

MR KARABO MODISE

Date: .....

This mini-dissertation has been submitted with my approval as a University supervisor and would certify that the requirements for the applicable Masters of Science degree rules and regulations have been fulfilled.

Signed:.....

DR GABRIEL MAGALAKWE

Date: .....

Dedication

I dedicate this work to my late mother Naomi Modise. To the Modise family and Sithole family, your unwavering support has played a tremendous role to drive this work to its completion. Also a special thanks to my girlfriend Phetheho Moleleki, your words of comfort encouraged me to soldier on. This work is dedicated to you all.

Acknowledgements

This research would not have been a success without the assistance, motivation and guidance of my supervisor Dr Gabriel Magalakwe. His support was vital in seeing this project to its completion. Also a special thanks to CSIR and DST for providing me with financial assistance when I was in great need of finances to pay for my tuition fees. Above all let the name of the Lord God Almighty be praised for his unfailing hand of guidance and source of strength throughout my Masters degree training.

Abstract

This research project presents semi-analytical solutions for flow and heat transfer during solid rocket motor operation. Proficient modelling process is followed to construct a mathematical representation based on conservation of mass, momentum and energy. According to the dynamics of flow behaviour and temperature distribution during solid rocket motor operation, forces affecting the flow and heat transfer are derived from physical postulates. To understand the dynamics of a solid rocket motor, the current study investigates the flow and heat transfer inside a pipe in two folds.

The first fold is to understand the effects of buoyancy force on axial-velocity and pressure field during solid rocket motor operation. The last fold is to understand temperature distribution inside the combustion chamber. Lie group analysis along with double perturbation method is used to carry out the integration of the problem at hand. To integrate equations representing the flow and heat transfer during solid rocket motor operation, momentum and energy equations are reduced to a single fourth order ordinary differential equation and second order differential equation respectively. Thereafter, double perturbation method is used to find the semi-analytical solutions of the resulting ordinary differential equations. The effects of dimensionless parameters arising from the design such as cross-flow Reynolds number R_e, wall expansion ratio α, Grashof number G_r, Prandtl number P_r and radiation R on axial-velocity and temperature are represented graphically. Lastly, analysis is performed to seek the best combination of dimensionless parameters that lead to optimal thrust during operation.

Key words: Lie group analysis; flow and heat transfer; perturbation method; porous medium; bouyancy and radiation effects.

List of symbols

Dimensional variables

$2a$-distance between walls, m

$\dot{a}$- wall dilation rate, m/s

t-time, s

$\bar{u}$-axial-velocity, m/s

$\bar{v}$-radial-velocity, m/s

$\bar{z}$-axial coordinate, m

$\bar{r}$-radial coordinate, m

$\bar{P}$-pressure, Pa

ν-kinematic viscosity, m^2/s

ρ-density, kg/m^3

$\bar{\Psi}$-stream function m^2/s

$\bar{T}$-Temperature, K

$\bar{T}_s$- surface Temperature, K

g-gravitational acceleration, m/s^2

Dimensionless variables

$\bar{t}$-dimensionless time

u-dimensionless axial-velocity

v-dimensionless radial-velocity

z-dimensionless axial coordinate

r-dimensionless radial coordinate

A-wall permeance (injection coefficient)

Ψ-dimensionless stream function

α-dimensionless wall dilation rate

P-dimensionless pressure

Θ-dimensional temperature

Θ_s-dimensionless surface temperature

R_e-Reynolds number

P_r-Prandtl number

α-wall dilation

R-radiation number

G_r-Grashof number

Contents

Introduction

Mathematical models which are used to predict the dynamics of real life events are difficult if not impossible to solve analytically. However a number of assumptions can be used to have simpler mathematical models that preserve the dynamics of what occurs in real-life. Differential equations, may it be partial differential equations or ordinary differential equations, form an integral part of mathematical modelling for natural sciences, engineering and biology to name a few.

For such models to be realistic, differential equations representing real-life events have to be multi-dimensional and it is often the number of dimensions in the models that determines to a large extent the complexity of the models. Most models which predict real life events with a reasonable accuracy have three space variables and they also depend on time. Thus, solutions of such models provide us with a better understanding of the physical phenomena that these models describe and for this reason, it is of primary importance to develop algorithms that lead to solutions of such models, analytically, but most often numerically.

To illustrate the significance of studying real life phenomena, the current study extends the problem of two-dimensional flow in a semi-infinite expanding or contracting pipe with injection or suction through a porous surface wall [1] which represent internal flow during solid rocket motor operation by incorporating body force and heat transfer effects given by the following

improved model:

$$
\begin{aligned}
&\frac{\partial(\bar{r}\bar{u})}{\partial\bar{z}}+\frac{\partial(\bar{r}\bar{v})}{\partial\bar{r}}=0,\\
&\frac{\partial\bar{u}}{\partial t}+\bar{u}\frac{\partial\bar{u}}{\partial\bar{z}}+\bar{v}\frac{\partial\bar{u}}{\partial\bar{r}}=-\frac{1}{\rho}\frac{\partial\bar{P}}{\partial\bar{z}}+\nu\left[\frac{\partial^2\bar{u}}{\partial\bar{z}^2}+\frac{1}{\bar{r}}\frac{\partial}{\partial\bar{r}}\left(\bar{r}\frac{\partial\bar{u}}{\partial\bar{r}}\right)\right],\\
&\frac{\partial\bar{v}}{\partial t}+\bar{\bar{u}}\frac{\partial\bar{v}}{\partial\bar{z}}+\bar{v}\frac{\partial\bar{v}}{\partial\bar{r}}=-\frac{1}{\rho}\frac{\partial\bar{P}}{\partial\bar{r}}+\nu\left[\frac{\partial^2\bar{v}}{\partial\bar{z}^2}+\frac{\partial}{\partial\bar{r}}\left(\frac{1}{\bar{r}}\frac{\partial(\bar{r}\bar{v})}{\partial\bar{r}}\right)\right]+g\beta(\bar{T}-\bar{T}_s),\\
&\frac{\partial\bar{T}}{\partial t}+\bar{u}\frac{\partial\bar{T}}{\partial\bar{z}}+\bar{v}\frac{\partial\bar{T}}{\partial\bar{r}}=\lambda\left[\frac{\partial^2\bar{T}}{\partial\bar{z^2}}+\frac{1}{\bar{r}}\frac{\partial}{\partial\bar{r}}\left(\bar{r}\frac{\partial\bar{T}}{\partial\bar{r}}\right)\right]-\frac{1}{\rho c_p}\frac{\partial q_r}{\partial\bar{r}}.
\end{aligned}
$$

The appropriate boundary conditions are:

$$
\begin{aligned}
&\text{(i)} \quad \bar{u}=0, \quad \bar{v}=-\bar{v}_s=-V=-A\dot{a}, \quad \bar{T}=\bar{T}_s \quad \text{at } \bar{r}=a(t),\\
&\text{(ii)} \quad \frac{\partial\bar{u}}{\partial\bar{r}}=0, \quad \bar{v}=0, \quad \frac{\partial\bar{T}}{\partial\bar{r}}=0 \quad \text{at } \bar{r}=0,\\
&\text{(iii)} \quad \bar{u}=0 \quad \text{at } \bar{z}=0.
\end{aligned}
$$

Here, we employ Lie group analysis along with double perturbation method to solve a system of differential equations representing propellant flow and heat transfer inside a combustion chamber of a solid rocket motor analytically. Furthermore, analytical solutions describing the flow-field and temperature distribution are analysed to study the effects of cross-flow Reynolds number R_e, wall expansion ratio α, Prandtl number P_r, Grashof number G_r and radiation R.

The mini-dissertation is organised as follows:

In Chapter One, we provide a brief introduction to Lie group analysis of PDEs and include the necessary results which will be used throughout this work. In particular, we provide the algorithm to determine the Lie point symmetries of PDEs.

In Chapter Two, we use the heat equation to illustrate how to determine the Lie point symmetries of a partial differential equation. We also show how to reduce a partial differential equation to an ordinary differential equation to obtain group-invariant solutions of the original equation.

In Chapter Three, uses Lie group method together with double perturbation method to study internal flow and heat transfer inside a combustion chamber of a solid rocket motor.

Finally, in Chapter Four we summarize the work done in this mini-dissertation and suggest future work.

References are given at the end.

Chapter 1

Preliminaries

This chapter presents a brief introduction of Lie group theory for partial differential equations, which will be used in this mini-dissertation.

1.1 Introduction

Modelling of real-life events lead to complex multi-variate differential equations. These differential equations, however can be extremely difficult to solve. It was in the nineteenth century when a Norwegian mathematician by the name of Sophus Lie, discovered a way of transforming system of equations representing real-life event to a simpler system of equations without changing the dynamics of the real-life event using Lie group method. Lie group method is a well-known technique which can be used to find group-invariant solutions for a system of equations such as equations representing the current case study. Over the years, several books have been written on this topic due to the ability of the method to transform complex systems to simplier systems and leave them invariant, a few are mentioned here, Ovsiannikov [2], Olver [3], Bluman and Kumei [4], Stephani [5], Ibragimov [6–8]. See also Mahomed [9].

The definitions and results presented in this chapter are taken from the books mentioned above and we will use them without referencing.

1.2 Local one-parameter Lie group

Here a transformation will be understood to mean an invertible transformation, i.e a bijective map. Let t and x be two independent variables and u be a dependent variable. We consider a change of the variables t, x and u:

$$T_a : \bar{t} = f(t, x, u, a),\ \bar{x} = g(t, x, u, a),\ \bar{u} = h(t, x, u, a) \tag{1.1}$$

with a being a real parameter, which continuously ranges in values from a neighbourhood $\mathcal{D}' \subset \mathcal{D} \subset \mathbb{R}$ of $a = 0$ and f, g and h are differentiable functions.

Definition 1.1 A *continuous one-parameter (local) Lie group of transformations* is a set G of transformations (1.1) which satisfies the following three conditions:

(i) For T_a, $T_b \in G$ where $a, b \in \mathcal{D}' \subset \mathcal{D}$ then T_b, $T_a = T_c \in G$, $c = \phi(a, b) \in \mathcal{D}$ (Closure)

(ii) $T_0 \in G$ if and only if $a = 0$ such that $T_0\, T_a = T_a\, T_0 = T_a$ (Identity)

(iii) For $T_a \in G$, $a \in \mathcal{D}' \subset \mathcal{D}$, $T_a^{-1} = T_{a^{-1}} \in G$, $a^{-1} \in \mathcal{D}$ such that
$T_a\, T_{a^{-1}} = T_{a^{-1}}\, T_a = T_0$ (Inverse)

From (i), we see that the associativity property is satisfied. Also, if the identity transformation occurs at $a = a_0 \neq 0$ i.e, $T_{a_0}$is the identity, then a shift of the parameter $a = \bar{a} + a_0$ will give T_0 as above. The property (i) can be written as

$$\begin{aligned}
\bar{\bar{t}} &\equiv f(\bar{t}, \bar{x}, \bar{u}, b) = f(t, x, u, \phi(a, b)), \\
\bar{\bar{x}} &\equiv g(\bar{t}, \bar{x}, \bar{u}, b) = g(t, x, u, \phi(a, b)), \\
\bar{\bar{u}} &\equiv h(\bar{t}, \bar{x}, \bar{u}, b) = h(t, x, u, \phi(a, b)).
\end{aligned} \tag{1.2}$$

The function ϕ is termed as the *group composition law*. A group parameter a is called *canonical* if $\xi(a, b) = a + b$.

Theorem 1.1 For any $\xi(a, b)$, there exists the canonical parameter $\tilde{a}$ defined by

$$\tilde{a} = \int_0^a \frac{ds}{w(s)},\ \text{where } w(s) = \left.\frac{\partial\, \xi(s, b)}{\partial b}\right|_{b=0}.$$

We now give the definition of a symmetry group for the second-order PDE

$$u_t = F(t, x, u, u_x, u_{xx}), \quad \frac{\partial F}{\partial u_{xx}} \neq 0. \tag{1.3}$$

Definition 1.2 (Symmetry group) A one-parameter group G of transformations (1.1) is called a *symmetry group* of (1.3) if it is form-invariant (has the same form) in the new variables $\bar{t}, \bar{x}$ and $\bar{u}$, i.e.

$$\bar{u}_{\bar{t}} = F(\bar{t}, \bar{x}, \bar{u}, \bar{u}_{\bar{x}}, \bar{u}_{\bar{x}\bar{x}}), \tag{1.4}$$

where the function F is the same as in (1.3).

1.3 Infinitesimal transformations

Lie's theory tells us that the construction of the symmetry group G is equivalent to the determination of the corresponding *infinitesimal transformations* :

$$\bar{t} \approx t + a\,\tau(t, x, u),\ \bar{x} \approx x + a\,\xi(t, x, u),\ \bar{u} \approx u + a\,\eta(t, x, u) \tag{1.5}$$

obtained from (1.1) by expanding the functions f, g and h into Taylor series in a about $a = 0$ and also taking into account the initial conditions

$$f|_{a=0} = t, \quad g|_{a=0} = x, \quad h|_{a=0} = u\,.$$

Thus, we have

$$\tau(t, x, u) = \left.\frac{\partial f}{\partial a}\right|_{a=0}, \quad \xi(t, x, u) = \left.\frac{\partial g}{\partial a}\right|_{a=0}, \quad \eta(t, x, u) = \left.\frac{\partial h}{\partial a}\right|_{a=0}. \tag{1.6}$$

Now one can write (1.5) as

$$\bar{t} \approx (1 + a\,X)t, \quad \bar{x} \approx (1 + a\,X)x, \quad \bar{u} \approx (1 + a\,X)u\,,$$

where

$$X = \tau(t, x, u)\frac{\partial}{\partial t} + \xi(t, x, u)\frac{\partial}{\partial x} + \eta(t, x, u)\frac{\partial}{\partial u}\,. \tag{1.7}$$

This differential operator X is known as the *infinitesimal operator (generator)* of the group G. If the group G is admitted by (1.3), we say that X is an *admitted operator* of (1.3) or X is an *infinitesimal symmetry* of (1.3).

1.4 Group invariants

Definition 1.3 A function $F(t,x,u)$ is called an *invariant of the group of transformation* (1.1) if

$$F(\bar{t},\bar{x},\bar{u}) \equiv F(f(t,x,u,a),g(t,x,u,a),h(t,x,u,a)) = F(t,x,u), \tag{1.8}$$

identically in t, x, u and a.

Theorem 1.2 (Infinitesimal criterion of invariance) A necessary and sufficient condition for a function $F(t,x,u)$ to be an invariant is that

$$X\,F \equiv \tau(t,x,u)\frac{\partial F}{\partial t} + \xi(t,x,u)\frac{\partial F}{\partial x} + \eta(t,x,u)\frac{\partial F}{\partial u} = 0\,. \tag{1.9}$$

From the above theorem it follows that every one-parameter group of point transformations (1.1) has two functionally independent invariants, which can be taken to be the left-hand side of any first integrals

$$J_1(t,x,u) = c_1, \quad J_2(t,x,u) = c_2,$$

of the characteristic equations

$$\frac{dt}{\tau(t,x,u)} = \frac{dx}{\xi(t,x,u)} = \frac{du}{\eta(t,x,u)}.$$

Theorem 1.3 Given the infinitesimal transformation (1.5) or its symbol X, the corresponding one-parameter group G is obtained by solving the Lie equations

$$\frac{d\bar{t}}{da} = \tau(\bar{t},\bar{x},\bar{u}), \quad \frac{d\bar{x}}{da} = \xi(\bar{t},\bar{x},\bar{u}), \quad \frac{d\bar{u}}{da} = \eta(\bar{t},\bar{x},\bar{u}) \tag{1.10}$$

subject to the initial conditions

$$\bar{t}|_{a=0} = t, \quad \bar{x}|_{a=0} = x, \quad \bar{u}|_{a=0} = u\,.$$

1.5 Construction of a symmetry group

Here we describe the algorithm to determine a symmetry group for a given PDE but first we give some definitions.

1.5.1 Prolongation of point transformations

Consider a second-order PDE

$$E(t, x, u, u_t, u_x, u_{tt}, u_{xx}, u_{tx}) = 0, \tag{1.11}$$

where t and x are two independent variables and u is a dependent variable. Let

$$X = \tau(t, x, u)\frac{\partial}{\partial t} + \xi(t, x, u)\frac{\partial}{\partial x} + \eta(t, x, u)\frac{\partial}{\partial u}, \tag{1.12}$$

be the infinitesimal generator of the one-parameter group G of transformation (1.1). The *first prolongation* of the operator X is denoted by $X^{[1]}$ and is given by

$$X^{[1]} = X + \zeta_1(t, x, u, u_t, u_x)\frac{\partial}{\partial u_t} + \zeta_2(t, x, u, u_t, u_x)\frac{\partial}{\partial u_x}$$

where

$$\begin{aligned} \zeta_1 &= D_t(\eta) - u_t D_t(\tau) - u_x D_t(\xi), \\ \zeta_2 &= D_x(\eta) - u_t D_x(\tau) - u_x D_x(\xi) \end{aligned}$$

and the total derivatives D_t and D_x are given by

$$D_t = \frac{\partial}{\partial t} + u_t\frac{\partial}{\partial u} + u_{tx}\frac{\partial}{\partial u_x} + u_{tt}\frac{\partial}{\partial u_t} + \cdots, \tag{1.13}$$

$$D_x = \frac{\partial}{\partial x} + u_x\frac{\partial}{\partial u} + u_{xx}\frac{\partial}{\partial u_x} + u_{tx}\frac{\partial}{\partial u_t} + \cdots. \tag{1.14}$$

Likewise, the the second prolongation of X is given by

$$X^{[2]} = X + \zeta_1\frac{\partial}{\partial u_t} + \zeta_2\frac{\partial}{\partial u_x} + \zeta_{11}\frac{\partial}{\partial u_{tt}} + \zeta_{12}\frac{\partial}{\partial u_{tx}} + \zeta_{22}\frac{\partial}{\partial u_{xx}}. \tag{1.15}$$

where

$$\begin{aligned} \zeta_{11} &= D_t(\zeta_1) - u_{tt} D_t(\tau) - u_{tx} D_t(\xi), \\ \zeta_{12} &= D_x(\zeta_1) - u_{tt} D_x(\tau) - u_{tx} D_x(\xi), \\ \zeta_{22} &= D_x(\zeta_2) - u_{tx} D_x(\tau) - u_{xx} D_x(\xi). \end{aligned}$$

Applying the definitions of D_t and D_x given above, we obtain

$$\begin{aligned}
\zeta_1 &= \eta_t + u_t\eta_u - u_t\tau_t - u_t^2\tau_u - u_x\xi_t - u_t u_x\xi_u. && (1.16)\\
\zeta_2 &= \eta_x + u_x\eta_u - u_t\tau_x - u_t u_x\tau_u - u_x\xi_x - u_x^2\xi_u. && (1.17)\\
\zeta_{11} &= \eta_{tt} + 2u_t\eta_{tu} + u_{tt}\eta_u + (u_t)^2\eta_{uu} - 2u_{tt}\tau_t - u_t\tau_{tt} - 2(u_t)^2\tau_{tu}\\
&\quad -3u_t u_{tt}\tau_u - (u_t)^3\tau_{uu} - 2u_{tx}\xi_t - u_x\xi_{tt} - 2u_t u_x\xi_{tu} - (u_t)^2 u_x\xi_{uu}\\
&\quad -(u_x u_{tt} + 2u_t u_{tx})\xi_u. && (1.18)\\
\zeta_{12} &= \eta_{tx} + u_x\eta_{tu} + u_t\eta_{xu} + u_{tx}\eta_u + u_t u_x\eta_{uu} - u_{tx}(\tau_t + \xi_x) - u_t\tau_{tx} - u_{tt}\tau_x\\
&\quad -u_t u_x(\tau_{tu} + \xi_{xu}) - u_t^2\tau_{xu} - (2u_t u_{tx} + u_x u_{tt})\tau_u - (u_t)^2 u_x\tau_{uu} - u_x\xi_{tx}\\
&\quad -u_{xx}\xi_t - (u_x)^2\xi_{tu} - (2u_x u_{tx} + u_t u_{xx})\xi_u - u_t(u_x)^2\xi_{uu}. && (1.19)\\
\zeta_{22} &= \eta_{xx} + 2u_x\eta_{xu} + u_{xx}\eta_u + (u_x)^2\eta_{uu} - 2u_{xx}\xi_x - u_x\xi_{xx} - 2(u_x)^2\xi_{xu}\\
&\quad -3u_x u_{xx}\xi_u - (u_x)^3\xi_{uu} - 2u_{tx}\tau_x - u_t\tau_{xx}\\
&\quad -2u_t u_x\tau_{xu} - (u_t u_{xx} + 2u_x u_{tx})\tau_u - u_t(u_x)^2\tau_{uu}. && (1.20)
\end{aligned}$$

1.5.2 Group admitted by a PDE

The operator

$$X = \tau(t,x,u)\frac{\partial}{\partial t} + \xi(t,x,u)\frac{\partial}{\partial x} + \eta(t,x,u)\frac{\partial}{\partial u} \tag{1.21}$$

is a *point symmetry* of the second-order PDE

$$E(t,x,u,u_t,u_x,u_{tt},u_{tx},u_{xx}) = 0 \tag{1.22}$$

if

$$X^{[2]}(E) = 0 \tag{1.23}$$

whenever $E = 0$. This can also be written as (symmetry condition)

$$X^{[2]}\,E\big|_{E=0} = 0, \tag{1.24}$$

where the symbol $|_{E=0}$ means evaluated on the equation $E = 0$.

Definition 1.4 Equation (1.24) is called the *determining equation* of (1.22), because it determines all the infinitesimal symmetries of (1.22).

The theorem below enables us to construct some solutions of (1.22) from known one.

Theorem 1.4 A symmetry of (1.22) transforms any solution of (1.22) into another solution of the same equation.

1.6 Lie algebras

Let us consider two operators X_1 and X_2 defined by

$$X_1 = \tau_1(t,x,u)\frac{\partial}{\partial t} + \xi_1(t,x,u)\frac{\partial}{\partial x} + \eta_1(t,x,u)\frac{\partial}{\partial u},$$

and

$$X_2 = \tau_2(t,x,u)\frac{\partial}{\partial t} + \xi_2(t,x,u)\frac{\partial}{\partial x} + \eta_2(t,x,u)\frac{\partial}{\partial u}.$$

Definition 1.5 (Commutator) The *commutator* of X_1 and X_2, written as $[X_1, X_2]$, is defined by $[X_1, X_2] = X_1(X_2) - X_2(X_1)$.

Definition 1.6 (Lie algebra) A Lie algebra is a vector space L of operators with the following property : For all $X_1, X_2 \in L$, the commutator $[X_1, X_2] \in L$.

The dimension of a Lie algebra is the dimension of the vector space L.

Theorem 1.5 The set of all solutions of any determining equation forms a Lie algebra.

1.7 Concluding remarks

In this chapter, we presented briefly some basic definitions and results of the Lie group analysis of PDEs. These included the algorithm to determine the Lie point symmetries of PDEs.

Chapter 2

Lie group analysis of the heat equation: illustrative example

In science and engineering, the heat equation is a partial differential equation that represent how heat spreads in a medium as well as how heat evolves with time through the medium.

In this chapter, we consider an example of a *linear* PDE, namely *heat equation* and calculate its symmetry Lie algebra. We also find group-invariant solutions under certain symmetry generators of the heat equation.

2.1 Lie symmetries of heat equation

Example 2.1 (see e.g., [3], [9])
Let us determine the Lie point symmetries of the heat equation

$$u_t - u_{xx} = 0, \tag{2.1}$$

in which the dependent variable is u and independent variables are t and x. This equation admits the one-parameter Lie group of transformations with infinitesimal generator

$$X = \tau(t, x, u)\frac{\partial}{\partial t} + \xi(t, x, u)\frac{\partial}{\partial x} + \eta(t, x, u)\frac{\partial}{\partial u}, \tag{2.2}$$

if and only if

$$X^{[2]}(u_t - u_{xx})\big|_{(2.1)} = 0. \tag{2.3}$$

Using the definition of $X^{[2]}$ from Chapter one, we obtain

$$\Big[\tau(t,x,u)\frac{\partial}{\partial t} + \xi(t,x,u)\frac{\partial}{\partial x} + \eta(t,x,u)\frac{\partial}{\partial u} + \zeta_1\frac{\partial}{\partial u_t} + \zeta_2\frac{\partial}{\partial u_x} + \zeta_{11}\frac{\partial}{\partial u_{tt}}$$
$$+\zeta_{12}\frac{\partial}{\partial u_{tx}} + \zeta_{22}\frac{\partial}{\partial_{xx}}\Big]\Big(u_t - u_{xx}\Big)\Big|_{u_t=u_{xx}} = 0,$$

and this gives

$$\zeta_1 - \zeta_{22}\Big|_{u_t=u_{xx}} = 0, \tag{2.4}$$

where ζ_1 and ζ_{22} are given by equations (1.16) and (1.20) respectively. Substituting the values of ζ_1 and ζ_{22} in equation (2.4) and replacing u_t by u_{xx}, we obtain

$$\eta_t + u_{xx}(\eta_u - \tau_t) - u_x\xi_t - u_xu_{xx}\xi_u - u_{xx}^2\tau_u - \Big[\eta_{xx} + u_x(2\eta_{xu} - \xi_{xx}) - u_{xx}\tau_{xx}$$
$$+u_x^2(\eta_{uu} - 2\xi_{xu}) - 2u_{xx}u_x\tau_{xu} - u_x^3\xi_{uu} - u_x^2u_{xx}\tau_{uu} + (\eta_u - 2\xi_x)u_{xx} - 2u_{tx}\tau_x$$
$$-3u_xu_{xx}\xi_u - u_{xx}^2\tau_u - 2\tau_uu_xu_{tx}\Big] = 0. \tag{2.5}$$

Since τ, ξ and η depend only on t, x and u and are independent of the derivatives of u, the coefficients of like derivatives of u can be equated to yield the following determined system of linear PDEs:

$$u_xu_{tx} \;:\; 2\tau_u = 0, \tag{2.6}$$
$$u_{tx} \;:\; 2\tau_x = 0, \tag{2.7}$$
$$u_x^2u_{xx} \;:\; \tau_{uu} = 0, \tag{2.8}$$
$$u_xu_{xx} \;:\; -\xi_u + 2\tau_{xu} + 3\xi_u = 0, \tag{2.9}$$
$$u_{xx} \;:\; \eta_u - \tau_t + \tau_{xx} - \eta_u + 2\xi_x = 0, \tag{2.10}$$
$$u_x^3 \;:\; \xi_{uu} = 0, \tag{2.11}$$
$$u_x^2 \;:\; \eta_{uu} - 2\xi_{xu} = 0, \tag{2.12}$$
$$u_x \;:\; \xi_t + 2\eta_{xu} - \xi_{xx} = 0, \tag{2.13}$$
$$1 \;:\; \eta_t - \eta_{xx} = 0. \tag{2.14}$$

From equations (2.6) and (2.7), we obtain

$$\tau \equiv \tau(t) = a(t), \tag{2.15}$$

where $a(t)$ is an arbitrary function of t. Equation (2.8) is also satisfied. Substituting the value of τ in equation (2.9) and integrating with respect to u, we get

$$\xi = b(t, x),$$

where $b(t, x)$ is an arbitrary function of t and x. Then equation (2.11) is satisfied too. Now, substituting the values of τ and ξ in equation (2.10) and integrating the equation obtained with respect to x, yields

$$b(t, x) = \frac{1}{2}\, a'(t)x + c(t), \tag{2.16}$$

where $c(t)$ is an arbitrary function of t and so

$$\xi = \frac{1}{2}\, a'(t)x + c(t). \tag{2.17}$$

After substitution the value of ξ in equation (2.12) and integrating with respect to u, we have

$$\eta = d(t, x)u + \alpha(t, x), \tag{2.18}$$

where $d(t, x)$ and $\alpha(t, x)$ are arbitrary functions of t and x. It follows from substitution equations (2.17) and (2.18) in (2.13) that

$$d = -\frac{1}{8}\, a''(t)x^2 - \frac{1}{2}\, c'(t)x + f(t),$$

where $f(t)$ is an arbitrary function of t and so

$$\eta = -\frac{1}{8}\, a''(t)ux^2 - \frac{1}{2}\, c'(t)ux + uf(t) + \alpha(t, x).$$

Substituting the values of η_t and η_{xx} in equation (2.14), yields

$$-\frac{1}{8}\, a'''(t)x^2u - \frac{1}{2}\, c''(t)xu + f'(t)u + \alpha_t + \frac{1}{4}\, a'''(t)u + \alpha_{xx} = 0.$$

Splitting the above equation on u, we obtain

$$u \;:\; -\frac{1}{8}a'''(t)x^2 - \frac{1}{2}c''(t)x + f'(t) + \frac{1}{4}a''(t) = 0, \tag{2.19}$$

$$1 \;:\; \alpha_t - \alpha_{xx} = 0. \tag{2.20}$$

Further splitting (2.19) with respect to powers of x, we get

$$x^2 \;:\; a'''(t) = 0, \tag{2.21}$$

$$x^1 \;:\; c''(t) = 0, \tag{2.22}$$

$$1 \;:\; f'(t) + \frac{1}{4}a''(t) = 0. \tag{2.23}$$

Integrating the above equations (2.21) and (2.22) with respect to t respectively, yields

$$a(t) = \frac{1}{2}A_1t^2 + A_2t + A_3, \tag{2.24}$$

$$c(t) = A_4t + A_5, \tag{2.25}$$

where A_1, A_2, A_3, A_4 and A_5 are arbitrary constants. It follows from equations (2.23) and (2.24) that

$$f(t) = -\frac{1}{4}A_1t + A_6,$$

where A_6 is an arbitrary constant. Hence the general solution of the system of equations (2.6)−(2.14) is

$$\begin{aligned}
\tau &= \frac{1}{2}A_1t^2 + A_2t + A_3,\\
\xi &= \frac{1}{2}(A_1t + A_2)x + A_4t + A_5,\\
\eta &= -\frac{1}{8}A_1x^2u - \frac{1}{2}A_4xu - (\frac{1}{4}A_1t - A_6)u + \alpha(t,x),
\end{aligned}$$

where the A_s are constants and $\alpha(t,x)$ satisfies $\alpha_t = \alpha_{xx}$.

Thus the Lie point symmetries of the heat equation are given by

$$\begin{aligned}
X_1 &= \frac{\partial}{\partial t},\\
X_2 &= \frac{\partial}{\partial x},\\
X_3 &= u\frac{\partial}{\partial u},\\
X_4 &= 2t\frac{\partial}{\partial t} + x\frac{\partial}{\partial x},\\
X_5 &= 2t\frac{\partial}{\partial x} - xu\frac{\partial}{\partial u},\\
X_6 &= 4t^2\frac{\partial}{\partial t} + 4tx\frac{\partial}{\partial x} - (x^2u + 2tu)\frac{\partial}{\partial u},\\
X_\beta &= \alpha(t,x)\frac{\partial}{\partial u},
\end{aligned}$$

which generates a Lie algebra of infinite dimension. We now calculate the commutation relations for all the symmetry generators. We first compute $[X_4, X_1]$. By the definition of the Lie bracket, we have

$$\begin{aligned}
[X_4, X_1] &= X_4X_1 - X_1X_4 \\
&= \left(2t\frac{\partial}{\partial t} + x\frac{\partial}{\partial x}\right)\frac{\partial}{\partial t} - \frac{\partial}{\partial t}\left(2t\frac{\partial}{\partial t} + x\frac{\partial}{\partial x}\right) \\
&= -2X_1.
\end{aligned}$$

Proceeding in a similar manner, we can compute other commutation relations. In a table form these commutation relations can be written as:

$[X_i, X_j]$	X_1	X_2	X_3	X_4	X_5	X_6	X_α
X_1	0	0	0	$2X_1$	$2X_2$	$4X_4 - 2X_3$	X_{α_t}
X_2	0	0	0	X_2	$-X_3$	$2X_5$	X_{α_x}
X_3	0	0	0	0	0	0	$-X_\alpha$
X_4	$-2X_1$	$-X_2$	0	0	X_5	$2X_6$	$X_{\alpha'}$
X_5	$-2X_2$	X_3	0	$-X_5$	0	0	$X_{\alpha''}$
X_6	$2X_3 - 4X_4$	$-2X_5$	0	$-2X_6$	0	0	$X_{\alpha'''}$
X_α	$-X_{\alpha_t}$	$-X_{\alpha_x}$	X_α	$-X_{\alpha'}$	$-X_{\alpha''}$	$-X_{\alpha'''}$	0

The values of α', α'' and α''' in the table above are given by,

$$\begin{aligned}
\alpha' &= x\alpha_x + 2t\alpha_t, \\
\alpha'' &= 2t\alpha_x + x\alpha, \\
\alpha''' &= 4tx\alpha_x + 4t^2\alpha_t + (x^2 + 2t)\alpha.
\end{aligned}$$

2.1.1 One parameter group

The one-parameter group can be obtained using the following Lie equations

$$\begin{aligned}
\frac{d\bar{t}}{da} &= \xi^1(t, x, u), \quad \bar{t}|_{a=0} = t, \\
\frac{d\bar{x}}{da} &= \xi^2(t, x, u), \quad \bar{x}|_{a=0} = x, \\
\frac{d\bar{u}}{da} &= \eta(t, x, u), \quad \bar{u}|_{a=0} = u.
\end{aligned}$$

We now compute the one-parameter groups. For each X_i, let T_{a_i} be the corresponding group. Let us first calculate the one-parameter group corresponding to infinitesimal generator X_4, namely

$$X_4 \;=\; 2t\frac{\partial}{\partial t} + x\frac{\partial}{\partial x}.$$

Using Lie equations, we have

$$\frac{d\bar{x}}{da} = \bar{x}, \quad \bar{x}|_{a=0} = x, \quad \frac{d\bar{t}}{da} = \bar{2}t, \quad \bar{t}|_{a=0} = t.$$

Solving the above equations, we get

$$\bar{x} = xe^a, \quad \bar{t} = te^{2a}.$$

Thus the one-parameter group T_{a_4} corresponding to the operator X_4 is given by

$$T_{a_4} : (\bar{t}, \bar{x}, \bar{u}) \longrightarrow (te^{2a_4}, xe^{a_4}, u).$$

If we continue in the same manner as above, we get the following one-parameter groups:

$$\begin{aligned}
T_{a_1} &: (\bar{t}, \bar{x}, \bar{u}) \longrightarrow (t + a_1, x, u),\\
T_{a_2} &: (\bar{t}, \bar{x}, \bar{u}) \longrightarrow (t, x + a_2, u),\\
T_{a_3} &: (\bar{t}, \bar{x}, \bar{u}) \longrightarrow (t, x, ue^{a_3}),\\
T_{a_5} &: (\bar{t}, \bar{x}, \bar{u}) \longrightarrow (t, x + 2a_5t, ue^{-a_5x - a_5^2t}),\\
T_{a_6} &: (\bar{x}, \bar{t}, \bar{u}) \longrightarrow \left(\frac{t}{1 - 4\alpha t a_6}, \frac{x}{1 - 4\alpha t a_6}, u\sqrt{(1 - 4\alpha t a_6}e^{\frac{-a_6x^2}{1-4a_6t}}\right),\\
T_\alpha &: (\bar{t}, \bar{x}, \bar{u}) \longrightarrow (t, x, u + a\alpha(t, x)).
\end{aligned}$$

2.2 The use of symmetry transformations

In this section, we make use of the symmetries calculated in the previous section to obtain special exact solutions for the heat equation. The Lie group analysis supply us with two basic ways for constructing exact solutions of PDEs: group transformations of known solutions and construction of group invariant solutions. These methods are described in detail by means of

examples.

If $\bar{u} = h(\bar{t}, \bar{x})$ is a solution of equation (2.1), then so is

$$\phi(t, x, u, a) = h(f_1(t, x, u, a), f_2(t, x, u, a))$$

or in solved form w.r.t $u : u = H_a(t, x)$ is a one-parameter family of solutions. For

$$T_{a_1} : \bar{t} = t + a_1, \quad \bar{x} = x, \quad \bar{u} = u,$$

if $\bar{u} = h(t, x)$ is a solution, then

$$u = h(t + a_1, x).$$

We now write down the generated solutions for the other cases:

$$\begin{aligned}
T_{a_2} : u &= h(t, x + a_2), \\
T_{a_3} : u &= h(t, x)e^{-a_3}, \\
T_{a_4} : u &= h(te^{2a_4}, xe^{a_4}), \\
T_{a_5} : u &= h(t, x + 2a_5 t)e^{(a_5 x - a_5^2 t)}, \\
T_{a_6} : u &= h\left(\frac{t}{1 - 4\alpha t a_6}, \frac{x}{1 - 4\alpha t a_6}\right)\frac{1}{\sqrt{(1 - 4\alpha t a_6)}}e^{\frac{ax^2}{1-4a_6 t}}, \\
T_{\alpha} : u &= h(t, x) - a\alpha(t, x).
\end{aligned}$$

2.3 Group invariant solutions

A group-invariant solution with respect to a subgroup of the symmetry group is an exact solution which is unchanged by all the transformations of the subgroup. Invariant solutions are expressed in terms of invariant of the subgroup. The number of independent variables in the reduced system is fewer than the original system. Thus, the solution of the original system can be obtained by a solution from a solution of the reduced ODE, which is invariant under the transformation G. Considering the heat equation, let G be a one-parameter symmetry group of equation (2.1). A solution $u = u(t, x)$ of equation (2.1) is invariant under G with generator X if

$$\eta - \xi^1 u_t - \xi^2 u_x = 0,$$

whenever $u = u(t, x)$. This is the invariant surface condition which provides the form of the invariant solution to the equation.

Let us now illustrate the above method by considering the heat equation which consist of six-parameter group of symmetries and infinite-dimensional subgroup. We will construct invariant solutions under the operators X_5 and form the linear combination of X_1 and X_2.

Traveling wave solutions

Consider the following linear combination of the translation operators X_1 and X_2:

$$c\,\frac{\partial}{\partial x} + \frac{\partial}{\partial t}.$$

The characteristic equations are

$$\frac{dx}{c} = \frac{dt}{1} = \frac{du}{0}.$$

Thus, one invariant is $I_1 = u$. The other is obtained from the equation

$$\frac{dx}{c} = \frac{dt}{1}$$

and is given by $I_2 = x - ct$.

The invariant solution can be written as $I_1 = h(I_2)$, i.e.,

$$u = h(x - ct),$$

where h is an arbitrary function of its argument. Differentiation of u with respect to x and t, gives us

$$u_t = -c\,h', \quad u_x = h', \quad u_{xx} = h''.$$

Substituting these expressions into equation (2.1), we obtain the following reduced ODE

$$h'' + ch' = 0,$$

which is a second-order ODE with constant coefficients. Its general solution is

$$h(I_2) = A_1 e^{-cI_2} + A_2 = A_1 e^{-c(x-ct)} + A_2,$$

where A_1 and A_2 are arbitrary constants of integration. Thus the most general traveling wave solution for the heat equation is of the form

$$u(t,x) = A_1 e^{-c(x-ct)} + A_2.$$

Galilean-invariant solutions

Secondly let us construct an invariant solution under operator X_5, namely

$$X_5 \;=\; 2t\frac{\partial}{\partial x} - xu\frac{\partial}{\partial u}.$$

The characteristic equations are

$$\frac{dx}{2t} = \frac{dt}{0} = \frac{du}{-xu}.$$

Thus, one invariant is $I_1 = t$. The other is obtained from the equation

$$\frac{dx}{2t} = \frac{du}{-xu}$$

and is given by $I_2 = ue^{\frac{x^2}{4t}}$.

Consequently, the invariant solution is $I_2 = h(I_1)$, i.e.

$$u = e^{-\frac{x^2}{4t}} h(t).$$

Similarly

$$\begin{aligned} u_t &= \left(\frac{x^2}{4t^2}h + h'\right)e^{-\frac{x^2}{4t}}, \\ u_{xx} &= \left(-\frac{1}{2t} + \frac{x^2}{4t^2}\right)he^{-\frac{x^2}{4t}}. \end{aligned}$$

Substitution of the above values of u_t and u_{xx} in equation (2.1), gives the following first-order ODE

$$h' = -\frac{1}{2t}h$$

which on integration gives

$$h(t) = \frac{C}{\sqrt{t}}.$$

Hence the most general Galilean-invariant solution is

$$u(t,x) = \frac{C}{\sqrt{t}}\, e^{-\frac{x^2}{4t}}.$$

2.4 Concluding remarks

In this chapter, we have looked at an example of a linear PDE, namely the heat equation. We calculated its Lie point symmetries, constructed solutions under transformation groups on known solutions and also obtained invariant solution under certain symmetry generators.

Chapter 3

Lie group analysis of an internal flow and heat transfer inside a combustion chamber of a solid rocket motor.

This chapter aims to study fluid flow and heat transfer inside a porous cylindrical pipe which has direct application when designing solid rocket motors. The gaseous flow inside the combustion chamber arises from burning solid propellant (fuel) grain due to the porous surface wall which is kept at constant temperature after ignition. Thus, the chapter studies gaseous mean flow dynamics and temperature distribution inside the combustion chamber of a solid rocket motor. Also effects of various parameters that arise from the design of the combustion chamber, internal gaseous flow dynamics and temperature distribution are studied and illustrated graphically.

3.1 Introduction

The subject of injection driven fluid flow inside cylindrical pipes with porous walls has received a great deal of attention in the past and recent. This attention stems from a broad spectrum of technical applications the subject covers. To mention a few, these technical applications include surface transpiration, boundary layer control and internal flow modelling of propellant

grain in solid rocket motors. Restricting our attention to solid rocket motors. Internal flow modelling of propellant grain has received a great deal of attention due to the vital role it plays in the assessment of aeroacoustic instabilities. Studies [11, 12] found that the stability of solid rocket motors depends strongly on the accurate description of unsteady velocity and pressure fields inside the combustion chamber of solid rocket motors.

On the quest to asses these aeroacoustic instabilities, Taylor and Culick were the first to study injection driven incompressible fluid inside a tube with porous wall and their solution later served as a good approximation for simulating the mean gaseous flow in solid rocket motors as mentioned in reference [13]. The desire to know more about the subject led to considerable amount of work being done by researchers to seek mathematical formulations and solutions that would better describe the gaseous dynamics (flow) inside solid rocket motor combustion chamber using a pipe with porous wall. Berman [14] was the first as mentioned in the studies [15, 16] to show that a system of equations representing laminar flow inside porous walls with uniform injection or suction at the walls can be transformed to single ordinary differential equation (ODE) while preserving the dynamics of the flow. Although similarity solutions have some disadvantages, that is they are not always valid in the entrance region. They provide a gateway to analyse the motion of fluid flow inside porous channels [17].

Terrill and Thomas [15] investigated laminar flow through a uniform (constant diameter) porous pipe with constant injection or suction through the wall and used similarity transformation to reduce a system of equations to single nonlinear ODE which they solved and obtained dual solutions. The analysis of the results obtained in their study show that the dual solutions exist everywhere except in the range $2.3 < R_e < 9.1$. Also the study illustrates that the flow is not fully developed within the same range. In the region, $R_e = 0$ to $R_e = 2.3$, the system permeates at a low rate, thus lead to reverse flow near the wall, for large injection $9.1 < R_e < \infty$, the velocity profiles are well-behaved (fully developed).

Quaile and Levy [18] similarly investigated theoretically and experimentally laminar flow in a constant diameter porous tube (pipe) with uniform mass suction at the wall. Upon conclusion, their theoretical (inlet region theory) and experimental results revealed that by assuming the transverse pressure to be zero gives good results however this can lead to inaccuracies towards

the wall, thus the flow field leads to reverse flow and results in turbulent flow which is not ideal during solid rocket motor operation. Both theoretical and experimental findings show that the pressure increases in the direction of the flow for $R_e > 1.25$.

From the results obtained in [15] and [18] one would argue that sucking fluid out of a porous pipe is not ideal, since it leads to reverse flow, as a result the velocity of the fluid decreases and lead to the decrease in thrust of the solid rocket motor. In addition to the above mentioned findings, it can be asked as much as the results are correct for a porous pipe of a fixed diameter, how correct or incorrect are the same findings for a porous pipe of variable diameter? Since in practice the radius of the rocket chamber increases as propellant burn, thus leads to time-dependent radius. The variation of radius changes the dynamics of the steady state flow to unsteady state flow, hence the dynamics of mean flow vary with time due to expansion or contraction of the combustion chamber.

To understand the effects of expansion or contraction, researchers saw the need to study unsteady state regime of fluid flow inside the porous pipe to understand the underlying dynamics. Galowin and Desantis [19] studied laminar flow in an expanding or contracting pipe with a porous wall, from their analysis authors observed that for fluid suction, the wall shear stress and static pressure decrease in the axial flow direction, also the rate at which these quantities decrease are functions of wall porosity, initial pressure gradient across the wall and inlet flow permeation Reynolds number.

Saad and Majdalani [20] studied incompressible laminar flow in a porous contracting or expanding pipe. They employed double perturbation method of a pair Reynolds number R_e and wall dilation α. Their analysis revealed that so long the control parameters were chosen at the prescribed asymptotic range both numerical and exact solution showed agreement. Zhou and Majdalani [21] investigated improved mean-flow for slab rocket motors with radially regressing walls using a porous pipe. Authors employed similarity transformations and reduced Navier-Stokes equations representing the internal flow to a single nonlinear classical Berman ODE. Analysis of their results revealed that for $R_e = 1000$, the mean-flow becomes practically equivalent to that of Taylor and Culick profile and also explains the use of Taylor and Culick's solution in practice as mentioned in [13]. Boutros et al [1] investigated unsteady flows

in a semi-infinite expanding or contracting pipe and similarly used similarity transformation and obtained a single non-linear ODE, which they solved and analyzed. The analysis thereof revealed that sucking whilst expanding is not desirable and leads to an error in the solution.

The burning of propellant grain introduces heat transfer to the system. In view of understanding heat transfer inside a pipe, a number of research works have been done to investigate thermal radiation and convection heat transfer. Pearce [22] motivated by the absence of a description (mathematical formulation) that accounts for radiative heat transfer studied radiative heat effects within a solid propellant rocket motor. From his findings, he observed that radiation is a dominant heat flux (heat source) in the combustion chamber and the heat flux drops to a small fraction of the convective heat flux near the rocket nozzle. Also radiation from fluid particles is large compared to that of the gaseous species. Xia et al [23] investigated the impact of thermal radiation on high-temperature laminar flow in a tube. Authors observed that thermal radiation weakens the convective heat transfer from the fluid to the surface wall of the tube. This study found that suppressive effects of radiative heat transfer on the flow weakens the convective transport capability of the fluid. Viskanta [24] studied the interaction of heat transfer by conduction, convection and radiation in a radiating fully developed laminar flow numerically. Huang and Lin [25] studied numerically the interaction of thermal radiation with laminar forced convection in a thermally developing circular pipe flow. Studies [24] and [25] revealed that axial radiation effects become significant for small conduction-to-radiation parameter and higher temperature ratio.

The dynamics of temperature difference within the fluid leads to variation of fluid density which lead to an important study of a parameter due to gravity, namely buoyancy force. Hariprasad et al [26] studied the influence of gravity on solid propellant burning rate experimentally and noticed a five percent rate augmentation when the propellant burning surface evolution was against the earth gravity. Ishigaki [27] studied the effects of buoyancy on laminar flow and heat transfer pipes (rotating and stationary) by employing similarity analysis and numerical computations. The author argued that buoyancy secondary induced flows in heated pipes rotating about a parallel axis are similar to those in a stationary horizontal heated pipes.

Lie group method was used to study unsteady flows in a semi-infinite expanding or contracting

pipe with injection or suction through a porous wall [1]. Authors studied the flow without investigating the effect of heat transfer and buoyancy force which are two parameters playing an essential role during both transient unsteady and steady regimes operation of a solid rocket motor. Motivated by the above study, the purpose of this project is to extend the study carried out in reference [1] by incorporating heat transfer and buoyancy effects during the steady state regime operation of a solid rocket motor. The project seeks to find analytical solutions of the improved model that represents the above phenomena (extension of the works in [1]) using Lie group analysis along with double perturbation method. Also, the effect of the cross-flow Reynolds number R_e, wall expansion ratio α, Grashof number G_r, Prandlt number P_r and radiation number R on the axial velocity and temperature distribution are studied. Lastly, results are represented graphically, analysed and discussed.

3.2 Mathematical modelling of the problem

This section provides a detailed mathematical formulation of a system of equations representing an unsteady two-dimensional laminar flow of an incompressible fluid in a circular pipe whose surface wall is kept at a constant temperature, representing propellant flow and heat transfer inside a solid rocket motor. The mathematical formulation of the above mentioned flow is derived based on conservation of mass, momentum and energy respectively. The boundary conditions will be given based on flow dynamics and the design of the system. Lastly, the mathematical model derived for flow and heat transfer inside the solid rocket motor combustion chamber will be represented as a flow inside a circular porous pipe in Section 3.3.

3.2.1 Flow configuration

We consider fluid flow and heat transfer in a porous cylindrical pipe which has a direct application when optimizing solid rocket motor thrust. The cylindrical propellant grain (fuel) dynamics inside the solid rocket motor is modelled as a long pipe with one end closed at the headwall, whose surface wall is kept at a constant temperature, as shown in Figure 3.1.

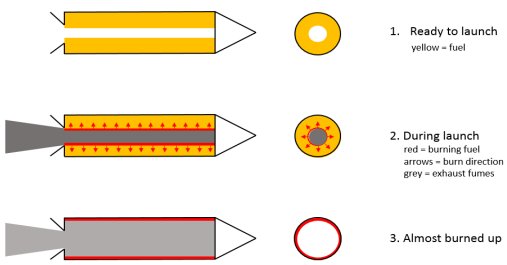

Figure 3.1: Solid rocket motor operational regimes

The solid propellant grain (yellow part in Figure 3.1.1) is initially bounded between the combustion chamber (white part in Figure 3.1.1) and the outer wall of the rocket case. The state of the grain changes to gaseous form due to the heated wall after ignition (Figure 3.1.2) which leads to flow injection inside the chamber. The gas inside the chamber will either flow in or out of the chamber through porous surface, thus, result in injection or suction. Figure 3.1.3 indicates how the burning of propellant grain regresses with time as it burns.

The physical model of the above specified flow is represented by the following laminar streams and cylindrical configuration as shown in Figure 3.2:

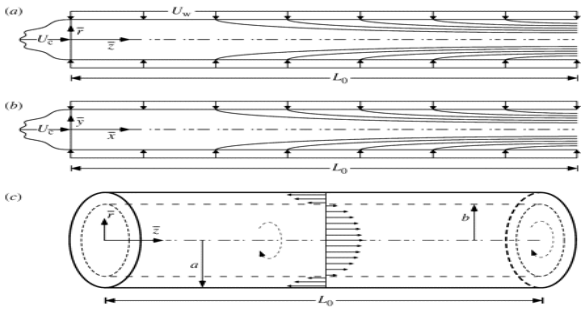

Figure 3.2: Geometry of the flow

The above case study is influenced by surfaces forces and body force. The current study investigates the influence of the buoyancy force (body force) and heat transfer effects due to temperature difference on the flow field studied in [1].

3.2.2 Conservation laws

This subsection lists and express the important conservation laws and thereafter use them to derive the equations representing flow and heat transfer inside the combustion chamber. The mathematical model of an internal flow inside a solid rocket motor is derived from the cylindrical coordinates system given in Figure 3.3 below.

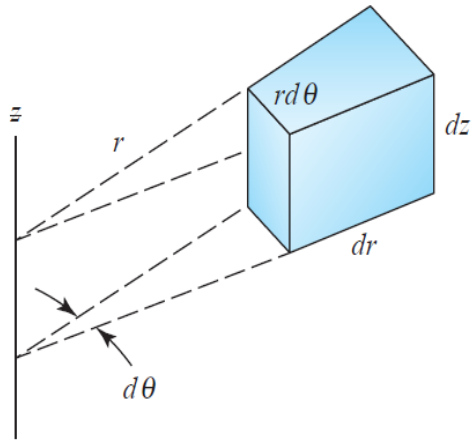

Figure 3.3: Bulk of fluid in cylindrical coordinate system

Conservation of mass

The principle of mass conservation states that the rate of change of a fluid mass in a closed system is constant [10]. Simply it means that the amount of fluid flowing into the system must equal the amount of fluid flowing out of the system. The equation of mass conservation in cylindrical coordinate is given by

$$\frac{\partial \rho}{\partial t} + \frac{1}{r}\frac{\partial}{\partial r}\left(r\rho v_r\right) + \frac{1}{r}\frac{\partial}{\partial \theta}\left(\rho v_\theta\right) + \frac{\partial}{\partial z}\left(\rho v_z\right) = 0, \tag{3.1}$$

where z, r and θ are axial, radial and transversal directions of flow respectively. The flow parameters under investigation have the gradients in axial and radial directions only. Since flow parameters do not vary in the transversal direction. Thus, the flow is two-dimensional along the z and r axis. The above equation (3.1) reduces to:

$$\frac{\partial \rho}{\partial t} + \frac{1}{r}\frac{\partial}{\partial r}\left(r\rho v_r\right) + \frac{\partial}{\partial z}\left(\rho v_z\right) = 0. \tag{3.2}$$

The density of the fluid does not change with time for an incompressible fluid, thus equation (3.2) becomes

$$\frac{1}{r}\frac{\partial}{\partial r}\Big(r\rho v_r\Big) + \frac{\partial}{\partial z}\Big(\rho v_z\Big) = 0, \tag{3.3}$$

where v_z and v_r are velocity components along the axial z and radial r directions respectively. Equivalently equation (3.3) can be written as follows:

$$\frac{\partial(\bar{r}\bar{u})}{\partial\bar{z}} + \frac{\partial(\bar{r}\bar{v})}{\partial\bar{r}} = 0, \tag{3.4}$$

by taking standard components $\bar{u}$ and $\bar{v}$ to be velocity components along the axial z and radial r direction respectively.

Conservation of momentum

The law of conservation of momentum states that the rate of change of the momentum of a fluid mass in a control volume is equal to the net external force acting on the fluid [10]. The external forces that act on a fluid mass are classed as either surface forces or body forces. Surface forces act across the surface of the fluid mass, examples of such forces are pressure and viscosity forces. Body forces act throughout the body of the fluid, which are gravitational force and electromagnetic force.

The flow under investigation is influenced by the surface force and body force. Similarly the variation of fluid parameters is along the radial and axial direction respectively as mentioned above. The equation of conservation of momentum is given by the following Naiver-Stokes equations in cylindrical coordinates in the r and z direction respectively,

$$\rho\left(\frac{\partial u_r}{\partial t} + u_r\frac{\partial u_r}{\partial r} + u_z\frac{\partial u_r}{\partial z}\right) = -\frac{\partial p}{\partial r} + \mu\left(\Delta^2 u_r - \frac{u_r}{r^2}\right) + \rho f_r, \tag{3.5}$$

$$\rho\left(\frac{\partial u_z}{\partial t} + u_r\frac{\partial u_z}{\partial r} + u_z\frac{\partial u_z}{\partial z}\right) = -\frac{\partial p}{\partial z} + \mu\Delta^2 u_z + \rho f_z. \tag{3.6}$$

where $\dfrac{\partial p}{\partial r}$ and $\dfrac{\partial p}{\partial z}$ are surface forces due to the work done by the surface wall in the r and z direction, f_r and f_z are the body forces affecting the flow in the r and z direction. Similarly equation (3.5) and (3.6) can be written in terms of $\bar{u}$ and $\bar{v}$:

$$\frac{\partial \bar{v}}{\partial t} + \bar{\bar{u}}\frac{\partial \bar{v}}{\partial \bar{z}} + \bar{v}\frac{\partial \bar{v}}{\partial \bar{r}} = -\frac{1}{\rho}\frac{\partial \bar{P}}{\partial \bar{r}} + \nu\left[\frac{\partial^2 \bar{v}}{\partial \bar{z}^2} + \frac{\partial}{\partial \bar{r}}\left(\frac{1}{\bar{r}}\frac{\partial(\bar{r}\bar{v})}{\partial \bar{r}}\right)\right] + f_r, \tag{3.7}$$

$$\frac{\partial \bar{u}}{\partial t} + \bar{u}\frac{\partial \bar{u}}{\partial \bar{z}} + \bar{v}\frac{\partial \bar{u}}{\partial \bar{r}} = -\frac{1}{\rho}\frac{\partial \bar{P}}{\partial \bar{z}} + \nu\left[\frac{\partial^2 \bar{u}}{\partial \bar{z}^2} + \frac{1}{\bar{r}}\frac{\partial}{\partial \bar{r}}\left(\bar{r}\frac{\partial \bar{u}}{\partial \bar{r}}\right)\right] + f_z. \tag{3.8}$$

Derivation of body force affecting momentum during solid rocket motor operation.

Propellant (fluid) flow inside a horizontally oriented pipe has the net force (net effect between the buoyancy and gravity) acting on a unit volume of the propellant in the vertical direction. Thus the net force is given by

$$\mathbf{F_n} = g(\rho_s - \rho), \tag{3.9}$$

where g is gravity, ρ_s is the density of the propellant close to the surface wall and ρ is the density of the propellant inside the combustion chamber far from the surface wall. For the problem at hand, the density of propellant is depended (function) on temperature, hence the variation of density of the propellant with temperature at constant pressure can be expressed in terms of cubical expansion coefficient β as follows:

$$\beta = -\frac{1}{\rho}\left(\frac{\partial \rho}{\partial T}\right)_p, \tag{3.10}$$

$$\approx -\frac{1}{\rho}\left(\frac{\triangle \rho}{\triangle T}\right). \tag{3.11}$$

Replacing differential quantities by differences, equation (3.11) can be expressed as

$$\beta \approx -\frac{1}{\rho}\left(\frac{\triangle \rho}{\triangle T}\right) = -\frac{1}{\rho}\frac{\rho - \rho_s}{\bar{T} - \bar{T}_s} \tag{3.12}$$

which can be rewritten as

$$\rho - \rho_\infty = \rho\beta(\bar{T} - \bar{T}_s), \tag{3.13}$$

where $\bar{T}$ and $\bar{T}_s$ are temperature of the fluid and temperature at the surface wall respectively. Substituting (3.13) into (3.9), the net body force in the r- direction is given by

$$\mathbf{F}_n = g\rho\beta(\bar{T} - \bar{T}_s). \tag{3.14}$$

Since the body force does not affect the flow in the axial-direction, equations (3.7) and (3.8) become

$$\frac{\partial \bar{v}}{\partial t} + \bar{\bar{u}}\frac{\partial \bar{v}}{\partial \bar{z}} + \bar{v}\frac{\partial \bar{v}}{\partial \bar{r}} = -\frac{1}{\rho}\frac{\partial \bar{P}}{\partial \bar{r}} + \nu\left[\frac{\partial^2 \bar{v}}{\partial \bar{z}^2} + \frac{\partial}{\partial \bar{r}}\left(\frac{1}{\bar{r}}\frac{\partial(\bar{r}\bar{v})}{\partial \bar{r}}\right)\right] + g\beta(\bar{T} - \bar{T}_s), \tag{3.15}$$

$$\frac{\partial \bar{u}}{\partial t} + \bar{u}\frac{\partial \bar{u}}{\partial \bar{z}} + \bar{v}\frac{\partial \bar{u}}{\partial \bar{r}} = -\frac{1}{\rho}\frac{\partial \bar{P}}{\partial \bar{z}} + \nu\left[\frac{\partial^2 \bar{u}}{\partial \bar{z}^2} + \frac{1}{\bar{r}}\frac{\partial}{\partial \bar{r}}\left(\bar{r}\frac{\partial \bar{u}}{\partial \bar{r}}\right)\right]. \tag{3.16}$$

Conservation of energy

The conservation of energy states that the change in internal energy due to an event is equal to the sum of the total work done on the system during the course of the event and any heat which was added to the system [10]. The net heat flux into the fluid bulk is due to:

- volumetric heating due to emission and absorption of radiation denoted by $\dot{q}$.
- heat transferred across the surface due to temperature gradients, i.e thermal conduction.

Thus, the conservation of energy is given by

$$\rho c_p\left(\frac{\partial T}{\partial t} + u_r\frac{\partial T}{\partial r} + \frac{u_\theta}{r}\frac{\partial T}{\partial \theta} + u_z\frac{\partial T}{\partial z}\right) = k\Delta^2 T + \dot{q}, \tag{3.17}$$

where k is thermal conductivity, ρ is the density and c_p is the specific heat. Similarly the temperature distribution does not vary along the transversal direction, thus energy equation with convection along the axial and the radial directions is given by

$$\rho c_p\left(\frac{\partial T}{\partial t} + u_r\frac{\partial T}{\partial r} + u_z\frac{\partial T}{\partial z}\right) = k\Delta^2 T + \dot{q}. \tag{3.18}$$

Equivalently equation (3.18) in terms velocity components $\bar{u}$ and $\bar{v}$

$$\frac{\partial \bar{T}}{\partial t} + \bar{u}\frac{\partial \bar{T}}{\partial \bar{z}} + \bar{v}\frac{\partial \bar{T}}{\partial \bar{r}} = \lambda\left[\frac{\partial^2 \bar{T}}{\partial \bar{z^2}} + \frac{1}{\bar{r}}\frac{\partial}{\partial \bar{r}}\left(\bar{r}\frac{\partial \bar{T}}{\partial \bar{r}}\right)\right] + \frac{\dot{q}}{\rho c_p}, \tag{3.19}$$

where $\lambda = \frac{k}{\rho c_p}$ is the thermal diffusivity.

Derivation of radiative flux affecting temperature distribution (energy).

A medium (fluid bulk) is said to be optically dense if some of the light incident rays energy is absorbed by medium, thus result in refracted waves moving at slow speed inside the fluid bulk due to loss in kinetic energy. For such optically dense absorbing and emitting medium, the spectral radiative flux may be determined from

$$\mathbf{q}_\gamma = -\frac{4}{3k_\gamma} \bigtriangledown \sigma E_{b,\gamma}, \tag{3.20}$$

where γ represents different wavelength of electromagnetic waves, k_γ is the radiative conductivity, σ is the scattering coefficient and $E_{b,\gamma}$ is the incident radiation. The above equation represents the general relation for local spectral radiative energy flux in terms of the local emissive power gradient. Since equation (3.20) has the same form as the Fourier heat conduction law for medium that is optically dense for all wavelengths which relates energy and temperature gradient, the radiative heat flux in terms of temperature is given by

$$\mathbf{q}_\gamma = -\frac{4\sigma}{3k_\gamma} \bigtriangledown T^4. \tag{3.21}$$

Based on the flow configuration, radiative heat variation is in the radial $\bar{r}$ and axial $\bar{z}$ - directions respectively, thus

$$\mathbf{q}_\gamma = -\frac{4\sigma}{3k_\gamma}\left[\frac{\partial \bar{T}^4}{\partial \bar{r}} + \frac{\partial \bar{T}^4}{\partial \bar{z}}\right], \tag{3.22}$$

which one can differentiate to get volumetric heating $\dot{q}$.

The radiative heat flux is very small in the z, hence it is negligible. Substituting the radial component of radiative heat flux (3.22) into equation (3.18), yields

$$\frac{\partial \bar{T}}{\partial t} + \bar{u}\frac{\partial \bar{T}}{\partial \bar{z}} + \bar{v}\frac{\partial \bar{T}}{\partial \bar{r}} = \lambda\left[\frac{\partial^2 \bar{T}}{\partial \bar{z}^2} + \frac{1}{\bar{r}}\frac{\partial}{\partial \bar{r}}\left(\bar{r}\frac{\partial \bar{T}}{\partial \bar{r}}\right)\right] - \frac{1}{\rho c_p}\frac{\partial q_r}{\partial \bar{r}}, \tag{3.23}$$

where $\lambda = \frac{k}{\rho c_p}$ is the thermal diffusivity and $q_r = \frac{-4}{3}\frac{\sigma}{k_r}\frac{\partial \bar{T}^4}{\partial \bar{r}}$ is the Rosseland or diffusion approximation for radiation.

Boundary conditions

The appropriate boundary conditions of fluid flow and temperature distribution are defined by the following physical conditions, as given in figure 3.2. We note that for this configuration, the symmetric nature of the flow is taken into account at $\bar{z} = 0$. At the wall, we have

$$\bar{u} = 0, \quad \bar{v} = V_s = -V = -A\dot{a}, \quad \bar{T} = \bar{T}_s, \quad \text{at } \bar{r} = a(t). \tag{3.24}$$

The above conditions arise from the following reasons. Due to no-slip condition there is no axial-velocity, thus $\bar{u} = 0$ at the surface wall, since the velocity closest to wall approximates the velocity of the surface wall. Furthermore the radial velocity $\bar{v}$ is given by $V_s = -V = -A\dot{a}$,

the condition is due to the fact that the surface wall is porous hence fluid can flow in or out of the system. Also the surface wall are kept at a constant temperature, thus $\bar{T} = \bar{T}_s$.

At the centre, we have

$$\frac{\partial \bar{u}}{\partial \bar{r}} = 0, \quad \bar{v} = 0, \quad \frac{\partial \bar{T}}{\partial \bar{r}} = 0 \quad \text{at} \quad \bar{r} = 0. \tag{3.25}$$

Similarly the above are due to the following reasons. The flow is symmetric, thus, posses a parabolic velocity profile. At the centre the axial-velocity is constant and gives the maximum velocity of the fluid due to the parabolic nature of the flow. Also the temperature is minimum at the centre since the fluid serves a coolant and absorb the heat away from the surface wall.

Along the radial axis we have,

$$\bar{u} = 0 \quad \text{at} \quad \bar{z} = 0. \tag{3.26}$$

Since the system is closed at the headwall and the headwall is fixed relative to the chamber axial length, the axial-velocity is zero at $z = 0$.

3.3 Mathematical representation of problem

The two-dimensional flow of an unsteady, incompressible, viscous fluid and heat transfer in a circular semi-infinite pipe is considered. The pipe surface wall is assumed to be porous and is kept at a constant surface wall temperature $\bar{T} = \bar{T}_s$. Also the radius of the pipe $r = a(t)$ varies with time, the coordinate system is chosen to be asymmetric due the parabolic behaviour of flow. The surface pipe wall has the ability to expand or contract uniformly in the radial direction at speed $\dot{a}$. Fluid can be injected or sucked uniformly through the surface wall at the velocity $v_s = -V$ perpendicular to the wall surface and that is proportional to the moving velocity of the surface wall. The current flow parameters do not vary in the transversal direction, thus the transversal component of velocity is taken to be zero and kinematic viscosity is assumed to be constant.

3.3.1 Governing equations and boundary conditions

Mathematical model representing flow and heat transfer during solid rocket motor operation is given by

$$\frac{\partial(\bar{r}\bar{u})}{\partial\bar{z}} + \frac{\partial(\bar{r}\bar{v})}{\partial\bar{r}} = 0, \tag{3.27}$$

$$\frac{\partial\bar{u}}{\partial t} + \bar{u}\frac{\partial\bar{u}}{\partial\bar{z}} + \bar{v}\frac{\partial\bar{u}}{\partial\bar{r}} = -\frac{1}{\rho}\frac{\partial\bar{P}}{\partial\bar{z}} + \nu\left[\frac{\partial^2\bar{u}}{\partial\bar{z}^2} + \frac{1}{\bar{r}}\frac{\partial}{\partial\bar{r}}\left(\bar{r}\frac{\partial\bar{u}}{\partial\bar{r}}\right)\right], \tag{3.28}$$

$$\frac{\partial\bar{v}}{\partial t} + \bar{u}\frac{\partial\bar{v}}{\partial\bar{z}} + \bar{v}\frac{\partial\bar{v}}{\partial\bar{r}} = -\frac{1}{\rho}\frac{\partial\bar{P}}{\partial\bar{r}} + \nu\left[\frac{\partial^2\bar{v}}{\partial\bar{z}^2} + \frac{\partial}{\partial\bar{r}}\left(\frac{1}{\bar{r}}\frac{\partial(\bar{r}\bar{v})}{\partial\bar{r}}\right)\right] + g\beta(\bar{T} - \bar{T}_s), \tag{3.29}$$

$$\frac{\partial\bar{T}}{\partial t} + \bar{u}\frac{\partial\bar{T}}{\partial\bar{z}} + \bar{v}\frac{\partial\bar{T}}{\partial\bar{r}} = \lambda\left[\frac{\partial^2\bar{T}}{\partial\bar{z}^2} + \frac{1}{\bar{r}}\frac{\partial}{\partial\bar{r}}\left(\bar{r}\frac{\partial\bar{T}}{\partial\bar{r}}\right)\right] - \frac{1}{\rho c_p}\frac{\partial q_r}{\partial\bar{r}}, \tag{3.30}$$

where $\bar{u}$ and $\bar{v}$ are the velocity components in the axial $\bar{z}$ and radial $\bar{r}$ directions respectively, and $\bar{T}$ is the temperature. Here, ρ is the fluid density, ν is the kinematic viscosity, k is the thermal conductivity of an incompressible fluid, g is the acceleration due to gravity, β is the coeffcient of thermal expansion, thermal diffusivity is $\lambda = \frac{k}{\rho c_p}$, where c_p is the specific heat, $\bar{P}$ is the pressure, t is time and $q_r = \frac{-4}{3}\frac{\sigma}{k_r}\frac{\partial\bar{T}^4}{\partial\bar{r}}$ is the Rosseland approximation.

The appropriate boundary conditions according to the design and the flow dynamics of a solid rocket motor are as follows:

$$\begin{aligned}
&\text{(i)} \quad \bar{u} = 0, \quad \bar{v} = -\bar{v}_s = -V = -A\dot{a}, \quad \bar{T} = \bar{T}_s \quad \text{at } \bar{r} = a(t),\\
&\text{(ii)} \quad \frac{\partial\bar{u}}{\partial\bar{r}} = 0, \quad \bar{v} = 0, \quad \frac{\partial\bar{T}}{\partial\bar{r}} = 0 \quad \text{at } \bar{r} = 0,\\
&\text{(iii)} \quad \bar{u} = 0 \quad \text{at } \bar{z} = 0.
\end{aligned} \tag{3.31}$$

Since the internal flow is in axial and radial directions, the momentum equation, energy equation and boundary conditions are express in terms of the stream function $\bar{\Psi}$. From the conservation of mass which gives the continuity equation (3.27), there exists a dimensional stream function $\bar{\Psi}(\bar{z}, \bar{r}, t)$ such that

$$\bar{u} = \frac{1}{\bar{r}}\frac{\partial\bar{\Psi}}{\partial\bar{r}}, \qquad \bar{v} = -\frac{1}{\bar{r}}\frac{\partial\bar{\Psi}}{\partial\bar{z}}, \tag{3.32}$$

which satisfies (3.27) identically.

Introducing the dimensionless radial coordinate $r = \bar{r}/a(t)$, equation (3.32) becomes

$$\bar{u} = \frac{1}{a^2 r}\frac{\partial\bar{\Psi}}{\partial r}, \qquad \bar{v} = -\frac{1}{ar}\frac{\partial\bar{\Psi}}{\partial\bar{z}}. \tag{3.33}$$

Substituting (3.33) into (3.28)-(3.29), we obtain the following momentum equations in the axial and radial directions respectively

$$a^2r^2\bar{\Psi}_{rt} - a\dot{a}r^3\bar{\Psi}_{rr} - a\dot{a}r^2\bar{\Psi}_r + r\bar{\Psi}_r\bar{\Psi}_{r\bar{z}} - r\bar{\Psi}_{rr}\bar{\Psi}_{\bar{z}} + \bar{\Psi}_{\bar{z}}\bar{\Psi}_r = -\frac{a^4r^3}{\rho}\bar{P}_{\bar{z}}$$
$$+\nu[a^2r^2\bar{\Psi}_{r\bar{z}\bar{z}} + r^2\bar{\Psi}_{rrr} - r\bar{\Psi}_{rr} + \bar{\Psi}_r], \tag{3.34}$$
$$-a^2r^2\bar{\Psi}_{\bar{z}t} + a\dot{a}r^3\bar{\Psi}_{\bar{z}r} - r\bar{\Psi}_r\bar{\Psi}_{\bar{z}\bar{z}} + r\bar{\Psi}_{\bar{z}}\bar{\Psi}_{\bar{z}r} - (\bar{\Psi}_{\bar{z}})^2 = -\frac{a^2r^3}{\rho}\bar{P}_r$$
$$+\nu[-a^2r^2\bar{\Psi}_{\bar{z}\bar{z}\bar{z}} - r^2\bar{\Psi}_{\bar{z}rr} + r\bar{\Psi}_{\bar{z}r}] + a^3r^3g\beta(\bar{T} - \bar{T}_s), \tag{3.35}$$

where $\dot{a}$ in the above equations denotes the expansion or contraction rate of the solid rocket motor combustion chamber in radial direction.

Similarly the energy equation (3.30) becomes

$$\frac{\partial\bar{T}}{\partial t} + \frac{1}{a^2r}\bar{\Psi}_{\bar{r}}\frac{\partial\bar{T}}{\partial\bar{z}} - \frac{1}{a^2r}\bar{\Psi}_{\bar{z}}\frac{\partial\bar{T}}{\partial r} = \lambda\left[\frac{\partial^2\bar{T}}{\partial\bar{z}^2} + \frac{1}{a^2r}\frac{\partial}{\partial r}\left(r\frac{\partial\bar{T}}{\partial r}\right)\right] - \frac{1}{a\rho c_p}\frac{\partial q_r}{\partial r}. \tag{3.36}$$

The variables in the equations (3.34)-(3.36) are dimensionless according to

$$u = \frac{\bar{u}}{V}, \quad v = \frac{\bar{v}}{V}, \quad z = \frac{\bar{z}}{a(t)}, \bar{t} = \frac{tV}{a}, \tag{3.37}$$
$$\Psi = \frac{\bar{\Psi}}{a^2V}, P = \frac{\bar{P}}{\rho V^2}, \alpha = \frac{a\dot{a}}{\nu}, \Theta = \frac{\bar{T} - \bar{T}_a}{T_w - T_a}.$$

Substituting (3.37) into momentum and energy equations (3.34)-(3.36), yields the following dimensionless system of equations

$$r^2\Psi_{r\bar{t}} + r\Psi_r\Psi_{rz} + \Psi_z[\Psi_r - r\Psi_{rr}] + r^3P_z + \frac{1}{R_e}\Big[(r - \alpha r^3)\Psi_{rr} - r^2\Psi_{rrr} - r^2\Psi_{rzz}$$
$$-(1 + \alpha r^2)\Psi_r\Big] = 0, \tag{3.38}$$
$$r^2\Psi_{z\bar{t}} + r\Psi_r\Psi_{zz} + \Psi_z[\Psi_z - r\Psi_{rz}] - r^3P_r + \frac{1}{R_e}\Big[(r - \alpha r^3)\Psi_{rz} - r^2\Psi_{zrr}$$
$$-r^2\Psi_{zzz}\Big] + r^3G_r\Theta = 0, \tag{3.39}$$
$$\Theta_{\bar{t}} + \frac{1}{r}\Psi_r\Theta_z - \frac{1}{r}\Psi_z\Theta_r - \frac{1}{P_rR_e}\left[\Theta_{zz} + \frac{\Theta_r}{r} + (1 + 4R)\Theta_{rr}\right] = 0, \tag{3.40}$$

where $\alpha = \dfrac{a\dot{a}}{\nu}$ is the wall dilation rate, $R_e = \dfrac{aV_s}{\nu}$ is the permeation Reynolds number, $G_r = \dfrac{a^3g\beta(T_s - T_a)}{\nu^2}$ is the Grashof number, $P_r = \frac{\nu\rho c_p}{k}$ is the Prandtl number and $R = \frac{4\sigma T_a^3}{3k_rk}$ is

the radiation number. Similarly substituting (3.37) into equation (3.33), yields the following dimensionless stream function

$$u = \frac{1}{r}\frac{\partial \Psi}{\partial r}, \qquad v = -\frac{1}{r}\frac{\partial \Psi}{\partial z}. \tag{3.41}$$

Also the dimensionless boundary conditions take the following forms

$$\begin{aligned} &\text{(i)} \quad \Psi_r = 0, \quad \Psi_z = 1, \quad \Theta = 1, \quad \text{at } r = 1, \\ &\text{(ii)} \quad \left(\frac{\Psi_r}{r}\right)_r = 0, \quad \Psi_z = 0, \quad \Theta_r = 0, \quad \text{at } r = 0, \\ &\text{(iii)} \quad \Psi_r = 0 \quad \text{at } z = 0. \end{aligned} \tag{3.42}$$

3.3.2 Parameters influencing the problem at hand

The dynamics of flow and heat transfer depend on the following five dimensionless parameters:

Wall dilation rate

The rate at which the combustion chamber expands or contracts is given by surface wall dilation rate α. This dimensionless parameter can either be positive or negative depending on whether the chamber expands (positive) or contracts (negative). When the rate is zero, the size of the combustion chamber remains unchanged. The surface wall dilation rate is given by

$$\alpha = \frac{a\dot{a}}{\nu}. \tag{3.43}$$

Permeation Reynolds number

Reynolds number is the measure of how fluid flow makes a transition from laminar to turbulent, it a dimensionless quantity which is the ratio of fluids speed at which the fluid enter through the porous surface wall of the pipe and viscosity of the fluid. This quantity is positive when, we inject fluid into the combustion chamber and negative when we suck out fluid from the combustion chamber. It is zero, when no fluid is injected or sucked out of the system. The

above parameter is given by

$$R_e = \frac{aV_s}{\nu}. \tag{3.44}$$

Grashof number

Grashof number is the measure of viscous forces resisting motion as the fluid density decrease or increase due to temperature gradients. It is the ratio of the buoyancy force to viscous force acting on a fluid which given by

$$G_r = \frac{ag\beta(T_s - T_a)}{V_s^2}. \tag{3.45}$$

Representing the surface wall V_s in terms of $\frac{\nu}{a}$, since they are dimensionally compatible, thus we obtain the following

$$G_r = \frac{a^3 g\beta(T_s - T_a)}{\nu^2}. \tag{3.46}$$

Prandtl Number

Prandtl number is the measure of heat transfer between a moving fluid and a solid body given by

$$P_r = \frac{\nu\rho c_p}{k}. \tag{3.47}$$

Radiation Number

Radiation number is the measure of how fluids emits or absorbs heat energy in a form of electromagnetic waves or subatomic particles. Radiation number is given by

$$R = \frac{4\sigma T_a^3}{3k_r k}. \tag{3.48}$$

3.4 Solutions of the problem under investigation

This section uses Lie-group method to derive similarity solutions under which (3.38)-(3.40) and boundary conditions (3.42) remains invariant.

3.4.1 Lie symmetry analysis

We consider the one-parameter (ε) Lie group of infinitesimal transformation in $(\bar{t}, r, z, \Psi, P, \Theta)$ given by

$$\begin{aligned} t^* &= \bar{t} + \varepsilon\tau(\bar{t}, r, z, \Psi, P, \Theta) + 0(\varepsilon^2), \\ r^* &= r + \varepsilon\xi(\bar{t}, r, z, \Psi, P, \Theta) + 0(\varepsilon^2), \\ z^* &= z + \varepsilon\eta(\bar{t}, r, z, \Psi, P, \Theta) + 0(\varepsilon^2), \\ \Psi^* &= \Psi + \varepsilon\phi(\bar{t}, r, z, \Psi, P, \Theta) + 0(\varepsilon^2), \\ P^* &= P + \varepsilon\varphi(\bar{t}, r, z, \Psi, P, \Theta) + 0(\varepsilon^2), \\ \Theta^* &= \Theta + \varepsilon L(\bar{t}, r, z, \Psi, P, \Theta) + 0(\varepsilon^2), \end{aligned} \tag{3.49}$$

with ε as a small parameter. In view of Lie's algorithm, the vector field is

$$X = \tau\frac{\partial}{\partial\bar{t}} + \xi\frac{\partial}{\partial r} + \eta\frac{\partial}{\partial z} + \phi\frac{\partial}{\partial\Psi} + \varphi\frac{\partial}{\partial P} + L\frac{\partial}{\partial\Theta}, \tag{3.50}$$

if it is left invariant by the transformation $(\bar{t}, r, z, \Psi, P, \Theta) \to (t^*, r^*, z^*, \Psi^*, P^*, \Theta^*)$.
The solutions $\Psi = \Psi(z, r, \bar{t})$, $P = P(z, r, \bar{t})$ and $\Theta = \Theta(z, r, \bar{t})$ are invariant under the symmetry if

$$\Phi_\Psi = X(\Psi) = 0, \quad \text{where} \quad \Psi = \Psi(z, r, \bar{t}), \tag{3.51}$$

$$\Phi_P = X(P) = 0, \quad \text{where} \quad P = P(z, r, \bar{t}). \tag{3.52}$$

and

$$\Phi_\Theta = X(\Theta) = 0, \quad \text{where} \quad \Theta = \Theta(z, r, \bar{t}). \tag{3.53}$$

We set

$$\begin{aligned}
\Delta_1 &= r^2\Psi_{r\bar{t}} + r\Psi_r\Psi_{rz} + \Psi_z[\Psi_r - r\Psi_{rr}] + r^3P_z + \frac{1}{R_e}\Big[(r-\alpha r^3)\Psi_{rr} - r^2\Psi_{rrr} \\
&\quad -r^2\Psi_{rzz} - (1+\alpha r^2)\Psi_r\Big], \qquad (3.54)\\
\Delta_2 &= r^2\Psi_{z\bar{t}} + r\Psi_r\Psi_{zz} + \Psi_z[\Psi_z - r\Psi_{rz}] - r^3P_r + \frac{1}{R_e}\Big[(r-\alpha r^3)\Psi_{rz} - r^2\Psi_{zrr} \\
&\quad -r^2\Psi_{zzz}\Big] + r^3G_r\Theta, \qquad (3.55)\\
\Delta_3 &= \Theta_{\bar{t}} + \frac{1}{r}\Psi_r\Theta_z - \frac{1}{r}\Psi_z\Theta_r - \frac{1}{P_rR_e}\Big[\Theta_{zz} + \frac{\Theta_r}{r} + (1+4R)\Theta_{rr}\Big].
\end{aligned}$$

The vector field X given by (3.50) is a symmetry generator of equations (3.38)-(3.40) if and only if

$$X^{[3]}(\Delta_j)\big|_{\Delta_j=0} = 0, \quad j = 1,2,3 \qquad (3.56)$$

in which

$$\begin{aligned}
X^{[3]} &= \tau\frac{\partial}{\partial\bar{t}} + \xi\frac{\partial}{\partial r} + \eta\frac{\partial}{\partial z} + \phi\frac{\partial}{\partial\Psi} + \varphi\frac{\partial}{\partial P} + L\frac{\partial}{\partial\Theta} + \phi^r\frac{\partial}{\partial\Psi_r} + \phi^z\frac{\partial}{\partial\Psi_z} + \varphi^r\frac{\partial}{\partial P_r} \\
&\quad +\varphi^z\frac{\partial}{\partial P_z} + L^r\frac{\partial}{\partial\Theta_r} + L^{\bar{t}}\frac{\partial}{\partial\Theta_{\bar{t}}} + L^z\frac{\partial}{\partial\Theta_z} + \phi^{rz}\frac{\partial}{\partial\Psi_{rz}} + \phi^{r\bar{t}}\frac{\partial}{\partial\Psi_{r\bar{t}}} + \phi^{z\bar{t}}\frac{\partial}{\partial\Psi_{z\bar{t}}} \\
&\quad +\phi^{zz}\frac{\partial}{\partial\Psi_{zz}} + \phi^{rr}\frac{\partial}{\partial\Psi_{rr}} + L^{zz}\frac{\partial}{\partial\Theta_{zz}} + L^{rr}\frac{\partial}{\partial\Theta_{rr}} + \phi^{zzr}\frac{\partial}{\partial\Psi_{zzr}} + \phi^{zrr}\frac{\partial}{\partial\Psi_{zrr}} \\
&\quad +\phi^{zzz}\frac{\partial}{\partial\Psi_{zzz}} + \phi^{rrr}\frac{\partial}{\partial\Psi_{rrr}} \qquad (3.57)
\end{aligned}$$

is the third prolongation of X.

We now introduce the total derivatives by differentiating (3.49) with respect to $\bar{t}, r, z$ and construct

$$\begin{aligned}
D_z &= \partial_z + \Psi_z\partial_\Psi + P_z\partial_P + \Theta_z\partial_\Theta + \Psi_{zz}\partial_{\Psi_z} + P_{zz}\partial_{P_z} + \Theta_{zz}\partial_{\Theta_z} + \Theta_{zr}\partial_{\Theta_r} + \cdots, \\
D_r &= \partial_r + \Psi_r\partial_\Psi + P_r\partial_P + \Theta_r\partial_\Theta + \Psi_{rr}\partial_{\Psi_r} + P_{rr}\partial_{P_r} + \Theta_{rr}\partial_{\Theta_r} + \Theta_{zr}\partial_{\Theta_z} + \cdots, \\
D_{\bar{t}} &= \partial_{\bar{t}} + \Psi_{\bar{t}}\partial_\Psi + P_{\bar{t}}\partial_P + \Theta_{\bar{t}}\partial_\Theta + \Psi_{\bar{t}\bar{t}}\partial_{\Psi_{\bar{t}}} + P_{\bar{t}\bar{t}}\partial_{P_{\bar{t}}} + \Theta_{\bar{t}\bar{t}}\partial_{\Theta_{\bar{t}}} + \Theta_{z\bar{t}}\partial_{\Theta_z} + \cdots \qquad (3.58)
\end{aligned}$$

Since $\tau, \xi, \eta, \phi, \varphi$ and L depend only on t, r, z, ψ, P and Θ and are independent of the derivatives of ψ, P and Θ. We obtain the following determining equation by splitting the resulting

equations from (3.56) on derivatives of ψ, P and Θ:

$$\phi_\Theta = 0, \tag{3.59}$$

$$\varphi_\Theta = 0, \tag{3.60}$$

$$\tau_\Theta = 0, \tag{3.61}$$

$$\xi_\Theta = 0, \tag{3.62}$$

$$\eta_\Theta = 0, \tag{3.63}$$

$$L_{\Theta\Theta} = 0, \tag{3.64}$$

$$\phi_p = 0, \tag{3.65}$$

$$L_p = 0, \tag{3.66}$$

$$\tau_p = 0, \tag{3.67}$$

$$\xi_p = 0, \tag{3.68}$$

$$\eta_p = 0, \tag{3.69}$$

$$L_\psi = 0, \tag{3.70}$$

$$\tau_\psi = 0, \tag{3.71}$$

$$\xi_\psi = 0, \tag{3.72}$$

$$\eta_\psi = 0, \tag{3.73}$$

$$\phi_{\psi\psi} = 0, \tag{3.74}$$

$$L_z = 0, \tag{3.75}$$

$$\tau_z = 0, \tag{3.76}$$

$$\xi_z = 0, \tag{3.77}$$

$$\phi_{z\psi} = 0, \tag{3.78}$$

$$\eta_{zz} = 0, \tag{3.79}$$

$$L_r = 0, \tag{3.80}$$

$$\tau_r = 0, \tag{3.81}$$

$$\eta_r = 0, \tag{3.82}$$

$$\phi_{r\psi} = 0, \tag{3.83}$$

$$\frac{1}{R_e}(r\xi + r^2\varphi_p - r^2\phi_\psi + r^2\eta_z + r^3\xi_r) = 0, \tag{3.84}$$

$$\frac{1}{R_e}(r\xi + r^2\varphi_p - r^2\phi_\psi - r^2\eta_z + 3r^3\xi_r) = 0, \tag{3.85}$$

$$-2\xi - r\varphi_p + 2r\phi_\psi - 2r\xi_r = 0, \tag{3.86}$$

$$2\xi + r\varphi_p - 2r\phi_\psi + 2r\xi_r = 0, \tag{3.87}$$

$$-r\xi - r^2\varphi_p + r^2\phi_\psi + r^2\eta_z - r^2\xi_r - r^2\tau_{\bar{t}} = 0, \tag{3.88}$$

$$[3(r^2\alpha - 1) + (1 - 3r^2\alpha)]\xi + (r^3\alpha - r)\varphi_p + (r - \alpha r^3)\phi_\psi$$

$$(r - r^3\alpha)\eta_z - 2(r - r^3\alpha)\xi_r + 3r^2\xi_{rr} - R_e r\phi_z + R_e r^2\xi_{\bar{t}} = 0, \tag{3.89}$$

$$r\phi_r - r^2\eta_{\bar{t}} = 0, \tag{3.90}$$

$$-\frac{3\xi}{r} - \varphi_p + 2\phi_\psi - \xi_r + r\xi_{rr} = 0, \tag{3.91}$$

$$R_e r^3\varphi_z + (-1 - r^2\alpha)\phi_r - r^2\phi_{rzz} + (r - r^3\alpha)\phi_{rr} - r^2\phi_{rrr} + R_e r^2\phi_{\bar{t}r} = 0, \tag{3.92}$$

$$\Big(\frac{3}{r} + r\alpha\Big)\xi + (1 + r^2\alpha)\varphi_p - (1 + r^2\alpha)\phi_\psi - (1 + r^2\alpha)\eta_z + (1 + r^2\alpha)\xi_r \tag{3.93}$$

$$+(1 + r^2\alpha)\xi_r + (r + r^3\alpha)\xi_{rr} + r^3\xi_{rrr} + R_e\phi_z + R_e r\phi_{rz} + R_e r^2\phi_{\bar{t}\psi} - R_e r^2\xi_{\bar{t}r} = 0,$$

$$r^3\varphi_\psi + \phi_r - r\phi_{rr} = 0, \tag{3.94}$$

$$\frac{1}{R_e}(-2r^2\eta_z + 2r^2\xi_r) = 0, \tag{3.95}$$

$$-r\xi + r\phi_\psi + r\eta_z - r\xi_r = 0, \tag{3.96}$$

$$\xi - r\phi_\psi - r\eta_z + r\xi_r = 0, \tag{3.97}$$

$$-r^2\xi - r^3\varphi_p + r^3\phi_\psi - 3r^3\eta_z + r^3\xi_r = 0, \tag{3.98}$$

$$2r^2\eta_z - r^2\tau_{\bar{t}} = 0, \tag{3.99}$$

$$[(2r^2\alpha - 2) + (1 - 3r^2\alpha)]\xi + [(r^3\alpha - r) + (r - r^3\alpha)]\phi_\psi + [(3r - 3r^3\alpha)$$

$$+(-r + r^3\alpha)]\eta_z - R_e r\phi_z + [-r + r^3\alpha]\xi_r + r^2\xi_{rr} - R_e r^2\xi_{\bar{t}} = 0, \tag{3.100}$$

$$r\phi_r - r^2\eta_{\bar{t}} = 0, \tag{3.101}$$

$$\frac{-2\xi}{r} + \phi_\psi + \eta_z = 0, \tag{3.102}$$

$$r^3 G_r R_e L + r^2 G_r R_e \Theta\xi - r^3 G_r R_e \Theta\phi_\psi + 3r^3 G_r R_e \Theta\eta_z$$

$$-r^2\phi_{zzz} - r^3 R_e\varphi_r + (r - r^3\alpha)\phi_{rz} - r^2\phi_{rrz} + R_e r^2\phi_{\bar{t}z} = 0, \tag{3.103}$$

$$-r^3\varphi_\psi + r\phi_{zz} = 0, \tag{3.104}$$

$$2\phi_z - r\phi_{rz} + r^2\phi_{\bar{t}\psi} - r^2\eta_{\bar{t}z} = 0, \tag{3.105}$$

$$\frac{\xi}{r^2} + \frac{\phi_\psi}{r} + \frac{\eta_z}{r} - \frac{\xi_r}{r} = 0, \tag{3.106}$$

$$\frac{\xi}{r^2} - \frac{\phi_\psi}{r} - \frac{\eta_z}{r} + \frac{\xi_r}{r} = 0, \tag{3.107}$$

$$\frac{1}{P_r R_e}\big(1 + 4R\big)L_\Theta + \frac{1}{P_r R_e}\big(-2 - 8R\big)\eta_z + L_{\bar{t}} = 0, \tag{3.108}$$

$$2\eta - \tau_{\bar{t}} = 0, \tag{3.109}$$

$$\frac{\xi}{r^2 R_e P_r} - \frac{2\eta_z}{r R_e P_r} - \frac{\phi_z}{r} + \frac{\xi_r}{r R_e P_r} - \xi_{\bar{t}} = 0, \tag{3.110}$$

$$\frac{\phi_r}{r} - \eta_{\bar{t}} = 0. \tag{3.111}$$

From equation (3.59-3.64), we obtain

$$\phi = a(\bar{t}, r, z, \psi, P), \tag{3.112}$$

$$\varphi = b(\bar{t}, r, z, \psi, P), \tag{3.113}$$

$$\tau = c(\bar{t}, r, z, \psi, P), \tag{3.114}$$

$$\xi = d(\bar{t}, r, z, \psi, P), \tag{3.115}$$

$$\eta = e(\bar{t}, r, z, \psi, P), \tag{3.116}$$

$$L = f(\bar{t}, r, z, \psi, P) + \Theta g(\bar{t}, r, z, \psi, P) \tag{3.117}$$

where $a(\bar{t}, r, z, \psi, P), b(\bar{t}, r, z, \psi, P), c(\bar{t}, r, z, \psi, P), d(\bar{t}, r, z, \psi, P), e(\bar{t}, r, z, \psi, P)$, $f(\bar{t}, r, z, \psi, P)$ and $g(\bar{t}, r, z, \psi, P)$ is an arbitrary functions of $\bar{t}, r, z, \psi$ and P. Substituting (3.117) into (3.66) and splitting on powers of Θ, we obtain

$$\Theta \;:\; f(\bar{t}, r, z, \psi, P)_P = 0, \tag{3.118}$$

$$1 \;:\; g(\bar{t}, r, z, \psi, P)_P = 0. \tag{3.119}$$

Integrating (3.118) and (3.119) with respect to P, gives

$$f = f_1(\bar{t}, r, z, \psi), \tag{3.120}$$

$$g = g_1(\bar{t}, r, z, \psi), \tag{3.121}$$

where f_1 and g_1 are arbitrary functions of $\bar{t}, r, z$ and ψ. Thus the value of L becomes

$$L = f_1(\bar{t}, r, z, \psi) + \Theta g_1(\bar{t}, r, z, \psi). \tag{3.122}$$

Now substituting (3.112) and (3.114-3.116) into equations (3.65) and (3.67)-(3.69), upon solving the resulting equations, we get

$$a = a_1(\bar{t}, r, z, \psi), \tag{3.123}$$

$$c = c_1(\bar{t}, r, z, \psi), \tag{3.124}$$

$$d = d_1(\bar{t}, r, z, \psi), \tag{3.125}$$

$$e = e_1(\bar{t}, r, z, \psi), \tag{3.126}$$

where a_1, c_1, d_1 and e_1 are arbitrary functions of $\bar{t}, r, z$ and ψ. Thus the values of ϕ, τ, ξ and η becomes

$$\phi = a_1(\bar{t}, r, z, \psi), \tag{3.127}$$

$$\tau = c_1(\bar{t}, r, z, \psi), \tag{3.128}$$

$$\xi = d_1(\bar{t}, r, z, \psi), \tag{3.129}$$

$$\eta = e_1(\bar{t}, r, z, \psi). \tag{3.130}$$

Substituting (3.122) into (3.70) and splitting on powers of Θ, we obtain

$$\Theta : f_1(\bar{t}, r, z, \psi)_\psi = 0, \tag{3.131}$$

$$1 : g_1(\bar{t}, r, z, \psi)_\psi = 0. \tag{3.132}$$

Integrating (3.131) and (3.132) with respect to ψ, yields

$$f = f_2(\bar{t}, r, z), \tag{3.133}$$

$$g = g_2(\bar{t}, r, z), \tag{3.134}$$

where f_2 and g_2 arbitrary functions of $\bar{t}, r$ and z. Thus the value of L becomes

$$L = f_2(\bar{t}, r, z) + \Theta g_2(\bar{t}, r, z). \tag{3.135}$$

Substituting (3.127)-(3.130) into (3.71)-(3.74) and solving the obtained equations, yields

$$\begin{aligned} a_1 &= a_2(\bar{t}, r, z) + \psi a_3(\bar{t}, r, z), && (3.136)\\ c_1 &= c_2(\bar{t}, r, z), && (3.137)\\ d_2 &= d_2(\bar{t}, r, z), && (3.138)\\ e_1 &= e_2(\bar{t}, r, z), && (3.139) \end{aligned}$$

where a_2, a_3, c_2, d_2 and e_2 are arbitrary functions of $\bar{t}, r$ and z. Thus the values of ϕ, τ, ξ and η become

$$\begin{aligned} \phi &= a_2(\bar{t}, r, z) + \psi a_3(\bar{t}, r, z), && (3.140)\\ \tau &= c_2(\bar{t}, r, z), && (3.141)\\ \xi &= d_2(\bar{t}, r, z), && (3.142)\\ \eta &= e_2(\bar{t}, r, z). && (3.143) \end{aligned}$$

Using (3.140) and (3.143) into (3.111), yields the following equation

$$a_2(\bar{t}, r, z)_r + \psi a_3(\bar{t}, r, z)_r - r e_2(\bar{t}, r, z)_{\bar{t}} = 0. \tag{3.144}$$

Splitting on powers of ψ from equation (3.144) above, yields

$$\begin{aligned} \psi &: a_3(\bar{t}, r, z)_r = 0, && (3.145)\\ 1 &: a_2(\bar{t}, r, z)_r - r e_2(\bar{t}, r, z)_{\bar{t}} = 0. && (3.146) \end{aligned}$$

Solving for (3.145), we get

$$a_3 = a_4(\bar{t}, z), \tag{3.147}$$

where a_4 is an arbitrary function of $\bar{t}$ and z, as a result ϕ becomes

$$\phi = a_2(\bar{t}, r, z) + \psi a_4(\bar{t}, z). \tag{3.148}$$

Using (3.141), (3.142) and (3.143) into (3.76), (3.77) and (3.79) and solving the resulting equations respectively, yields

$$c_2 = c_3(\bar{t}, r), \tag{3.149}$$

$$d_2 = d_3(\bar{t}, r), \tag{3.150}$$

$$e_2 = e_3(\bar{t}, r) + ze_4(\bar{t}, r), \tag{3.151}$$

where c_3, d_3, e_3 and e_4 are arbitrary functions of $\bar{t}$ and r. Thus the value of τ, ξ and η takes the form

$$\tau = c_3(\bar{t}, r), \tag{3.152}$$

$$\xi = d_3(\bar{t}, r), \tag{3.153}$$

$$\eta = e_3(\bar{t}, r) + ze_4(\bar{t}, r), \tag{3.154}$$

where c_3, d_3, e_3 and e_4 are arbitrary functions of t and r. Thus (3.146) becomes

$$a_2(\bar{t}, r, z)_r - r[e_3(\bar{t}, r)_{\bar{t}} + ze_4(\bar{t}, r)_{\bar{t}}] = 0. \tag{3.155}$$

Now substituting (3.135) into (3.75) and splitting on powers of Θ, yields

$$\Theta : f_2(\bar{t}, r, z)_z = 0, \tag{3.156}$$

$$1 : g_2(\bar{t}, r, z)_z = 0. \tag{3.157}$$

Integrating (3.156) and (3.157) with respect to z respectively, yields

$$f_2 = f_3(\bar{t}, r), \tag{3.158}$$

$$g_2 = g_3(\bar{t}, r), \tag{3.159}$$

where f_3 and g_3 are arbitrary functions of t and r respectively. Thus the value of L becomes

$$L = f_3(\bar{t}, r) + \Theta g_3(\bar{t}, r). \tag{3.160}$$

Substituting (3.148) into (3.78) and thereafter solving the result, yields

$$a_4 = a_5(\bar{t}), \tag{3.161}$$

where a_5 is an arbitrary function of $\bar{t}$. Thus the value of ϕ becomes

$$\phi = a_2(\bar{t}, r, z) + \psi a_5(\bar{t}). \tag{3.162}$$

By substituting (3.113) and (3.162) into (3.104) and solving for b from the resulting equation, yields

$$b = b_1(\bar{t}, r, z, P) + \frac{\psi a_2(\bar{t}, r, z)_{zz}}{r^2}, \tag{3.163}$$

where b_1 is an arbitrary function of $\bar{t}, r$ and z. Thus φ becomes

$$\varphi = b_1(\bar{t}, r, z, P) + \frac{\psi a_2(\bar{t}, r, z)_{zz}}{r^2}. \tag{3.164}$$

Using the result from (3.152) into (3.81) and solving the resulting equation, yields

$$c_3 = c_4(\bar{t}), \tag{3.165}$$

where c_4 is a arbitrary function of $\bar{t}$. Thus the value of τ becomes

$$\tau = c_4(\bar{t}). \tag{3.166}$$

Using (3.160) into (3.80) and splitting on powers of Θ, we get

$$\Theta \quad : \quad f_3(\bar{t}, r)_r = 0, \tag{3.167}$$

$$1 \quad : \quad g_3(\bar{t}, r)_r = 0. \tag{3.168}$$

Integrating (3.167) and (3.168) with respect to r, yields

$$f_3 = f_4(\bar{t}), \tag{3.169}$$

$$g_3 = g_4(\bar{t}), \tag{3.170}$$

where the f_4 and g_4 are arbitrary functions of t. Thus the value of L becomes

$$L = f_4(\bar{t}) + \Theta g_4(\bar{t}). \tag{3.171}$$

Now substituting equations (3.154) and (3.171) into equation (3.108), yields the power of Θ as

$$\Theta \quad : \quad g_4'(\bar{t}) = 0, \tag{3.172}$$

$$1 \quad : \quad f_4'(\bar{t}) + \big(\frac{1}{R_e P_r} + \frac{4R}{R_e P_r}\big) g_4(\bar{t}) + \big(\frac{-2}{R_e P_r} - \frac{8R}{R_e P_r}\big) e_4(\bar{t}, r) = 0. \tag{3.173}$$

Solving (3.172), yields

$$g_4(\bar{t}) = g_5 \tag{3.174}$$

where g_5 is a constant. Thus the value of L becomes

$$L = f_4(\bar{t}) + \Theta g_5. \tag{3.175}$$

Substituting (3.153), (3.162) and (3.164) into equation (3.86) and solving for b_1 yields

$$b_1 = b_2(\bar{t}, r, z) - \frac{2P(d_3(\bar{t}, r) - ra_5(\bar{t}) + rd_3(\bar{t}, r)_r)}{r}, \tag{3.176}$$

where b_2 is an arbitrary function of t, r and z, thus the value of φ becomes the following

$$\varphi = b_2(\bar{t}, r, z) - \frac{2P(d_3(\bar{t}, r) - ra_5(\bar{t}) + rd_3(\bar{t}, r)_r)}{r} + \frac{\psi a_2(\bar{t}, r, z)_{zz}}{r^2}. \tag{3.177}$$

Substituting (3.154) into (3.82) and splitting the result on powers of z, yields

$$z \;:\; e_3(\bar{t}, r)_r = 0, \tag{3.178}$$

$$1 \;:\; e_4(\bar{t}, r)_r = 0. \tag{3.179}$$

Integrating and (3.178) and (3.179) with respect to r, yields

$$e_3 = e_5(\bar{t}), \tag{3.180}$$

$$e_4 = e_6(\bar{t}), \tag{3.181}$$

where e_5 and e_6 are arbitrary functions of $\bar{t}$. Thus the value of η takes the form

$$\eta = e_5(\bar{t}) + ze_6(\bar{t}). \tag{3.182}$$

Also the equation (3.155) becomes

$$a_2(\bar{t}, r, z)_r - r[e_5(\bar{t})_{\bar{t}} + ze_4(\bar{t})_{\bar{t}}] = 0. \tag{3.183}$$

Using (3.153) and (3.182) into equation (3.95) and thereafter solving for d_3, yields

$$d_3 = d_4(\bar{t}) + re_6(\bar{t}), \tag{3.184}$$

where d_4 is an arbitrary function of $\bar{t}$. Thus the value of ξ becomes

$$\xi = d_4(\bar{t}) + re_6(\bar{t}). \tag{3.185}$$

Using the value of d_3 from equation (3.184) into equation (3.177), yields

$$\varphi = b_2(\bar{t}, r, z) - \frac{2P(d_4(\bar{t}) + re_6(\bar{t}) - ra_5(\bar{t}) + e_6(\bar{t}))}{r} + \frac{\psi a_2(\bar{t}, r, z)_{zz}}{r^2}. \tag{3.186}$$

Now substituting (3.162) and (3.182) into (3.101) and solving for a_2, gives

$$a_2 = a_6(\bar{t}, z) + \frac{r^2}{2}\big[e_5'(\bar{t}) + ze_6'(\bar{t})\big], \tag{3.187}$$

where a_6 is an arbritary function of $\bar{t}$ and r, thus the value of ϕ becomes

$$\phi = a_6(\bar{t}, z) + \frac{r^2}{2}(e_5'(t) + ze_6'(\bar{t})) + \psi a_5(\bar{t}). \tag{3.188}$$

Using the value of a_2 from equation (3.187) into (3.186), we get

$$\varphi = b_2(\bar{t}, r, z) - \frac{2P(d_4(\bar{t}) + re_6(\bar{t}) - ra_5(\bar{t}) + e_6(\bar{t}))}{r} + \frac{\psi a_6(\bar{t}, z)_{zz}}{r^2}. \tag{3.189}$$

Substituting (3.182), (3.185) and (3.188) into (3.97) and splitting the resulting equation on powers of r, yields

$$r \;:\; d_4(\bar{t}) = 0, \tag{3.190}$$

$$1 \;:\; e_6(\bar{t}) = a_5(\bar{t}). \tag{3.191}$$

Thus values of ξ, ϕ, η and φ become

$$\xi = ra_5(\bar{t}), \tag{3.192}$$

$$\phi = a_6(\bar{t}, z) + \frac{r^2}{2}(e_5'(\bar{t}) + za_5'(\bar{t})) + \psi a_5(\bar{t}), \tag{3.193}$$

$$\eta = e_5(\bar{t}) + za_5(\bar{t}), \tag{3.194}$$

$$\varphi = b_2(\bar{t}, r, z) - \frac{2P(a_5(\bar{t}))}{r} + \frac{\psi a_6(\bar{t}, z)_{zz}}{r^2}. \tag{3.195}$$

By using (3.192), (3.193) and (3.194) into (3.110) and thereafter solving for a_6, we obtain

$$a_6 = a_7(\bar{t}) - z\frac{3}{2}r^2 a_5'(\bar{t}), \tag{3.196}$$

where a_7 is an abitrary function of $\bar{t}$. Using the value of a_6 from (3.196) into equation (3.195), we obtain

$$\varphi = b_2(\bar{t}, r, z) - \frac{2Pa_5(\bar{t})}{r}. \tag{3.197}$$

Also the value for ϕ becomes

$$\phi = a_7(\bar{t}) - z\frac{3}{2}r^2 a_5'(\bar{t}) + \frac{r^2}{2}(e_5'(\bar{t}) + z a_5'(\bar{t})) + \psi a_5(\bar{t}). \tag{3.198}$$

Using (3.194) and (3.198) into equation (3.105), thereafter solving for a_5, yields

$$a_5(\bar{t}) = a_8. \tag{3.199}$$

where a_6 is an arbitrary constant. Thus the values of ϕ, η, ξ and φ becomes

$$\xi = r a_8, \tag{3.200}$$

$$\phi = a_7(\bar{t}) + \frac{r^2}{2}e_5'(\bar{t}) + \psi a_8, \tag{3.201}$$

$$\eta = e_5(\bar{t}) + z a_8, \tag{3.202}$$

$$\varphi = b_2(\bar{t}, r, z) - \frac{2P a_8}{r}. \tag{3.203}$$

Using (3.166) and (3.202) into (3.109) and thereafter integrating yields

$$c_4(\bar{t}) = c_5 + 2\bar{t}a_8, \tag{3.204}$$

where c_5 is an arbitrary constant. Thus τ becomes

$$\tau = c_5 + 2\bar{t}a_8. \tag{3.205}$$

Using ξ, ϕ, η and L into (3.103) and splitting on powers of Θ, gives

$$\Theta \;:\; r^3 f_4(\bar{t}) - r^3 b_2(\bar{t}, r, z)_r = 0, \tag{3.206}$$

$$1 \;:\; r^3 G_r g_5 + 3r^3 G_r a_8 = 0. \tag{3.207}$$

Solving for b_2 from equation (3.206) and making g_5 subject of the formula from equation (3.207) respectively, yields

$$b_2 = b_3(\bar{t}, z) + r G_r f_4(\bar{t}), \tag{3.208}$$

$$g_5 = -3a_8. \tag{3.209}$$

Thus L and φ take the form

$$\varphi = b_3(\bar{t}, z) + r G_r f_4(\bar{t}) - \frac{2P(a_8)}{r}, \tag{3.210}$$

$$L = f_4(\bar{t}) - 3\Theta a_8. \tag{3.211}$$

Solving for f_4 from (3.173), we get

$$f_4(\bar{t}) = f_5 + \frac{5\bar{t}(a_8 + 4Ra_8)}{P_r R_e}, \tag{3.212}$$

where f_5 is an arbitrary constant. Using f_4 from equation (3.212), the value of φ is now given by

$$\varphi = b_3(\bar{t}, z) + rG_r\left(f_5 + \frac{5\bar{t}(a_8 + 4Ra_8)}{P_r R_e}\right) - \frac{2P(a_8)}{r}. \tag{3.213}$$

Substituting (3.200)-(3.202) and (3.210) into (3.93) and solving for b_3 from the obtained equation, yields

$$b_3(\bar{t}) = b_4(\bar{t}) + \frac{z(2\alpha e_5'(\bar{t}) - R_e e_5''(\bar{t}))}{R_e}. \tag{3.214}$$

where b_4 is an arbritary function of $\bar{t}$, thus the value for φ becomes

$$\varphi = b_4(\bar{t}) + \frac{z(2\alpha e_5'(\bar{t}) - R_e e_5''(\bar{t}))}{R_e} + rG_r\left(f_5 + \frac{5\bar{t}(a_8 + 4Ra_8)}{P_r R_e}\right) - \frac{2P(a_8)}{r}. \tag{3.215}$$

Substituting the values from (3.200), (3.201) and (3.202) into (3.100), yields

$$a_8 = 0. \tag{3.216}$$

Thus the values of $\xi, \eta, \varphi, \phi, \tau$ and L satisfying equations (3.59)-(3.111) are given

$$\xi = 0, \tag{3.217}$$

$$\tau = c_5, \tag{3.218}$$

$$L = f_5, \tag{3.219}$$

$$\varphi = b_4(\bar{t}) + \frac{z(2\alpha e_5'(\bar{t}) - R_e e_5''(\bar{t}))}{R_e} + rG_r f_5, \tag{3.220}$$

$$\phi = a_7(\bar{t}) + \frac{r^2}{2} e_5'(\bar{t}), \tag{3.221}$$

$$\eta = e_5(\bar{t}). \tag{3.222}$$

The system of equations (3.59)-(3.111) has the following five Lie symmetries

$$\begin{aligned} &X_1 = (2zK\alpha e_5'(\bar{t}) - z e_5''(\bar{t}))\frac{\partial}{\partial P} + \frac{r^2}{2} e_5'(\bar{t})\frac{\partial}{\partial \Psi} - z\frac{\partial}{\partial z}, \quad X_2 = \frac{\partial}{\partial \bar{t}}, \\ &X_3 = a_7(\bar{t})\frac{\partial}{\partial \Psi}, \quad X_4 = b_4(\bar{t})\frac{\partial}{\partial P}, \quad X_5 = rG_r\frac{\partial}{\partial P} + \frac{\partial}{\partial \Theta}. \end{aligned} \tag{3.223}$$

3.4.2 Invariant solutions

This subsection uses Lie group symmetries that leave the dynamics of propellant flow, temperature distribution and boundary conditions during solid rocket motor operation unchanged. When calculating invariant solutions under the group generators, X_2 is the only symmetry that preserve the steady state dynamics of the system of equations representing the phenomenon and the boundary conditions. Thus

from X_2, the characteristic $\Phi = (\Phi_\Psi, \Phi_P, \Phi_\Theta)$ shows that stream function, pressure and temperature do not vary with time, thus

$$\Phi_\Psi = -\Psi_{\bar{t}}, \quad \Phi_P = -P_{\bar{t}}, \quad \Phi_\Theta = -\Theta_{\bar{t}}.$$

Therefore, the steady state solutions according to the invariant conditions (3.51)-(3.53) are given by

$$\Psi = h(r)H(z,r), \qquad P = \Gamma(z,r), \qquad \Theta = \omega(z,r), \tag{3.224}$$

which gives the steady state operation of a solid rocket motor.

Substituting (3.224) into (3.38) and letting $K = \frac{1}{R_e}$ yields

$$\begin{aligned}
&-r^2K\frac{d^3h}{dr^3} + \left[-rhH_z + Kr - \alpha Kr^3 - 3Kr^2\frac{H_r}{H}\right]\frac{d^2h}{dr^2}\\
&+\left[hH_z - rh\frac{H_zH_r}{H} + 2K(r-\alpha r^3)\frac{H_r}{H} - 3Kr^2\frac{H_{rr}}{H} - Kr^2\frac{H_{zz}}{H} - K - \alpha Kr^2 + rhH_{rz}\right]\frac{dh}{dr}\\
&+rH_z\left(\frac{dh}{dr}\right)^2 + \left[K(r-\alpha r^3)\frac{H_{rr}}{H} - Kr^2\frac{H_{rrr}}{H} - Kr^2\frac{H_{rzz}}{H} - K(1+\alpha r^2)\frac{H_r}{H}\right]\\
&+\left[r\frac{H_rH_{rz}}{H} + \frac{H_rH_z}{H} - r\frac{H_zH_{rr}}{H}\right]h^2 + \frac{r^3}{H}\frac{\partial\Gamma}{\partial z} = 0.
\end{aligned} \tag{3.225}$$

Simplifying the above equation, we obtain

$$\begin{aligned}
&-r^2K\frac{d^3h}{dr^3} + \left[-rhK_1 + Kr - \alpha Kr^3 - 3Kr^2K_2\right]\frac{d^2h}{dr^2}\\
&+\left[hK_1 - rhK_3 + 2K(r-\alpha r^3)K_2 - 3Kr^2K_5 - Kr^2K_4 - K - \alpha Kr^2 + rhK_8\right]\frac{dh}{dr}\\
&+rK_1\left(\frac{dh}{dr}\right)^2 + \left[K(r-\alpha r^3)K_5 - Kr^2K_7 - Kr^2K_6 - K(1+\alpha r^2)K_2\right]h\\
&+\left[rK_9 + K_3 + rK_{10}\right]h^2 + \frac{r^3}{H}\frac{\partial\Gamma}{\partial z} = 0
\end{aligned} \tag{3.226}$$

by taking

$$K_1 = H_z, \quad K_2 = \frac{H_r}{H}, \quad K_3 = \frac{H_z H_r}{H}, \quad K_4 = \frac{H_{zz}}{H}, \quad K_5 = \frac{H_{rr}}{H}, \quad K_6 = \frac{H_{rzz}}{H},$$
$$K_7 = \frac{H_{rrr}}{H}, \quad K_8 = H_{rz}, \quad K_9 = \frac{H_r H_{rz}}{H}, \quad K_{10} = \frac{H_z H_{rr}}{H}. \tag{3.227}$$

Since h is function of a single variable r, whereas H and Γ are functions of both z and r. To make equation (3.226) a function of r, set K_i, i = 0,1,2...,10, to be a constants or function of r only by setting the derivatives of H to yield constant or function of r only.

Integrating the function $K_1 = H_z$ from (3.227) with respect to z, gives

$$H(z, r) = zK_1(r) + K_{11}(r). \tag{3.228}$$

Thus by using the above value of $H(z, r)$, the stream function from (3.224) becomes

$$\Psi = (zK_1(r) + K_{11}(r))h(r). \tag{3.229}$$

Differentiating the stream function (3.229) with respect to r and using the boundary condition of the stream function from (3.42) (iii), yields

$$K_{11}(r)h(r) = K_{12}, \tag{3.230}$$

where K_{12} is an integration constant.

Using the value of the above integration constant K_{12} from (3.230), the stream function (3.229) becomes

$$\Psi = zG(r) + K_{12}, \tag{3.231}$$

where $G(r) = K_1(r)h(r)$.

Substitution the steady state pressure $P = \Gamma(r, z)$ from (3.224) and stream function (3.231) into (3.38), yields

$$r^3 \frac{\partial \Gamma}{\partial z} = z\Bigg[\Big\{(1 + \alpha r^2)K - G\Big\}\frac{dG}{dr} + \Big\{rG - (r - \alpha r^3)K\Big\}\frac{d^2G}{dr^2}$$
$$-r\left(\frac{dG}{dr}\right)^2 + r^2 K \frac{d^3G}{dr^3}\Bigg]. \tag{3.232}$$

Using (3.228) and (3.232) into (3.226), yields

$$K_{11} = 0. \tag{3.233}$$

Substituting the value of K_{11} into (3.228), one obtains

$$H(z, r) = zK_1(r). \tag{3.234}$$

Also when K_{11} is zero, $K_{12} = 0$ from (3.230), thus the stream function (3.231) becomes

$$\Psi = zG(r). \tag{3.235}$$

Using the stream function (3.235) into (3.41) yields the axial and radial components of the propellant velocity inside the combustion chamber as follows

$$\frac{u}{z} = \frac{1}{r}\frac{dG}{dr} \quad \text{and} \quad v = -\frac{G}{r} \tag{3.236}$$

respectively. It can be noted that the flow is laminar since both the radial-velocity and axial-velocity per length z, are functions of r. These components show that the axial-velocity per length z varies with respect to r only while the radial component indicates that the propellant injection through the chamber surface wall is a function of r.

Using the stream function (3.235) and the value of steady state temperature from equation (3.224) into (3.39) and thereafter differentiating the resulting equation with respect to z, one arrives at the following result

$$P_{rz} = G_r\omega_z. \tag{3.237}$$

Substituting the stream function (3.235) into momentum equation along the axial direction (3.38) and thereafter differentiating the resulting momentum equation with respect to r and using pressure variation (3.237), we obtain

$$\begin{aligned} &K\left[r^2\frac{d^4G}{dr^4} + (\alpha r^3 - 2r)\frac{d^3G}{dr^3} + (\alpha r^2 + 3)\frac{d^2G}{dr^2} - \left(\alpha r + \frac{3}{r}\right)\frac{dG}{dr}\right] - r\frac{dG}{dr}\frac{d^2G}{dr^2} \\ &+\left(\frac{dG}{dr}\right)^2 - 3G\frac{d^2G}{dr^2} + \frac{3}{r}G\frac{dG}{dr} + rG\frac{d^3G}{dr^3} - \frac{r^3G_r\omega_z}{z} = 0. \end{aligned} \tag{3.238}$$

Differentiating the above equation twice with respect to z, gives

$$r^3G_r\omega_{zzz} = 0. \tag{3.239}$$

According to the dynamics of the propellant flow, there is bouyancy effects due to temperature difference and the radius cannot be zero, thus G_r and r^3 are non-zero variables. Therefore $\omega_{zzz} = 0$, which gives

$$\omega_{zz} = F_1(r), \tag{3.240}$$

where $F_1(r)$ is a function of r. Integrating (3.240) again, we obtain

$$\theta_z = zF_1(r) + F_2(r), \tag{3.241}$$

where $F_2(r)$ is a function of r. The system design is such that there is no heat transfer at the headwall (the headwall is insulated), thus at $z = 0$ temperature change $\omega_z = 0$, thus (3.241) yields $F_2(r) = 0$. Hence temperature difference per length of the combustion chamber is given by

$$\frac{\omega_z}{z} = F_1(r), \tag{3.242}$$

which shows that the temperature changes along the axial direction z of the combustion chamber does not change along the length of the combustion chamber. According to equation (3.242), temperature from the surface of the rocket chamber affects the propellant in the r-direction only, thus there is no temperature diffusion in the z-direction. This dynamics implies that $\frac{\omega_{zz}}{z} = 0$.

Taking in account the fact that there is no heat diffusion in the axial direction and setting temperature difference $F_1(r) = H(r)$ from equation (3.242), thereafter using both velocity components (3.236) and temperature difference (3.242) into (3.238) and (3.40) and invoking $\frac{r^2}{2} = \beta$, momentum and energy equations become

$$K\left[2\beta\frac{d^4G}{d\beta^4} + (2\alpha\beta + 4)\frac{d^3G}{d\beta^3} + 4\alpha\frac{d^2G}{d\beta^2}\right] + G\frac{d^3G}{d\beta^3} - \frac{dG}{d\beta}\frac{d^2G}{d\beta^2} - \frac{HG_r}{\sqrt{2\beta}} = 0, \tag{3.243}$$

$$\frac{dG}{d\beta}H - \frac{G}{2}\frac{dH}{d\beta} - \frac{K}{P_r}\left[\frac{dH}{d\beta} + \beta\frac{dH^2}{d\beta^2}\right] - \frac{2RK}{P_r}\left[\frac{dH}{d\beta} + 2\beta\frac{dH^2}{d\beta^2}\right] = 0. \tag{3.244}$$

Similarly the boundary conditions become

$$\begin{aligned} &\text{(i) } \frac{dG(1/2)}{d\beta} = 0,\ \text{(ii) } G(1/2) = 1,\ \text{(iii) } G(0) = 0, \\ &\text{(iv) } \lim_{\beta\to 0}\sqrt{2\beta}\,\frac{d^2G}{d\beta^2} = 0,\ \text{(v) } H(1/2) = 1,\ \text{(vi)}\frac{dH(0)}{d\beta} = 0. \end{aligned} \tag{3.245}$$

3.4.3 Analytical solutions

The main purpose of this subsection is to obtain semi-analytical solutions of the fourth-order non-linear differential equation (3.243) representing momentum variation and the second-order non-linear differential equation (3.244) representing temperature distribution during solid rocket motor operation using double perturbation [28]. The solid rocket motor is designed to allow propellant injection inside the combustion chamber such that $K = \frac{1}{R_e}$ is small and the density variation within the fluid bulk is such that Grashof number G_r is also small. For such small parameters, the velocity G and temperature H can be represented in a series form as

$$\begin{aligned} G &= G_1 + KG_2 + O(K^2), \\ H &= H_1 + KH_2 + O(K^2), \end{aligned} \tag{3.246}$$

where the zero-th order terms G_1, H_1 and first order terms G_2, H_2 of K are given by equations

$$\begin{aligned} G_1 &= G_{10} + G_r G_{11} + O(G_r^2), \\ H_1 &= H_{10} + G_r H_{11} + O(G_r^2), \\ G_2 &= G_{20} + G_r G_{21} + O(G_r^2), \\ H_2 &= H_{20} + G_r H_{21} + O(G_r^2), \end{aligned} \tag{3.247}$$

respectively. Using the velocity G and temperature H from (3.246) into equations (3.243), (3.244) and boundary conditions (3.245), we obtain momentum and energy equations as

$$\begin{aligned} &G_1\frac{d^3G_1}{d\beta^3} - \frac{G_1}{d\beta}\frac{d^2G_1}{d\beta^2} + K\left[\beta\frac{d^4G_1}{d\beta^4} + (2\alpha\beta+4)\frac{d^3G_1}{d\beta^3} + 4\alpha\frac{d^2G_1}{d\beta^2} + G_1\frac{d^3G_2}{d\beta^3}\right. \\ &\left. + G_2\frac{d^3G_1}{d\beta^3} - \frac{dG_1}{d\beta}\frac{d^2G_2}{d\beta^2} - \frac{dG_2}{d\beta}\frac{d^2G_1}{d\beta^2}\right] - \frac{H_1G_r + KH_2G_r}{\sqrt{2\beta}} + O(K^2) \end{aligned} \tag{3.248}$$

and

$$\begin{aligned} &\left[\frac{dG_1}{d\beta} + K\frac{dG_2}{d\beta}\right]\left[H_1 + KH_2\right] - \left[\frac{G_1}{2} + K\frac{G_2}{2}\right]\left[\frac{dH_1}{d\beta} + K\frac{dH_2}{d\beta}\right] \\ &-\frac{K}{P_r}\left[\frac{dH_1}{d\beta} + K\frac{dH_2}{d\beta} + \beta\frac{dH_1^2}{d\beta^2} + K\beta\frac{dH_2^2}{d\beta^2}\right] - \frac{2RK}{P_r}\left[\frac{dH_1}{d\beta} + K\frac{dH_2}{d\beta} + 2\beta\frac{dH_1^2}{d\beta^2}\right. \\ &\left. + 2K\beta\frac{dH_2^2}{d\beta^2}\right] + O(K^2). \end{aligned} \tag{3.249}$$

The boundary conditions becomes

$$\text{(i) } \frac{dG_1(1/2)}{d\beta} + K\frac{dG_2(1/2)}{d\beta} = 0, \text{ (ii) } G_1(1/2) + KG_2(1/2) = 1,$$
$$\text{(iii) } G_1(0) + KG_2(0) = 0, \text{ (iv) } \lim_{\beta\to 0}\sqrt{2\beta}\,\frac{d^2G_1}{d\beta^2} + K\lim_{\beta\to 0}\sqrt{2\beta}\,\frac{d^2G_2}{d\beta^2} = 0,$$
$$\text{(v) } H_1(1/2) + KH_2(1/2) = 1, \text{ (vi)}\frac{dH_1(0)}{d\beta} + K\frac{dH_1(0)}{d\beta} = 0. \tag{3.250}$$

Comparing powers of K from equations (3.248), (3.249) and boundary conditions (3.250) yields two equations arising from zero-th order terms and two equations, arising from first-order terms from momentum (3.248) and energy (3.249) equations respectively.

The zero-th order terms of K from the momentum equation (3.248), is given by

$$K^0 : G_1\frac{d^3G_1}{d\beta^3} - \frac{dG_1}{d\beta}\frac{d^2G_1}{d^2\beta} - \frac{G_rH_1}{\sqrt{2\beta}} = 0 \tag{3.251}$$

with the following corresponding boundary conditions

$$\text{(i) } \frac{dG_1(1/2)}{d\beta} = 0, \text{ (ii) } G_1(1/2) = 1, \text{ (iii) } G_1(0) = 0,$$
$$\text{(iv) } \lim_{\beta\to 0}\sqrt{2\beta}\,\frac{d^2G_2}{d\beta^2} = 0, \text{ (v) } H_1(1/2) = 1, \text{ (vi) } \frac{dH_1(0)}{d\beta} = 0. \tag{3.252}$$

The first-order term of K from the momentum equation (3.248), yields

$$K^1 : \quad \left[\beta\frac{d^4G_1}{d\beta^4} + (2\alpha\beta + 4)\frac{d^3G_1}{d\beta^3} + 4\alpha\frac{d^2G_1}{d\beta^2} + G_1\frac{d^3G_2}{d\beta^3} + G_2\frac{d^3G_1}{d\beta^3}\right.$$
$$\left. - \frac{dG_1}{d\beta}\frac{d^2G_2}{d\beta^2} - \frac{dG_2}{d\beta}\frac{d^2G_1}{d\beta^2}\right] - \frac{H_2G_r}{\sqrt{2\beta}} = 0 \tag{3.253}$$

with corresponding boundary conditions

$$\text{(i) } \frac{dG_2(1/2)}{d\beta} = 0, \text{ (ii) } G_2(1/2) = 0, \text{ (iii) } G_2(0) = 0,$$
$$\text{(iv) } \lim_{\beta\to 0}\sqrt{2\beta}\,\frac{d^2G_2}{d\beta^2} = 0, \text{(v) } H_2(1/2) = 0, \text{ (vi)}\frac{dH_2(0)}{d\beta} = 0. \tag{3.254}$$

Similarly the energy equation (3.249), yields

$$K^0 : H_1\frac{dG_1}{d\beta} - \frac{1}{2}G_1\frac{dH_1}{d\beta} = 0 \tag{3.255}$$

with boundary conditions

$$\text{(i) } \frac{dG_1(1/2)}{d\beta} = 0, \text{ (ii) } G_1(1/2) = 1, \text{ (iii) } G_1(0) = 0, \tag{3.256}$$
$$\text{(iv) } \lim_{\beta\to 0}\sqrt{2\beta}\,\frac{d^2G_1}{d\beta^2} = 0, \text{ (v) } H_1(1/2) = 1, \text{ (vi)}\frac{dH_1(0)}{d\beta} = 0.$$

and

$$K^1: \quad H_2\frac{dG_1}{d\beta}+H_1\frac{dG_2}{d\beta}-\frac{1}{P_r}\frac{dH_1}{d\beta}-\frac{2R}{P_r}\frac{dH_1}{d\beta} \\ -\frac{1}{2}G_2\frac{dH_1}{d\beta}-\frac{1}{2}G_1\frac{dH_2}{d\beta}-\frac{\beta}{P_r}\frac{d^2H_2}{d\beta^2}-\frac{4R\beta}{P_r}\frac{d^2H_2}{d\beta^2}=0, \tag{3.257}$$

with the boundary conditions

$$\text{(i) } \frac{dG_2(1/2)}{d\beta}=0,\ \text{(ii) } G_2(1/2)=0,\ \text{(iii) } G_2(0)=0, \\ \text{(iv) } \lim_{\beta\to 0}\sqrt{2\beta}\,\frac{d^2G_2}{d\beta^2}=0,\ \text{(v) } H_2(1/2)=0,\ \text{(vi) } \frac{dH_2(0)}{d\beta}=0, \tag{3.258}$$

respectively.

Substituting equations from (3.247) into momentum equations (3.251) and (3.253) and their respective boundary conditions (3.252) and (3.254), yields the following equations arising from zero-th and first order term of G_r.

The momentum equation (3.251), yields zero-th and first-order terms of G_r respectively as

$$G_r^0: G_{10}\frac{d^3G_{10}}{d\beta^3}-\frac{G_{10}}{d\beta}\frac{d^2G_{10}}{d\beta^2}=0, \tag{3.259}$$

with the corresponding boundaries

$$\text{(i) } \frac{dG_{10}(1/2)}{d\beta}=0, \qquad \text{(ii) } G_{10}(1/2)=1, \\ \text{(iii) } G_{10}(0)=0, \qquad \text{(iv) } \lim_{\beta\to 0}\sqrt{2\beta}\,\frac{d^2G_{10}}{d\beta^2}=0. \tag{3.260}$$

and

$$G_r^1: \quad G_{10}\frac{d^3G_{11}}{d\beta^3}+G_{11}\frac{d^3G_{10}}{d\beta^3}-\frac{dG_{10}}{d\beta}\frac{d^2G_{11}}{d\beta^2}-\frac{G_{11}}{d\beta}\frac{d^2}{d\beta^2}-\frac{H_{10}}{\sqrt{2\beta}}=0 \tag{3.261}$$

with the following corresponding boundary conditions

$$\text{(i) } \frac{dG_{11}(1/2)}{d\beta}=0, \qquad \text{(ii) } G_{11}(1/2)=0, \\ \text{(iii) } G_{11}(0)=0, \qquad \text{(iv) } \lim_{\beta\to 0}\sqrt{2\beta}\,\frac{d^2G_{11}}{d\beta^2}=0. \tag{3.262}$$

Similarly equation (3.253), yields two equations of zero-th and first order of G_r as

$$G_r^0: \quad 2\beta\frac{d^4G_{10}}{d\beta^4}+(2\alpha\beta+4)\frac{d^3G_{10}}{d\beta^3}+4\alpha\frac{d^2G_{10}}{d\beta^2}+G_{10}\frac{d^3G_{20}}{d\beta^3}+G_{20}\frac{d^3G_{10}}{d\beta^3}-\frac{dG_{10}}{d\beta}\frac{d^2G_{20}}{d\beta^2}, \\ \frac{dG_{20}}{d\beta}\frac{d^2G_{10}}{d\beta^2}=0, \tag{3.263}$$

with corresponding boundaries

$$\text{(i) } \frac{dG_{20}(1/2)}{d\beta} = 0, \qquad \text{(ii) } G_{20}(1/2) = 0,$$
$$\text{(iii) } G_{20}(0) = 0, \qquad \text{(iv) } \lim_{\beta\to 0} \sqrt{2\beta}\, \frac{d^2G_{20}}{d\beta^2} = 0. \tag{3.264}$$

and

$$\begin{aligned} G_r^1 : \quad & 2\beta\frac{d^4G_{11}}{d\beta^4} + (2\beta\alpha + 4)\frac{d^3G_{11}}{d\beta^3} + 4\alpha\frac{d^2G_{11}}{d\beta} - \frac{dG_{20}}{d\beta}\frac{d^2G_{11}}{d\beta^2} - \frac{dG_{11}}{d\beta}\frac{d^2G_{20}}{d\beta^2} \\ & + G_{20}\frac{d^3G_{11}}{d\beta^3} - G_{11}\frac{d^3G_{20}}{d\beta^3} + G_{10}\frac{d^3G_{21}}{d\beta^3} + G_{21}\frac{d^3G_{10}}{d\beta^3} - \frac{dG_{21}}{d\beta}\frac{d^2G_{10}}{d\beta^2} \\ & - \frac{dG_{10}}{d\beta}\frac{d^2G_{21}}{d\beta^2} - \frac{H_{20}}{\sqrt{2\beta}} = 0. \end{aligned} \tag{3.265}$$

with the boundary conditions

$$\text{(i) } \frac{dG_{21}(1/2)}{d\beta} = 0, \qquad \text{(ii) } G_{21}(1/2) = 1,$$
$$\text{(iii) } G_{21}(0) = 0, \qquad \text{(iv) } \lim_{\beta\to 0} \sqrt{2\beta}\, \frac{d^2G_{21}}{d\beta^2} = 0, \tag{3.266}$$

respectively.

Substituting equation (3.247) into the energy equations (3.255) and (3.257) and their respective boundary conditions (3.256) and (3.258), yields the following equation arising from zero-th and first-order term of G_r.

The equation arising from energy equation (3.255), yields two equations of zero-th order and first order terms in G_r respectively as

$$G_r^0 : H_{10}\frac{dG_{10}}{d\beta} - \frac{1}{2}G_{10}\frac{dH_{10}}{d\beta} = 0, \tag{3.267}$$

with corresponding boundaries

$$\text{(i) } H_{10}(1/2) = 1, \text{ (ii) } \frac{dH_{10}(0)}{d\beta} = 0 \tag{3.268}$$

and

$$G_r^1 : \quad H_{11}\frac{dG_{10}}{d\beta} + H_{10}\frac{dG_{11}}{d\beta} - \frac{1}{2}G_{11}\frac{dH_{10}}{d\beta} - \frac{1}{2}G_{10}\frac{dH_{11}}{d\beta} = 0, \tag{3.269}$$

with corresponding boundary conditions

$$\text{(i) } H_{11}(1/2) = 0, \text{ (ii) } \frac{dH_{11}(0)}{d\beta} = 0, \tag{3.270}$$

respectively.

Similarly the energy equation (3.257), yields the following two equations

$$G_r^0: \quad H_{20}\frac{dG_{10}}{d\beta} + H_{10}\frac{dG_{20}}{d\beta} - \frac{1}{P_r}\frac{dH_{10}}{d\beta} - \frac{2R}{P_r}\frac{dH_{10}}{d\beta} - \frac{1}{2}G_{20}\frac{dH_{10}}{d\beta} - \frac{1}{2}G_{10}\frac{dH_{20}}{d\beta} - \frac{\beta}{P_r}\frac{d^2H_{10}}{d\beta^2} - \frac{4R\beta}{P_r}\frac{d^2H_{10}}{d\beta^2} = 0, \tag{3.271}$$

with corresponding boundary conditions

$$\text{(i) } H_{20}(1/2) = 0, \text{ (ii) } \frac{dH_{20}(0)}{d\beta} = 0 \tag{3.272}$$

and

$$G_r^1: \quad H_{21}\frac{dG_{10}}{d\beta} + H_{20}\frac{dG_{11}}{d\beta} + H_{11}\frac{dG_{20}}{d\beta} + H_{10}\frac{dG_{21}}{d\beta} - \frac{1}{2}G_{21}\frac{dH_{10}}{d\beta} - \frac{1}{P_r}\frac{dH_{11}}{d\beta} - \frac{2R}{P_r}\frac{dH_{11}}{d\beta} - \frac{1}{2}G_{20}\frac{dH_{11}}{d\beta} - \frac{1}{2}G_{11}\frac{dH_{20}}{d\beta} - \frac{1}{2}G_{10}\frac{H_{21}}{d\beta} - \frac{\beta}{P_r}\frac{d^2H_{11}}{d\beta^2} - \frac{4R\beta}{P_r}\frac{d^2H_{11}}{d\beta} = 0$$

and corresponding boundaries

$$\text{(i) } H_{21}(1/2) = 0, \text{ (ii) } \frac{dH_{21}(0)}{d\beta} = 0. \tag{3.273}$$

Solving (3.259) together with boundary conditions (3.260), yields

$$G_{10} = \sin\theta, \tag{3.274}$$

where

$$\theta = \pi\beta. \tag{3.275}$$

Using the value of θ from (3.275) into (3.267) and boundary conditions (3.268), yields

$$H_{10}\frac{dH_{10}}{d\theta} - \frac{1}{2}G_{10}\frac{dH_{10}}{d\theta} = 0 \tag{3.276}$$

and boundary conditions

$$\text{(i) } H_{10}(\pi/2) = 1, \text{ (ii) } \frac{dH_{10}(0)}{d\theta} = 0. \tag{3.277}$$

Substitution of G_{10} from (3.274) into (3.276) and solving the resulting equation together with boundary conditions (3.277), yields

$$H_{10} = -\frac{\cos 2\theta}{2} + \frac{1}{2}. \tag{3.278}$$

Similarly by substituting (3.275) into (3.261) and boundary conditions (3.262), yields

$$G_{10}\frac{d^3G_{11}}{d\theta^3} + G_{10}\frac{d^3G_{10}}{d\theta^3} - \frac{dG_{10}}{d\theta}\frac{d^2G_{11}}{d\theta^2} - \frac{dG_{11}}{d\theta}\frac{d^2G_{10}}{d\theta^2} - \frac{\pi^{\frac{-5}{2}}H_{10}}{\sqrt{2\theta}} = 0 \tag{3.279}$$

and boundary conditions become

$$\begin{aligned} &\text{(i)}\ \frac{dG_{11}(\pi/2)}{d\theta} = 0, \qquad \text{(ii)}\ G_{11}(\pi/2) = 0, \\ &\text{(iii)}\ G_{11}(0) = 0, \qquad \text{(iv)}\ \lim_{\theta\to 0}\sqrt{\theta}\,\frac{d^2G_{11}}{d\theta^2} = 0. \end{aligned} \tag{3.280}$$

Substituting the values of G_{10} from (3.274) and H_{10} from (3.278) into equation (3.279), yields

$$\sin\theta\frac{d^3G_{11}}{d\theta^3} - \cos\theta\frac{d^2G_{11}}{d\theta^2} + \sin\theta\frac{dG_{11}}{d\theta} - \cos\theta G_{11} = \frac{\pi^{\frac{-5}{2}}\big(-\frac{\cos 2\theta}{2} + \frac{1}{2}\big)}{\sqrt{2\theta}}. \tag{3.281}$$

The solution of equation (3.281) needs to be carefully constructed. To solve (3.281), we follow the approach in [21]. The homogeneous part of the above equation is satisfied by the following solution

$$G_{11h} = cos\theta. \tag{3.282}$$

Using variation of parameters based on the correction multiplier $A(\theta)$, the improved solution of homogeneous solution (3.282) is given by

$$G_{11h} = A(\theta)\cos\theta. \tag{3.283}$$

Substituting the solution (3.283) into the homogenous part of (3.281), yields the following homogeneous equation

$$A'''\sin\theta\cos\theta - 2A''\sin\theta^2 - A'' = 0. \tag{3.284}$$

Integrating the above equation (3.284), yields

$$A(\theta) = C_1\tan\theta + C_2\theta + C_3, \tag{3.285}$$

where C_1, C_2 and C_3 are constants to be determined. Thus by substituting equation (3.285) into (3.283), yields

$$G_{11h} = C_1 \sin\theta + C_2\theta\cos\theta + C_3\cos\theta. \tag{3.286}$$

Using variation of parameters to improve the solution (3.286) requires the integration constant to vary with θ. Hence we take the integration constants to be function of θ, thus G_{11} becomes

$$\begin{aligned} G_{11} &= C_1(\theta)\sin\theta + C_2(\theta)\theta\cos\theta + C_3(\theta)cos\theta, \\ &= C_1(\theta)G_{11A}(\theta) + C_2(\theta)G_{11B}(\theta) + C_3(\theta)G_{11C}(\theta). \end{aligned} \tag{3.287}$$

The improved solution in equation (3.287) needs to be differentiated three times prior substitution into equation (3.281). The first differentiation yields the following

$$G'_{11} = C'_1G_{11A} + C_1G'_{11A} + C'_2G_{11B} + C_2G'_{11B} + C'_3G_{11C} + C_3G'_{11C}. \tag{3.288}$$

The constraint binding derivatives of the parameters varying with θ is given by

$$C'_1G_{11A} + C'_2G_{11B} + C'_3G_{11C} = 0, \tag{3.289}$$

which gives

$$G'_{11} = C'_1\sin\theta + C'_2\theta\cos\theta + C'_3\cos\theta = 0. \tag{3.290}$$

Hence C_1 becomes

$$G'_{11} = C_1\cos\theta + C_2[\cos\theta - \theta\sin\theta] - C_3\sin\theta. \tag{3.291}$$

Similarly taking the second derivative, we obtain

$$G''_{11} = C'_1G'_{11A} + C_1G''_{11A} + C'_2G'_{11B} + C_2G''_{11B} + C'_3G'_{11C} + C_3G''_{11C}. \tag{3.292}$$

Thus letting $C'_1G'_{11A} + C'_2G'_{11B} + C'_3G'_{11C} = 0$, gives

$$C'_1\cos\theta + C'_2[\sin\theta - \theta\sin\theta] - C'_3\sin\theta = 0. \tag{3.293}$$

Thus equation (3.292), becomes

$$G''_{11} = -C_1\sin\theta - C'_2[2\sin\theta + \theta\cos\theta] - C_3\cos\theta. \tag{3.294}$$

Taking the third derivative of G_{11}, yields the following

$$\begin{aligned} G'''_{11} = \quad & -C'_1 \sin\theta - C_1 \cos\theta - C'_2[2\sin\theta + \theta\cos\theta] \\ & -C_2[3\cos\theta - \theta\sin\theta] - C'_3\cos\theta + C_3\sin\theta. \end{aligned} \tag{3.295}$$

Substituting the improved solution of G_{11} (3.287) and its derivatives into equation (3.281) yields

$$\begin{aligned} & -C'_1\sin^2\theta - 2C'_2\sin^2\theta - C'_2\theta\sin\theta\cos\theta \\ & C'_3\sin\theta\cos\theta = \frac{\pi^{\frac{-5}{2}}\big(-\frac{\cos 2\theta}{2} + \frac{1}{2}\big)}{\sqrt{2\theta}}. \end{aligned} \tag{3.296}$$

which can be simplified to

$$\begin{aligned} \sin\theta C'_1 + \theta\cos\theta C'_2 + \cos\theta C'_3 &= 0, \\ \cos\theta C'_1 + (\cos\theta - \theta\sin\theta)C'_2 - \sin\theta C'_3 &= 0 \\ -\sin^2\theta C'_1 - (2\sin^2\theta + \theta\sin\theta\cos\theta)C'_2 - \sin\theta\cos\theta C'_3 &= \frac{\pi^{\frac{-5}{2}}\big(-\frac{\cos 2\theta}{2} + \frac{1}{2}\big)}{\sqrt{2\theta}} \end{aligned}$$

The matrix representation of the (3.290), (3.293) and (3.296) is given by

$$\begin{bmatrix} \sin\theta & \theta\cos\theta & \cos\theta \\ \cos\theta & \cos\theta - \theta\sin\theta & -\sin\theta \\ -\sin\theta & -2\sin\theta - \theta\cos\theta & -\cos\theta \end{bmatrix} \begin{bmatrix} C'_1 \\ C'_2 \\ C'_3 \end{bmatrix} = \begin{bmatrix} 0 \\ 0 \\ \frac{\pi^{\frac{-5}{2}}\left(-\frac{\cos 2\theta}{2} + \frac{1}{2}\right)}{\sqrt{2\theta}\sin\theta} \end{bmatrix}$$

Solving the above matrix yields the values of C'_1, C'_2 and C'_3. Which on integration, yields the following values of correction multiplier as

$$\begin{aligned} C_1(\theta) &= I_1 + 0.02\sqrt{\theta} + a_1, \\ C_2(\theta) &= I_2 - 0.02\sqrt{\theta} + a_2, \\ C_3(\theta) &= I_3 + I_4 + 0.0066667\theta^{\frac{3}{2}} + I_5 + a_3, \end{aligned} \tag{3.297}$$

where $I_1 = \int_0^\theta \frac{-0.01\cos^2\theta\cos 2\theta}{\sqrt{\theta}}d\theta$, $I_2 = \int_0^\theta \frac{0.01\cos 2\theta}{\sqrt{\theta}}d\theta$, $I_3 = \int_0^\theta -0.01\sqrt{\theta}\cos 2\theta d\theta$, $I_4 = \int_0^\theta \frac{0.01\sin\theta\cos 2\theta\cos\theta}{\sqrt{\theta}}d\theta$, $I_5 = \int_0^\theta \frac{-0.01\sin\theta\cos\theta}{\sqrt{\theta}}d\theta$ and a_1, a_2 and a_3 are constants.

Substituting the multipliers (3.297) into (3.287), yields the solution of (3.281) as

$$\begin{aligned} & G_{11} = 0.02\sqrt{\theta}\big[\sin\theta - \theta\cos\theta\big] + I_1\sin\theta + \cos\theta\big[\theta I_2 + I_3 + I_4 + I_5\big] \\ & + a_1\sin\theta + a_2\theta\cos\theta + a_3\cos\theta. \end{aligned} \tag{3.298}$$

Using the boundary conditions (3.280) into equation (3.298), we get the values of the integration constants as

$$a_1 = 0.0137593, \tag{3.299}$$

$$a_2 = \frac{-0.118586}{1.9687}, \tag{3.300}$$

$$a_3 = 0. \tag{3.301}$$

The integrals I_1, I_2, I_3, I_4 and I_5 can be rewritten in series form as

$$I_1 \cong \sqrt{\theta}\big(-0.02 - 2.24346 \times 10^{-18}\theta + 0.012\theta^2 - 1.66533 \times 10^{-18}\theta^3 - 0.0066666 7\theta^4\big) + ..., \tag{3.302}$$

$$I_2 \cong \sqrt{\theta}\big(0.02 - 0.008\theta^2 + 0.00148148\theta^4\big) + ..., \tag{3.303}$$

$$I_3 \cong \theta^{\frac{3}{2}}\big(-0.0066666 + 0.00571429\theta^2 - 0.0066666\theta^{\frac{9}{2}}\big) + ..., \tag{3.304}$$

$$I_4 \cong \theta^{\frac{3}{2}}\big(0.00666667 - 1.25673 \times 10^3\theta^2 - 1.09176 \times 10^{-18}\theta^3 0.00387879\theta^4\big) + ..., \tag{3.305}$$

$$I_5 \cong \theta^{\frac{3}{2}}\big(-0.00666667 + 6.48634 \times 10^{-19}\theta + 0.00190476\theta^2 + 1.31582 \times 10^{-19}\theta^3 - 0.00024242 4\theta^4\big) + ... \tag{3.306}$$

Thus substituting (3.274) and (3.298) into equation (3.247), yield G_1 as

$$G_1 = \sin\theta + G_r\big[0.02\sqrt{\theta}\big(\sin\theta - \theta\cos\theta\big) + I_1\sin\theta + \cos\theta\big(\theta I_2 + I_3 + I_4 + I_5\big) + a_1\sin\theta + a_2\theta\cos\theta + a_3\cos\theta\big], \tag{3.307}$$

where a_1, a_2, a_3 and I_1, I_2, I_3, I_4, I_5 are defined by equations (3.196)-(3.198) and (3.199)-(3.203) respectively. Substituting (3.275) into equation (3.269) and the corresponding boundary conditions (3.270), yields

$$H_{11}\frac{dG_{10}}{d\theta} + H_{10}\frac{dG_{11}}{d\theta} - \frac{1}{2}G_{11}\frac{dH_{10}}{d\theta} - \frac{1}{2}G_{10}\frac{dH_{11}}{d\theta} = 0 \tag{3.308}$$

and boundary conditions

$$\text{(i) } H_{11}(\pi/2) = 0, \text{ (ii) } \frac{dH_{11}(0)}{d\theta} = 0. \tag{3.309}$$

The series forms of G_{10}, H_{10} and H_{11} which are used to integrate the non-integrable equation (3.308) from equations (3.274), (3.278) and (3.298) are as follows

$$\begin{aligned} G_{10} &= \theta - \frac{\theta^3}{6} + O(\theta^4), \\ H_{10} &= \theta^2 + O(\theta^4), \\ G_{11} &= -0.01375939\theta - 1.04038 \times 10^{-17}\theta^{\frac{3}{2}} - 2.24346 \times 10^{-18}\theta^{\frac{5}{2}} \\ &+0.00229321\theta^3 + O(\theta^{\frac{7}{2}}). \end{aligned} \tag{3.310}$$

Using the series representation of G_{10}, H_{10} and H_{11} defined in (3.310) into (3.308) yields a simplied first order linear equation which gives the following solution satisfying the boundary conditions (3.309) as

$$H_{11} = 3.49232 \times 10^{-17}\big[\theta^2 - 0.059607\theta^{\frac{5}{2}} - 0.128479\theta^{\frac{7}{2}}\big]. \tag{3.311}$$

Substituting (3.278) and (3.311) into equation (3.247), yields

$$H_1 = -\frac{\cos 2\theta}{2} + \frac{1}{2} + G_r\big[3.49232 \times 10^{17}\big(\theta^2 - 0.059607\theta^{\frac{5}{2}} - 0.128479\theta^{\frac{7}{2}}\big)\big]. \tag{3.312}$$

Also substituting (3.275) into (3.263) and the boundary conditions (3.264), yields

$$\begin{aligned} &\sin\theta\frac{d^3G_2}{d\theta^3} - \cos\theta\frac{d^2G_2}{d\theta^2} + \sin\theta\frac{dG_2}{d\theta} - \cos\theta G_2 = \left(\frac{2}{\pi}\theta + 4\right)\cos\theta \\ &+\frac{4}{\pi}\alpha\sin\theta - 2\theta\sin\theta \end{aligned} \tag{3.313}$$

and boundary conditions (3.245) becomes

$$\begin{aligned} &\text{(i) } \frac{dG_{20}(\pi/2)}{d\theta} = 0, \qquad \text{(ii) } G_{20}(\pi/2) = 0, \\ &\text{(iii) } G_{20}(0) = 0, \qquad \text{(iv) } \lim_{\theta\to 0}\sqrt{\theta}\,\frac{d^2G_{20}}{d\theta^2} = 0. \end{aligned} \tag{3.314}$$

A solution of the homogeneous part of (3.313) is given by

$$G_{20h} = \cos\theta. \tag{3.315}$$

Similarly the correction multiplier of G_{20} using variation of parameters is given by

$$G_{20h} = W(\theta)\cos\theta. \tag{3.316}$$

Substituting (3.316) into the homogeneous part of (3.313), yields the following third order ODE

$$W''' \sin\theta \cos\theta - 2W'' \sin\theta^2 - W'' = 0. \tag{3.317}$$

Integrating (3.317) with respect to θ, gives

$$W(\theta) = D_1 \tan\theta + D_2\theta + D_3. \tag{3.318}$$

Using (3.318) into (3.316), we get

$$G_{20h} = D_1 \sin\theta + D_2\theta\cos\theta + D_3\cos\theta. \tag{3.319}$$

Using method of variation of parameters, we assume

$$\begin{aligned} G_{20} &= D_1(\theta)\sin(\theta) + D_2(\theta)\theta\cos(\theta) + D_3(\theta)\cos\theta, \\ &= D_1(\theta)G_{20A}(\theta) + D_2(\theta)G_{20B}(\theta) + D_3(\theta)G_{20C}(\theta). \end{aligned} \tag{3.320}$$

Similarly differentiating (3.320) three times prior substituting into (3.313), yields the first differentiation as

$$G'_{20} = D'_1G_{20A} + D_1G'_{20A} + D'_2G_{20B} + D_2G'_{20B} + D'_3G_{20C} + D_3G'_{20C}, \tag{3.321}$$

similarly letting

$$D'_1G_{20A} + D'_2G_{20B} + D'_3G_{20C} = 0, \tag{3.322}$$

which gives

$$D'_1\sin\theta + D'_2\theta\cos\theta + D'_3\cos\theta = 0. \tag{3.323}$$

Hence G'_{20} becomes

$$G'_{20} = D'_1\cos\theta + D'_2[\cos\theta - \theta\sin\theta] - D'_3\sin\theta. \tag{3.324}$$

Also, taking the second derivative, we obtain

$$G''_{20} = D'_1G'_{20A} + D_1G''_{20A} + D'_2G'_{20B} + D_2G''_{20B} + D'_3G'_{20C} + D_3G''_{20C}. \tag{3.325}$$

Thus letting $D_1'G_{20A}' + D_2'G_{20B}' + D_3'G_{20C}' = 0$, gives

$$D_1' \cos\theta + D_2'[\sin\theta - \theta\sin\theta] - D_3' \sin\theta = 0. \tag{3.326}$$

Thus equation (3.325), becomes

$$G_{20}'' = -D_1 \sin\theta - D_2'[2\sin\theta + \theta\cos\theta] - D_3\cos\theta. \tag{3.327}$$

Lastly the third differentiation yields

$$\begin{aligned} G_{20}''' = \quad & -D_1' \sin\theta - D_1\cos\theta - D_2'[2\sin\theta + \theta\cos\theta] \\ & -D_2[3\cos\theta - \theta\sin\theta] - D_3'\cos\theta + D_3\sin\theta. \end{aligned} \tag{3.328}$$

Substituting equation (3.320) and its derivatives (3.324), (3.327) and (3.328) into (3.313), yields

$$\begin{aligned} & -D_1'\sin^2\theta - 2D_2'\sin^2\theta - D_2'\theta\sin\theta\cos\theta \\ & D_3'\sin\theta\cos\theta = \left(\frac{2}{\pi}\theta + 4\right)\cos\theta + \frac{4}{\pi}\alpha\sin\theta - 2\theta\sin\theta. \end{aligned} \tag{3.329}$$

Representing (3.323), (3.326) and (3.329) as a systems, yields

$$\begin{aligned} \sin\theta D_1' + \theta\cos\theta D_2' + \cos\theta D_3' &= 0, \\ \cos\theta D_1' + (\cos\theta - \theta\sin\theta)D_2' - \sin\theta D_3' &= 0, \\ -\sin^2\theta D_1' - (2\sin^2\theta + \theta\sin\theta\cos\theta)D_2' - \sin\theta\cos\theta D_3' &= \left(\frac{2}{\pi}\alpha\,\theta + 4\right)\cos\theta + \frac{4}{\pi}\alpha\sin\theta - 2\theta\sin\theta \end{aligned}$$

and takes the matrix form

$$\begin{bmatrix} \sin\theta & \theta\cos\theta & \cos\theta \\ \cos\theta & \cos\theta - \theta\sin\theta & -\sin\theta \\ -\sin\theta & -2\sin\theta - \theta\cos\theta & -\cos\theta \end{bmatrix} \begin{bmatrix} D_1' \\ D_2' \\ D_3' \end{bmatrix} = \begin{bmatrix} 0 \\ 0 \\ \left(\frac{2}{\pi}\alpha\,\theta + 4\right)\cot\theta + \frac{4}{\pi}\alpha - 2\theta \end{bmatrix}$$

Solving the above matrix yields the values of D_1', D_2' and D_3'. Which on integration, yields the following values of correction multiplier $D_1(\theta)$, $D_2(\theta)$ and $D_3(\theta)$ as

$$\begin{aligned} D_1(\theta) &= \frac{\alpha}{\pi}\Big[\cos\theta - \theta\sin\theta + 3\ln\tan(\theta/2) - \theta\ \mathrm{cosec}\theta\Big] - \sin\theta - 2\mathrm{cosec}\theta - \theta\cos\theta - I_6 + b_1, \\ D_2(\theta) &= \frac{\alpha}{\pi}\Big[\theta\mathrm{cosec}\theta - 3\ln\tan(\theta/2)\Big] + 2\mathrm{cosec}\theta + I_6 + b_2, \\ D_3(\theta) &= \frac{\alpha}{\pi}\Big[-\theta^2\mathrm{cosec}\theta - \theta\cos\theta - \sin\theta + 3I_6\Big] + \theta\sin\theta - 2\theta\mathrm{cosec} - \cos\theta - I_7 + b_3, \end{aligned} \tag{3.330}$$

where

$$I_6 = \int_0^\theta \theta \text{cosec}\theta \, d\theta, \quad I_7 = \int_0^\theta \theta^2 \text{cosec}\theta \, d\theta$$

and b_1, b_2 and b_3 are constants.

Substituting (3.330) into (3.320), we get

$$G_{20} = \frac{\alpha}{\pi}\left[3\ln\tan(\theta/2)(\sin\theta - \theta\cos\theta) - 2\theta\right] - 3 + (\theta\cos\theta - \sin\theta)I_6,$$
$$+\left(\frac{3\alpha}{\pi}I_6 - I_7\right)\cos\theta + b_1\sin\theta + b_2\theta\cos\theta + b_3\cos\theta. \tag{3.331}$$

The boundary conditions (3.314) together with equation (3.331), yields

$$b_1 = \alpha + 3 + \frac{\pi}{2} + \frac{\pi^3}{144} + \frac{7\pi^5}{57600}, \tag{3.332}$$

$$b_2 = \frac{-16\pi\left(43200 + 1800\pi^2 + \frac{45\pi^4}{2} + \frac{7\pi^6}{45}\right)}{86400\pi^2} \tag{3.333}$$
$$+\frac{172800\alpha\pi}{86400\pi^2} - \frac{144\pi\alpha\left(1800 + 25\pi^2 + \frac{7\pi^4}{16}\right)}{86400\pi^2},$$

$$b_3 = 3. \tag{3.334}$$

The integrals I_1 and I_2 can be rewritten in series form as

$$I_6 \approxeq \theta + \frac{\theta^3}{6} + \frac{7\theta^5}{360} + ..., \tag{3.335}$$

$$I_7 \approxeq \frac{\theta^2}{2} + \frac{\theta^4}{24} + \frac{7\theta^6}{2160} + ... \tag{3.336}$$

Substituting θ from (3.275) into (3.271) and boundary conditions (3.272), we get

$$H_{20}\frac{dG_{10}}{d\theta} + H_{10}\frac{dG_{20}}{d\theta} - \frac{1}{P_r}\frac{dH_{10}}{d\theta} - \frac{2R}{P_r}\frac{dH_{10}}{d\theta} \tag{3.337}$$
$$-\frac{1}{2}G_{20}\frac{dH_{10}}{d\theta} - \frac{1}{2}G_{10}\frac{dH_{20}}{d\theta} - \frac{\theta}{P_r}\frac{d^2H_{10}}{d\theta^2} - \frac{4R\theta}{P_r}\frac{d^2H_{10}}{d\theta^2} = 0,$$

with corresponding boundaries given by

$$\text{(i) } H_{20}(\pi/2) = 0, \text{ (ii) } \frac{dH_{20}(0)}{d\theta} = 0. \tag{3.338}$$

Equation (3.337) is not easily integrable or solvable, we now represent G_{20} in series form as follows

$$G_{20} = \bigg(3 - \frac{8}{\pi} + \frac{\pi}{6} + \frac{\pi^3}{360} + \frac{7\pi^5}{69120} + \alpha + \frac{2\alpha}{\pi^2} - \frac{2\alpha}{\pi} - \frac{\pi\alpha}{24} - \frac{7\pi^3\alpha}{9600}\bigg)\theta - 2\theta^2 + O(\theta^3). \tag{3.339}$$

Using series form of G_{10} and H_{10} defined by (3.310), G_{20} defined by (3.339) into (3.337) thereafter solving the simplified equation and boundary conditions (3.338), yields the solution of H_{20} as

$$H_{20} = \frac{2}{\pi P_r}\bigg(4\pi\theta + 12\pi R\theta - 8\theta^2 - 24R\theta^2 + \pi^2\theta^2 P_r - 2\pi\theta^3 P_r\bigg). \tag{3.340}$$

Substituting (3.275) into (3.265) and the boundary conditions (3.266), yields

$$\begin{aligned} &G_{10}\frac{d^3G_{21}}{d\theta^3} + G_{21}\frac{d^3G_{10}}{d\theta^3} - \frac{dG_{21}}{d\theta}\frac{d^2G_{10}}{d\theta^2} - \frac{dG_{10}}{d\theta}\frac{d^2G_{21}}{d\theta^2} = -\frac{-\pi^{\frac{5}{2}}H_{20}}{\sqrt{2\theta}} \\ &-\frac{4\alpha}{\pi}\frac{d^2G_{11}}{d\theta^2} + \frac{dG_{20}}{d\theta}\frac{d^2G_{11}}{d\theta^2} + \frac{dG_{11}}{d\theta}\frac{d^2G_{20}}{d\theta^2} - \big(\frac{2\theta\alpha}{\pi} + 4\big)\frac{d^3G_{11}}{d\theta^3} - G_{11}\frac{d^3G_{20}}{d\theta^3} \\ &-2\theta\frac{d^4G_{11}}{d\theta^4}, \end{aligned} \tag{3.341}$$

with corresponding boundary conditions

$$\begin{aligned} &\text{(i)}\frac{dG_{21}(\pi/2)}{d\theta} = 0, \qquad \text{(ii)}\, G_{21}(\pi/2) = 0, \\ &\text{(iii)}G_{21}(0) = 0, \qquad \text{(iv)}\lim_{\theta\to 0}\sqrt{\theta}\,\frac{d^2G_{21}}{d\theta^2} = 0. \end{aligned} \tag{3.342}$$

Substituting $G_{10}, G_{11}, G_{20}, H_{20}$ previously obtained into (3.341), we get the following nonhomegous equations

$$\begin{aligned} &\sin\theta\frac{d^3G_{21}}{d\theta^3} - \cos\theta\frac{d^2G_{21}}{d\theta^2} + \sin\theta\frac{dG_{21}}{d\theta} - \cos\theta G_{21} = -\frac{4\alpha}{\pi}\frac{d^2G_{11}}{d\theta^2} \\ &+\frac{dG_{20}}{d\theta}\frac{d^2G_{11}}{d\theta^2} + \frac{dG_{11}}{d\theta}\frac{d^2G_{20}}{d\theta^2} - \bigg(\frac{2\theta\alpha}{\pi} + 4\bigg)\frac{d^3G_{11}}{d\theta^3} - G_{11}\frac{d^3G_{20}}{d\theta^3} \\ &-2\theta\frac{d^4G_{11}}{d\theta^4}. \end{aligned} \tag{3.343}$$

The homogeneous solution of the homogenous part of (3.343) is given by

$$G_{21h} = \cos\theta. \tag{3.344}$$

Using variation of parameters approach to find the correction multiplier $J(\theta)$, equation (3.344) above becomes

$$G_{21h} = J(\theta)\cos\theta. \tag{3.345}$$

Substituting (3.345) into the homogeneous part of (3.343), yields

$$J'''\sin\theta\cos\theta - 2J''\sin\theta^2 - J'' = 0. \tag{3.346}$$

Integrating (3.346), we obtain

$$J(\theta) = V_1\tan\theta + V_2\theta + V_3. \tag{3.347}$$

Using (3.347) into (3.345), we get

$$G_{21h} = V_1\sin\theta + V_2\theta\cos\theta + V_3\cos\theta. \tag{3.348}$$

Using variation of parameters to improve the solution of G_{21}, we assume

$$\begin{aligned} G_{21} &= V_1(\theta)\sin\theta + V_2(\theta)\theta\cos\theta + V_3(\theta)\cos\theta \\ &= V_1(\theta)G_{21A}(\theta) + V_2(\theta)G_{21B}(\theta) + V_3(\theta)G_{21C}(\theta). \end{aligned} \tag{3.349}$$

Similarly equation (3.349) must be differentiated three times before substituting into (3.343). The first derivative, yields

$$G'_{21} = V'_1G_{21A} + V_1G'_{21A} + V'_2G_{21B} + V_2G'_{21B} + V'_3G_{21C} + V_3G'_{21C}, \tag{3.350}$$

similarly letting

$$V'_1G_{21A} + V'_2G_{21B} + V'_3G_{21C} = 0, \tag{3.351}$$

we get

$$V'_1\sin\theta + V'_2\theta\cos\theta + V'_3\cos\theta = 0. \tag{3.352}$$

Thus G'_{21} becomes

$$G'_{21} = V'_1\cos\theta + V'_2[\cos\theta - \theta\sin\theta] - V'_3\sin\theta \tag{3.353}$$

Similarly taking the second derivative, we obtain

$$G''_{21} = V'_1 G'_{21A} + V_1 G''_{21A} + V'_2 G'_{21B} + V_2 G''_{21B} + V'_3 G'_{21C} + V_3 G''_{21C}. \tag{3.354}$$

Letting, $V'_1 G'_{21A} + V'_2 G'_{21B} + V'_3 G'_{21C} = 0$, yields

$$V'_1 \cos\theta + V'_2[\sin\theta - \theta\sin\theta] - V'_3 \sin\theta = 0. \tag{3.355}$$

Thus equation (3.354), becomes

$$G''_{21} = -V_1 \sin\theta - V'_2[2\sin\theta + \theta\cos\theta] - V_3 \cos\theta. \tag{3.356}$$

Lastly the third differentiation, yields

$$\begin{aligned} G'''_{21} = \quad & -V'_1 \sin\theta - V_1 \cos\theta - V'_2[2\sin\theta + \theta\cos\theta] \\ & -V_2[3\cos\theta - \theta\sin\theta] - V'_3 \cos\theta + V_3 \sin\theta. \end{aligned} \tag{3.357}$$

Finally substituting equation (3.349) and its derivatives (3.353), (3.356) and (3.357) into (3.343), yields

$$\begin{aligned} & -V'_1 \sin^2\theta - 2V'_2 \sin^2\theta - V'_2 \theta \sin\theta\cos\theta \\ & V'_3 \sin\theta\cos\theta = AA, \end{aligned} \tag{3.358}$$

where

$$AA = -\frac{4\alpha}{\pi}\frac{d^2G_{11}}{d\theta^2} + \frac{dG_{20}}{d\theta}\frac{d^2G_{11}}{d\theta^2} + \frac{dG_{11}}{d\theta}\frac{d^2G_{20}}{d\theta^2} - \Big(\frac{2\theta\alpha}{\pi} + 4\Big)\frac{d^3G_{11}}{d\theta^3} - G_{11}\frac{d^3G_{20}}{d\theta^3} - 2\theta\frac{d^4G_{11}}{d\theta^4}.$$

where equations (3.352), (3.355) and (3.358) in a system form, we have

$$\begin{aligned} \sin\theta V'_1 + \theta\cos\theta V'_2 + \cos\theta V'_3 &= 0, \\ \cos\theta V'_1 + (\cos\theta - \theta\sin\theta)V'_2 - \sin\theta V'_3 &= 0, \\ -\sin^2\theta V'_1 - (2\sin^2\theta + \theta\sin\theta\cos\theta)V'_2 - \sin\theta\cos\theta V'_3 &= AA. \end{aligned}$$

The above system takes the following matrix form

$$\begin{bmatrix} \sin\theta & \theta\cos\theta & \cos\theta \\ \cos\theta & \cos\theta - \theta\sin\theta & -\sin\theta \\ -\sin\theta & -2\sin\theta - \theta\cos\theta & -\cos\theta \end{bmatrix} \begin{bmatrix} V'_1 \\ V'_2 \\ V'_3 \end{bmatrix} = \begin{bmatrix} 0 \\ 0 \\ \frac{AA}{\sin\theta} \end{bmatrix}$$

Solving the above matrix yields the values of V_1', V_2' and V_3'. Which on integration yields the following values of correction multiplier $V_1(\theta)$, $V_2(\theta)$ and $V_3(\theta)$ as

$$V_1(\theta) = -1.7348 \times 10^{-18}\alpha\big(\cos\theta - \ln[\cos(\theta/2)] + \ln[\sin(\theta 2)]\big) + A_1 \tag{3.359}$$
$$+4.3368 \times 10^{-18}\big(\cos\theta - \ln[\cos([\theta/2)] + \ln[\sin(\theta/2)]\big) + j_1,$$
$$V_2(\theta) = -1.7348 \times 10^{-18}\alpha\big(\cos\theta - \ln[\cos(\theta/2)] + \ln[\sin(\theta/2)]\big) \tag{3.360}$$
$$+A_2 - 4.3368 \times 10^{-18}\alpha\big(\cos\theta - \ln[\cos(\theta/2)] + \ln[\sin(\theta/2)]\big) + j_2,$$
$$V_3(\theta) = A_3 + j_3. \tag{3.361}$$

Here $A_1 = I_8 + I_9 + I + I_{10} + I_{11} + I_{12} + I_{13} + I_{14} + I_{15} + I_{16} + I_{17} + I_{18} + I_{19}$, $A_2 = I_{20} + I_{21} + I_{22} + I_{23} + I_{24} + I_{25} + I_{26} + I_{27} + I_{28} + I_{29} + I_{30} + I_{31} + I_{32} + I_{33} + I_{34}$ and $A_3 = I_{35} + I_{36} + I_{37} + I_{38} + I_{39} + I_{40} + I_{41}$,

where the above integrals I_i for $i = 8, ...41$ are defined as follows

$$I_8 = \int_0^\theta \frac{-\cos^2\theta}{2\sin\theta}\frac{0.9709R}{P_r\sqrt{\theta}}d\theta, \qquad I_9 = \int_0^\theta \frac{1.1654\times10^{-17}\cos^2\theta}{2\sin\theta\sqrt{\theta}}d\theta, \tag{3.362}$$

$$I_{10} = \int_0^\theta \frac{-\cos^2\theta}{2\sin\theta}\frac{0.32337}{P_r\sqrt{\theta}}d\theta, \qquad I_{11} = \int_0^\theta \frac{-0.7875\cos^2\theta}{2\sin\theta\sqrt{\theta}}d\theta,$$

$$I_{12} = \int_0^\theta \frac{3.0791\times10^{-18}\alpha\cos^2}{2\sin\theta\theta^{\frac{3}{2}}}d\theta, \qquad I_{13} = \int_0^\theta \frac{-2.8112\times10^{-19}\cos^2}{2\sin\theta\theta^{\frac{3}{2}}}d\theta,$$

$$I_{14} = \int_0^\theta \frac{-2.2446\times10^{-34}\alpha\theta\cos^2\theta}{2\sin\theta}d\theta, \qquad I_{15} = \int_0^\theta \frac{-0.2556\alpha\sqrt{\theta}\cos^2\theta}{2\sin\theta}d\theta,$$

$$I_{16} = \int_0^\theta \frac{0.6176R\sqrt{\theta}\cos^2\theta}{2\sin\theta P_r}d\theta, \qquad I_{17} = \int_0^\theta \frac{-1.8498\times10^{-17}\sqrt{\theta}\ln\theta}{2\sin\theta}d\theta,$$

$$I_{18} = \int_0^\theta \frac{2.0586\sqrt{\theta}\cos^2\theta}{2\sin\theta P_r}d\theta, \qquad I_{19} = \int_0^\theta \frac{-0.3114\sqrt{\theta}\cos^2\theta}{2\sin\theta}d\theta,$$

$$I_{20} = \int_0^\theta \frac{0.97091R}{2P_r\sin\theta\sqrt{\theta}}d\theta, \qquad I_{21} = \int_0^\theta \frac{-1.1654\times10^{-17}}{2\sin\theta\sqrt{\theta}}d\theta,$$

$$I_{22} = \int_0^\theta \frac{0.32337}{2P_r\sin\theta\sqrt{\theta}}d\theta, \qquad I_{23} = \int_0^\theta \frac{0.7875}{2\sin\theta\sqrt{\theta}}d\theta,$$

$$I_{24} = \int_0^\theta \frac{-3.079\times10^{-18}\alpha}{2\sin\theta\theta^{\frac{3}{2}}}d\theta, \qquad I_{25} = \int_0^\theta \frac{2.8112\times10^{-19}}{2\sin\theta\theta^{\frac{3}{2}}}d\theta,$$

$$I_{26} = \int_0^\theta \frac{2.2446\times10^{-34}\alpha\theta}{2\sin\theta}d\theta, \qquad I_{27} = \int_0^\theta \frac{-6.9389\times10^{-18}\theta}{2\sin\theta}d\theta,$$

$$I_{28} = \int_0^\theta \frac{0.2556\sqrt{\theta}\alpha}{2\sin\theta}d\theta, \qquad I_{29} = \int_0^\theta \frac{-0.6176R\sqrt{\theta}}{2P_r\sin\theta}d\theta,$$

$$I_{30} = \int_0^\theta \frac{1.8498\times10^{-17}\sqrt{\theta}\ln\theta}{2P_r\sin\theta}d\theta, \qquad I_{31} = \int_0^\theta \frac{-2.0586\sqrt{\theta}}{2P_r\sin\theta}d\theta,$$

$$I_{32} = \int_0^\theta \frac{0.3114\sqrt{\theta}}{2\sin\theta}d\theta, \qquad I_{33} = \int_0^\theta \frac{3.4696\times10^{-18}\alpha(\theta-\sin\theta\cos\theta)}{2\sin\theta}d\theta,$$

$$I_{34} = \int_0^\theta \frac{0.97091R(\theta-\sin\theta\cos\theta)}{2P_r\sin\theta\sqrt{\theta}}d\theta, \qquad I_{35} = \int_0^\theta \frac{-1.1654\times10^{-17}(\theta-\sin\theta\cos\theta)}{2\sin\theta\sqrt{\theta}}d\theta,$$

$$I_{36} = \int_0^6 \frac{0.32337(\theta-\sin\theta\cos\theta)}{2P_r\sin\theta\sqrt{\theta}}d\theta, \qquad I_{37} = \int_0^\theta \frac{0.7875(\theta-\sin\theta\cos\theta)}{2\sin\theta\sqrt{\theta}}d\theta,$$

$$I_{38} = \frac{-3.0791\times10^{-18}\alpha(\theta-\sin\theta\cos\theta)}{2\sin\theta\theta^{\frac{3}{2}}}d\theta, \qquad I_{39} = \int_0^\theta \frac{2.8112\times10^{-19}(\theta-\sin\theta\cos\theta)}{2\sin\theta\theta^{\frac{3}{2}}}d\theta,$$

$$I_{40} = \int_0^\theta \frac{-8.6736\times10^{-18}(\theta-\sin\theta\cos\theta)}{2\sin\theta}d\theta, \qquad I_{41} = \int_0^\theta \frac{6.9389\times10^{-18}\cos^2\theta}{2\sin\theta}d\theta.$$

with j_1, j_2 and j_3 as integration constants.

Substituting V_1, V_2 and V_3 into (3.349), we get

$$\begin{aligned} G_{21} = \quad & \sin\theta\Big[-1.7348\times10^{-18}\alpha\big(\cos\theta-\ln[\cos(\theta/2)]+\ln[\sin(\theta 2)]\big)+A_1 \\ & +4.3368\times10^{-18}\big(\cos\theta-\ln[\cos([\theta/2)]+\ln[\sin(\theta/2)]\big)+j_1\Big]+ \\ & +\theta\cos\theta\Big[-1.7348\times10^{-18}\alpha\big(\cos\theta-\ln[\cos(\theta/2)]+\ln[\sin(\theta/2)]\big) \\ & +A_2-4.3368\times10^{-18}\alpha\big(\cos\theta-\ln[\cos(\theta/2)]+\ln[\sin(\theta/2)]\big)+j_2\Big] \\ & +\cos\theta(A_3+j_3). \end{aligned} \tag{3.363}$$

Using boundary conditions (3.342) into (3.363), yields

$$\begin{aligned} j_1 &= 0.18861\alpha-0.829203-\frac{1}{P_r}\Big[1.95391+1.76136R\Big], \\ j_2 &= -0.63662\Big[-0.205958+0.43689\alpha-1\times10^{-21}\Big(2.98817\times10^{12}\alpha+ \\ &\quad \frac{1.02259\times10^{10}}{P_r}+\frac{3.07029\times10^{10}R}{P_r}\Big)-\frac{3.82184}{P_r}-\frac{1.9658}{P_r}\Big], \\ j_3 &= 0, \end{aligned} \tag{3.364}$$

where the integrals I_i for $i=8,.....41$ in series form are written as

$$\begin{aligned} I_8 &\cong \frac{0.97091R}{P_r\sqrt{\theta}}+\frac{0.26967R\theta^{\frac{3}{2}}}{Pr}+\cdots, \\ I_9 &\cong \frac{-1.1654\times10^{-17}}{\sqrt{\theta}}-3.23722\times10^{-18}\theta^{\frac{3}{2}}+\cdots, \\ I_{10} &\cong \frac{0.32337}{P_r\sqrt{\theta}}+\frac{0.089825\theta^{\frac{3}{2}}}{P_r}+\cdots, \\ I_{11} &\cong \frac{0.7875}{\sqrt{\theta}}+0.21875\theta^{\frac{3}{2}}+\cdots, \\ I_{12} &\cong \frac{-1.02637\times10^{-18}\alpha}{\theta^{\frac{3}{2}}}-\frac{1.56482\times10^{-33}\theta}{\theta^{\frac{3}{2}}}-\frac{2.56592\times10^{-18}\theta^2\alpha}{\theta^{\frac{3}{2}}} \\ &+ \frac{6.561\times10^{-35}\theta^3\alpha}{\theta^{\frac{3}{2}}}+\frac{1.14611\times10^{-19}\theta^4\alpha}{\theta^{\frac{3}{2}}}+\cdots, \end{aligned}$$

$$
\begin{aligned}
I_{13} &\cong \frac{9.37067\times^{-20}}{\theta^{\frac{3}{2}}} + \frac{1.54225\times 10^{-34}\theta}{\theta^{\frac{3}{2}}} + \frac{2.34267\times 10^{-19}\theta^2}{\theta^{\frac{3}{2}}} \\
&- \frac{7.50282\times 10^{-36}\theta^3}{\theta^{\frac{3}{2}}} - \frac{-1.04639\times 10^{-20}\theta^4}{\theta^{\frac{3}{2}}} + \cdots, \\
I_{14} &\cong -1.1223\times 10^{-34}\alpha\theta + 3.1175\times 10^{-35}\alpha\theta^3 + \cdots, \\
I_{15} &\cong -0.2556\alpha\sqrt{\theta} + 0.0426\alpha\theta^{\frac{5}{2}} + \cdots, \\
I_{16} &\cong \frac{0.6176R\sqrt{\theta}}{P_r} - \frac{0.102933R\theta^{\frac{5}{2}}}{P_r} + \cdots, \\
I_{17} &\cong 3.6996\times 10^{-17}\sqrt{\theta} - 1.2332\times 10^{-18}\theta^{\frac{5}{2}} - 1.8498\times 10^{-17}\sqrt{\theta}\ln\theta \\
&+ 3.083\times 10^{-18}\theta^{\frac{5}{2}}\ln\theta + \cdots, \\
I_{18} &\cong \frac{2.0586\sqrt{\theta}}{P_r} - \frac{0.3431\theta^{\frac{5}{2}}}{P_r} + \cdots, \\
I_{19} &\cong -0.3114\sqrt{\theta} + 0.0519\theta^{\frac{5}{2}} + \cdots, \\
I_{20} &\cong -\frac{0.97091R}{P_r\sqrt{\theta}} + \frac{0.0539394R\theta^{\frac{3}{2}}}{P_r} + \cdots, \\
I_{21} &\cong \frac{1.1654\times 10^{-17}}{\sqrt{\theta}} - 6.7444\times 10^{-19}\theta^{\frac{3}{2}} + \cdots, \\
I_{22} &\cong \frac{-0.32337}{P_r\sqrt{\theta}} + \frac{0.089825\theta^{\frac{3}{2}}}{P_r} + \cdots, \\
I_{23} &\cong \frac{-0.7875}{\sqrt{\theta}} + 0.21875\theta^{\frac{3}{2}} + \cdots, \\
I_{24} &\cong \frac{1.02637\times 10^{-18}\alpha}{\theta^{\frac{3}{2}}} - \frac{5.77779\times 10^{-34}\alpha\theta}{\theta^{\frac{3}{2}}} - \frac{5.13183\times 10^{-19}\alpha\theta^2}{\theta^{\frac{3}{2}}} \\
&+ \frac{1.77255\times 10^{-35}\alpha\theta^3}{\theta^{\frac{3}{2}}} - \frac{1.19743\times 10^{-20}\alpha\theta^4}{\theta^{\frac{3}{2}}} + \cdots, \\
I_{25} &\cong \frac{9.37067\times 10^{-20}}{\theta^{\frac{3}{2}}} + \frac{9.62965\times 10^{-35}\theta}{\theta^{\frac{3}{2}}} + \frac{4.68533\times 10^{-20}\theta^2}{\theta^{\frac{3}{2}}} \\
&- \frac{1.61833\times 10^{-36}\theta^3}{\theta^{\frac{3}{2}}} + \frac{1.09324\times 10^{-21}\theta^4}{\theta^{\frac{3}{2}}} + \cdots, \\
I_{26} &\cong 1.223\times 10^{-34}\alpha\theta + 6.235\times 10^{-36}\alpha\theta^3 + \cdots, \\
I_{27} &\cong -3.46945\times 10^{-18} - 1.92747\times 10^{-19}\theta^3 + \cdots, \\
I_{28} &\cong 0.2556\alpha\sqrt{\theta} + 0.00852\alpha\theta^{\frac{5}{2}} + \cdots, \\
I_{29} &\cong \frac{-0.6176R\sqrt{\theta}}{P_r} - \frac{0.0205867R\theta^{\frac{5}{2}}}{P_r} + \cdots, \\
I_{30} &\cong -3.6996\times 10^{-17}\sqrt{\theta} - 2.4664\times 10^{-19}\theta^{\frac{5}{2}} \\
&+ 1.8498\times 10^{-17}\sqrt{\theta}\ln\theta + 6.166\times 10^{-19}\theta^{\frac{5}{2}}\ln\theta + \cdots, \\
I_{31} &\cong \frac{-2.0586\sqrt{\theta}}{P_r} - \frac{0.06862\theta^{\frac{5}{2}}}{P_r} + \cdots,
\end{aligned}
$$

$$
\begin{aligned}
I_{32} &\cong 0.3114\sqrt{\theta} + 0.01038\theta^{\frac{5}{2}} + \cdots, \\
I_{33} &\cong 3.85511 \times 10^{-19}\theta^3\alpha + \cdots, \\
I_{34} &\cong \frac{0.129455R\theta^{\frac{5}{2}}}{P_r} + \cdots, \\
I_{35} &\cong -1.55387 \times 10^{-18}\theta^{\frac{5}{2}} + \cdots, \\
I_{36} &\cong -1.55387 \times 10^{-18}\theta^{\frac{5}{2}} + \cdots, \\
I_{37} &\cong \frac{0.043116\theta^{\frac{5}{2}}}{P_r} + \cdots, \\
I_{38} &\cong 0.105\theta^{\frac{5}{2}} + ..., \\
I_{39} &\cong -6.84244 \times 10^{-19}\theta^{\frac{3}{2}}\alpha + \cdots, \\
I_{40} &\cong 6.24711 \times 10^{-20}\theta^{\frac{3}{2}} + \cdots, \\
I_{41} &\cong -9.63733 \times 10^{-19}\theta^3 + \cdots.
\end{aligned}
$$

Substituting (3.331) and (3.363) into (3.247), gives the value momentum first order (3.246) as

$$
\begin{aligned}
G_2 \;=\; & \frac{\alpha}{\pi}\big[3\ln\tan(\theta/2)(\sin\theta - \theta\cos\theta) - 2\theta\big] - 3 + (\theta\cos\theta - \sin\theta)I_6 \\
& + \big(\frac{3\alpha}{\pi}I_6 - I_7\big)\cos\theta + b_1\sin\theta + b_2\theta\cos\theta + b_3\cos\theta \qquad (3.365) \\
& + G_r\Big\{\sin\theta\Big[- 1.7348 \times 10^{-18}\alpha\big(\cos\theta - \ln[\cos(\theta/2)] + \ln[\sin(\theta 2)]\big) + A_1 \\
& + 4.3368 \times 10^{-18}\big(\cos\theta - \ln[\cos([\theta/2)] + \ln[\sin(\theta/2)]\big) + j_1\Big] \\
& + \theta\cos\theta\Big[- 1.7348 \times 10^{-18}\alpha\big(\cos\theta - \ln[\cos(\theta/2)] + \ln[\sin(\theta/2)]\big) \\
& + A_2 - 4.3368 \times 10^{-18}\alpha\big(\cos\theta - \ln[\cos(\theta/2)] + \ln[\sin(\theta/2)]\,\big) + j_2\Big] \\
& + \cos\theta(A_3 + j_3)\Big\}. \qquad (3.366)
\end{aligned}
$$

Thus from equation (3.246), we get momentum variation inside the solid rocket chamber as

$$\begin{aligned}
G &= \sin\theta + G_r\Big[0.02\sqrt{\theta}\big[\sin\theta - \theta\cos\theta\big] + I_1\sin\theta \\
&\quad + \cos\theta\big[\theta I_2 + I_3 + I_4 + I_5\big] + a_1\sin\theta + a_2\theta\cos\theta + a_3\cos\theta\Big] \\
&\quad + K\Big[\frac{\alpha}{\pi}\big[3\ln\tan(\theta/2)(\sin\theta - \theta\cos\theta) - 2\theta\big] - 3 + (\theta\cos\theta - \sin\theta)I_6 \\
&\quad + \big(\frac{3\alpha}{\pi}I_6 - I_7\big)\cos\theta + b_1\sin\theta + b_2\theta\cos\theta + b_3\cos\theta \\
&\quad + G_r\Big\{\sin\theta\Big[-1.7348\times10^{-18}\alpha\big(\cos\theta - \ln[\cos(\theta/2)] + \ln[\sin(\theta 2)]\big) + A_1 \\
&\quad + 4.3368\times10^{-18}\big(\cos\theta - \ln[\cos([\theta/2)] + \ln[\sin(\theta/2)]\big) + j_1\Big] \\
&\quad + \theta\cos\theta\Big[-1.7348\times10^{-18}\alpha\big(\cos\theta - \ln[\cos(\theta/2)] + \ln[\sin(\theta/2)]\big) \\
&\quad + A_2 - 4.3368\times10^{-18}\alpha\big(\cos\theta - \ln[\cos(\theta/2)] + \ln[\sin(\theta/2)]\big) + j_2\Big] \\
&\quad + \cos\theta(A_3 + j_3)\Big\}\Big]. \qquad (3.367)
\end{aligned}$$

Using the value of θ given by (3.275) into equation (3.273) and boundary conditions (3.273), yields

$$\begin{aligned}
&H_{21}\frac{dG_{10}}{d\theta} + H_{20}\frac{dG_{11}}{d\theta} + H_{11}\frac{dG_{20}}{d\theta} + H_{10}\frac{dG_{21}}{d\theta} - \frac{1}{2}G_{21}\frac{dH_{10}}{d\theta} - \frac{1}{P_r}\frac{dH_{11}}{d\theta} - \frac{2R}{P_r}\frac{dH_{11}}{d\theta} \\
&-\frac{1}{2}G_{20}\frac{dH_{11}}{d\theta} - \frac{1}{2}G_{11}\frac{dH_{20}}{d\theta} - \frac{1}{2}G_{10}\frac{H_{21}}{d\theta} - \frac{\theta}{P_r}\frac{d^2H_{11}}{d\theta^2} - \frac{4R\theta}{P_r}\frac{d^2H_{11}}{d\theta} = 0, \qquad (3.368)
\end{aligned}$$

and corresponding boundaries

$$\text{(i) } H_{21}(\pi/2) = 0, \text{ (ii) } \frac{dH_{21}(0)}{d\theta} = 0. \qquad (3.369)$$

Equation (3.368) is not easily solvable and requires G_{21}, G_{20}, G_{11}, G_{10}, H_{20}, H_{11} and H_{10} in

series form before solving. Thus the series form of G_{21} is given by

$$
\begin{aligned}
G_{21} &= \frac{1.08334\times10^{-34} - 1.73334\times10^{-33}\alpha}{\sqrt{\theta}} + \\
&\left(1.73472\times10^{-17} + 1.38778\times10^{-16}\alpha - \frac{5.55112\times10^{-16}}{P_r} + \frac{1.11022\times10^{-16}R}{P_r}\right) \\
&-\frac{2.1426\times10^{-33}\big(-1.5545\times10^{17} - 4.6635\times10^{17}R + \alpha P_r\big)\sqrt{\theta}}{P_r} + \Bigg(-0.698086 \\
&-0.0895229\alpha + \frac{0.479149}{P_r} - \frac{0.50989R}{P_r}\Bigg)\theta + \Bigg(-2.77556\times10^{-16} - 2.77556\times10^{-16}\alpha \\
&+3.08149\ln\theta + \frac{2.22045\times10^{-15}}{P_r} + \frac{6.66134\times10^{-16}R}{P_r}\Bigg)\theta^{\frac{3}{2}} + \Bigg(-1.21431\times10^{-17} \\
&-6.93889\times10^{-17}\alpha + \frac{2.77556\times10^{-16}}{P_r} - \frac{5.55112\times10^{-17}R}{P_r}\Bigg)\theta^2 + O(\theta^{\frac{5}{2}}).
\end{aligned} \tag{3.370}
$$

Using (3.339), (3.340), (3.370) and (3.310) into (3.368), thereafter solving the obtained equation together with boundary (3.369), yields

$$
\begin{aligned}
H_{21} &= \frac{2.77556\times10^{-16}}{P_r\theta^3}\Bigg(3.96584\times10^{14}\theta^4 + 1.18975\times10^{15}R\theta^4 + 0.725\theta^{4.5} \\
&+4.8R\theta^{4.5} - 2.52473\times10^{14}\theta^5 - 7.57419\times10^{14}R\theta^5 + 16.6568\theta^{5.5} + 7.10985R\times10^{5.5} \\
&+2\theta^6 - 0.4R\theta^6 + 0.0823318\theta^{6.5} + 0.246995R\theta^{6.5} + 0.4\theta^5\ln\theta \\
&+7.80626\times10^{-19}\theta^{3.5}P_r + 0.125\theta^4P_r + 3.11476\times10^5P_r - 2.38917\theta^{5.5}P_r \\
&-1.98292\times10^{14}\theta^6P_r + 0.0661165\theta^{6.5}P_r + 0.0323316\theta^{7.5}P_r - 1.249\times10^{-17}\theta^{3.5}\alpha P_r \\
&\theta^4\alpha P_r - 1.5439\times10^{-17}\theta^{4.5}\alpha P_r + 2.6035\theta^5\alpha P_r - 1.96906\theta^{5.5}\alpha P_r - 0.5\theta^6\alpha P_r \\
&+0.00666862\theta^{6.5}\alpha P_r + 1.50303\times10^{-16}\theta^5\ln\theta P_r \\
&+2.22045\times10^{-17}\theta^{5.5}\ln\theta P_r - 3.75759\times10^{-17}\theta^5\alpha\ln\theta P_r\Bigg).
\end{aligned} \tag{3.371}
$$

Substituting (3.340) and (3.371) into (3.247), gives the value of energy first order term (3.247)

as

$$
\begin{aligned}
H_2 &= \frac{2}{\pi P_r}\Big(4\pi\theta + 12\pi R\theta - 8\theta^2 - 24R\theta^2 + \pi^2\theta^2 P_r - 2\pi\theta^3 P_r\Big) \\
&\quad + G_r\Bigg[\frac{2.77556\times 10^{-16}}{P_r\theta^3}\Big(3.96584\times 10^{14}\theta^4 + 1.18975\times 10^{15}R\theta^4 + 0.725\theta^{4.5} \\
&\quad + 4.8R\theta^{4.5} - 2.52473\times 10^{14}\theta^5 - 7.57419\times 10^{14}R\theta^5 + 16.6568\theta^{5.5} + 7.10985R\times 10^{5.5} \\
&\quad + 2\theta^6 - 0.4R\theta^6 + 0.0823318\theta^{6.5} + 0.4\theta^5\ln\theta + 7.80626\times 10^{-19}\theta^{3.5}P_r + 0.125\theta^4 P_r \\
&\quad + 0.246995R\theta^{6.5} + 3.11476\times 10^5 P_r - 2.38917\theta^{5.5}P_r - 1.98292\times 10^{14}\theta^6 P_r \\
&\quad + 0.0661165\theta^{6.5}P_r + 0.0323316\theta^{7.5}P_r - 1.249\times 10^{-17}\times\theta^{3.5}\alpha P_r - 1.96906\theta^{5.5}\alpha P_r \\
&\quad - 0.5\theta^6\alpha P_r + 0.00666862\theta^{6.5}\alpha P_r + 1.50303\times 10^{-16}\theta^5\ln\theta P_r \\
&\quad + 2.22045\times 10^{-17}\theta^{5.5}\ln\theta P_r + -3.75759\times 10^{-17}\theta^5\alpha\ln\theta P_r\Big)\Bigg].
\end{aligned}
\tag{3.372}
$$

Using the values of H_1 and H_2 into (3.247), yields temperature distribution inside the solid rocket chamber as

$$
\begin{aligned}
H &= -\frac{\cos 2\theta}{2} + \frac{1}{2} + G_r\big[3.49232\times 10^{17}\big(\theta^2 - 0.059607\theta^{\frac{5}{2}} - 0.128479\theta^{\frac{7}{2}}\big)\big] \\
&\quad + K\Bigg\{\frac{2}{\pi P_r}\Big(4\pi\theta + 12\pi R\theta - 8\theta^2 - 24R\theta^2 + \pi^2\theta^2 P_r - 2\pi\theta^3 P_r\Big) \\
&\quad + G_r\Bigg[\frac{2.77556\times 10^{-16}}{P_r\theta^3}\Big(3.96584\times 10^{14}\theta^4 + 1.18975\times 10^{15}R\theta^4 + 0.725\theta^{4.5} + 4.8R\theta^{4.5} \\
&\quad - 2.52473\times 10^{14}\theta^5 - 7.57419\times 10^{14}R\theta^5 + 16.6568\theta^{5.5} + 7.10985R\times 10^{5.5} + 2\theta^6 - 0.4R\theta^6 \\
&\quad + 0.0823318\theta^{6.5} + 0.4\theta^5\ln\theta + 7.80626\times 10^{-19}\theta^{3.5}P_r + 0.125\theta^4 P_r + 0.246995R\theta^{6.5} \\
&\quad + 3.11476\times 10^5 P_r - 2.38917\theta^{5.5}P_r - 1.98292\times 10^{14}\theta^6 P_r + 0.0661165\theta^{6.5}P_r \\
&\quad + 0.0323316\theta^{7.5}P_r - 1.249\times 10^{-17}\times\theta^{3.5}\alpha P_r - 1.96906\theta^{5.5}\alpha P_r - 0.5\theta^6\alpha P_r \\
&\quad + 0.00666862\theta^{6.5}\alpha P_r + 1.50303\times 10^{-16}\theta^5\ln\theta P_r + 2.22045\times 10^{-17}\theta^{5.5}\ln\theta P_r \\
&\quad - 3.75759\times 10^{-17}\theta^5\alpha\ln\theta P_r\Big)\Bigg]\Bigg\}.
\end{aligned}
\tag{3.373}
$$

In terms of β, equation (3.236) can be rewritten as

$$
\frac{u}{z} = G_\beta, \qquad v = -\frac{G}{\sqrt{2\beta}}. \tag{3.374}
$$

To determine the radial pressure drop, we substitute (3.235) into (3.39) and also the fact that the temperature is in terms of H from the previous calculation, thus

$$
P_\beta = \Big[-\frac{G^2}{(2\beta)^2} - \frac{GG_\beta}{2\beta} - \alpha K G_\beta - K G_{\beta\beta}\Big] + \frac{G_r H}{\sqrt{2\beta}}. \tag{3.375}
$$

The radial pressure distribution is obtain by integrating (3.375) with boundary conditions (3.245) and letting P_c to be the pressure at the centreline and $P(\beta)$ surface pressure, thus

$$\begin{aligned}\int_{P_c}^{P(\beta)} dP &= -\int_0^{\beta}\Bigg[-\frac{G^2}{(2\beta)^2}-\frac{GG_\beta}{2\beta}-\alpha KG_\beta \\ &- KG_{\beta\beta}\Bigg]d\beta+\int_0^{\beta}\frac{G_rH}{\sqrt{2\beta}}d\beta.\end{aligned} \tag{3.376}$$

The resulting pressure drop in the radial direction is given by

$$\begin{aligned}\Delta P_r &= P(\beta)-P_c, \\ &= KG_\beta(0)-\left[\frac{1}{\beta}\left(\frac{G}{2}\right)^2+\alpha KG+KG_\beta\right]+\chi,\end{aligned} \tag{3.377}$$

where $\chi=\int_0^{\beta}\frac{G_rH}{\sqrt{2\beta}}d\beta$. This integral indicates that bouyancy force contributes to the increase in pressure inside the combustion chamber in the radial direction.

3.5 Results and Analysis

In this section, we give graphical representations of axial-velocity per length u/z and temperature distribution H. The analysis is carried out to understand the dynamics of solid rocket motor operation under the effects of dimensionless quantities such as wall expansion rate α, Grashof number G_r, Reynolds number R_e, Prandtl number P_r and radiation number R on axial-velocity and temperature distribution respectively.

3.5.1 Behaviour of axial-velocity under the influence of dimensionless quantities

This subsection studies the effects of various parameters on axial-velocity of propellant as it flows inside a combustion chamber during solid rocket motor operation.

Effects of wall dilation α on axial-velocity ratio

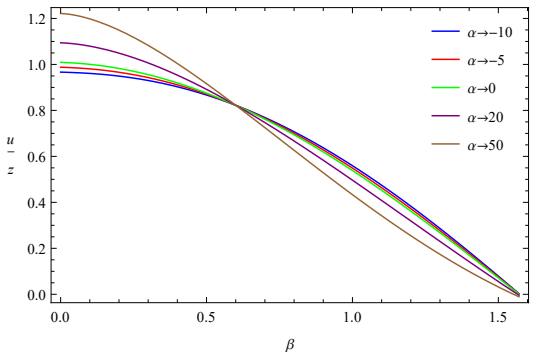

Figure 3.4: Axial-velocity profiles over a range of α at $K = 0.01$, $P_r = 6$, $R = 10$ and $G_r = 0.02$.

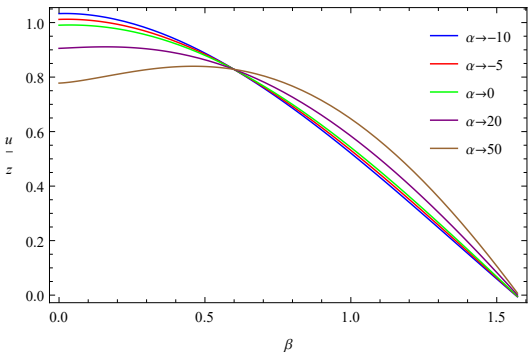

Figure 3.5: Axial-velocity profiles over a range of α at $K = -0.01$, $P_r = 6$, $R = 10$ and $G_r = 0.02$.

Figure 3.4 illustrates the behaviour of self-axial velocity profiles over a range of wall dilation rate α for cross-flow Reynolds number $K = 0.01$. In the case of wall expansion ratio, that is ($\alpha > 0$), we observe that the increase of combustion chamber volume leads to a higher axial-velocity of propellant (fluid) at the center and lower towards the surface wall. This observation is due to the additional space created by expanding the surface wall which is filled by fluid injected inside the combustion chamber, hence the net work done inside the chamber is positive work done. The net positive work done propels the fluid bulk, thus result in the high axial-velocity at the centre due to no slip condition, it can also be shown from Figure 3.4 that axial- velocity increases with the decrease of injection.

In the case of contraction ($\alpha < 0$), which lead to the decrease in combustion chamber volume and yields positive work done by the surface wall of the combustion chamber and fluid injection such that the net work done inside the chamber is high towards the surface wall and low towards the centre, thus the fluid bulk's axial-velocity becomes high towards the surface wall and low towards the centre of the combustion chamber. However in the case of wall contraction rate while sucking fluid out of the combustion chamber, it is observed that the decrease in combustion chamber volume leads to a higher axial-velocity of fluid at the centre and lower towards surface wall. This is due to the decrease in space resulting from the contracting wall surface and sucking fluid out of the chamber (positive work done), thus the fluid moves faster

at the centre and slower towards the surface wall. See Figure 3.5.

Effects of Reynolds number K on axial velocity

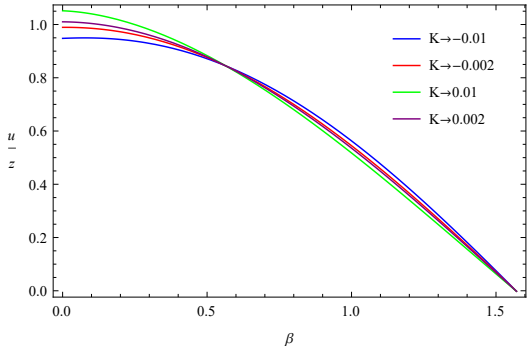

Figure 3.6: Axial-velocity profiles over a range of K at $\alpha = 10$, $P_r = 6$, $R = 10$ and $G_r = 0.02$.

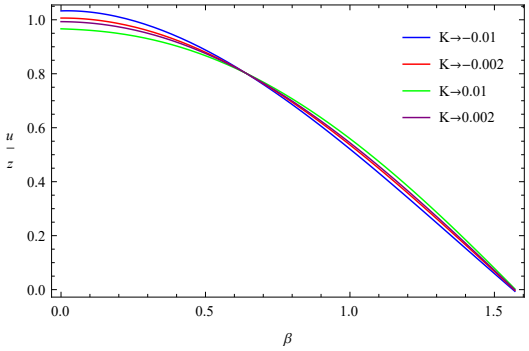

Figure 3.7: Axial-velocity profiles over a range of K at $\alpha = -10$, $P_r = 6$, $R = 10$ and $G_r = 0.02$.

Figure 3.6 illustrates the behaviour of self axial-velocity profiles over a range of Reynolds number R_e and wall dilation $\alpha = -10$ and $\alpha = 10$ respectively.

In the case of injecting fluid inside the combustion chamber, that is $(K > 0)$, we observe that the increase of combustion chamber volume while injecting fluid inside the chamber leads to a higher axial-velocity of fluid at the centre and lower towards surface wall. This observation is due to the additional space created by expanding the surface wall which allows more fluid to flow inside the combustion chamber, that result in positive net work done. The net positive work done propels the fluid bulk which lead to high axial-velocity at the centre due to no slip condition.

In the case of suction $(K < 0)$, sucking fluid out of the combustion chamber while increasing the volume yields to negative work done inside the chamber, thus the fluid axial-velocity will be low towards the centre and high towards the surface wall when fluid is removed out the combustion chamber. This behaviour is due to the additional space created by expanding the surface wall which allows fluid to flow towards the wall instead of flowing towards the centre and thereafter to rocket nozzle, thus sucking fluid decreases net flow towards the rocket nozzle, thus decrease velocity. See Figure 3.6.

In the case of injecting fluid inside the chamber, that is ($K > 0$) while decreasing the volume of the chamber ($\alpha < 0$), it observed that the decrease in combustion chamber volume while injecting fluid inside the chamber leads to the decrease in axial-velocity towards the centre and increase in axial-velocity towards surface wall. This observation is due to the decrease in combustion chamber space and the introduction of more fluid inside the combustion chamber which decreases the free movement of fluid particles inside the combustion chamber, thus decrease velocity which leads to the decrease in thrust during operation.

In the case of suction ($K < 0$) while decreasing the chamber volume, the flow field is such that the axial-velocity increases towards the centre while decreases towards the surface wall. This behaviour is due to the fact that the fluid inside the combustion chamber has more space to flow freely when fluid particles decreases during suction. See Figure 3.7.

Effects of Prandtl number on axial-velocity

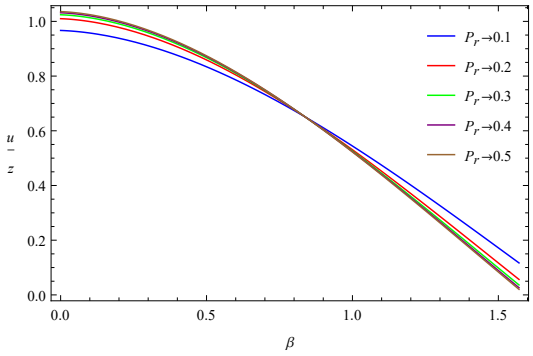

Figure 3.8: Axial-velocity profiles over a range of P_r at $\alpha = 10$, $G_r = 0.02$, $R = 10$ and $K = 0.01$.

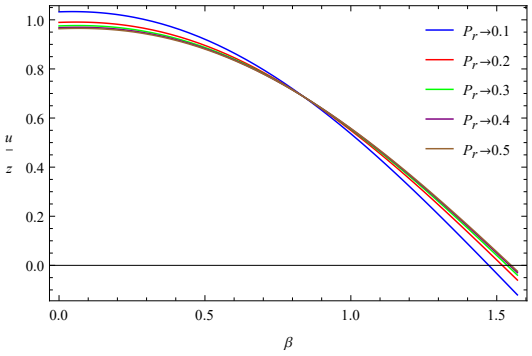

Figure 3.9: Axial-velocity profiles over a range of P_r at $\alpha = 10$, $G_r = 0.02$, $R = 10$ and $K = -0.01$.

Figures 3.8 and 3.9 respectively show the behaviour of self-axial velocity profiles over a range of Prandtl number P_r for injection and suction. The increase in Prandtl number Pr, leads to high axial-velocity towards the centre and low towards the surface wall during injection; however the increase in Prandtl number leads to a decrease in velocity towards the centre while increase the axial-velocity towards the wall during suction. This behaviour is caused by the effect of heat diffusion which decreases the density of the fluid such that the fluid can flow

easily. Thus fluid can be injected or sucked easily in or out of the chamber as a result increase or decrease velocity receptively. See Figures 3.8 and 3.9 respectively.

Effects of radiation on the axial-velocity

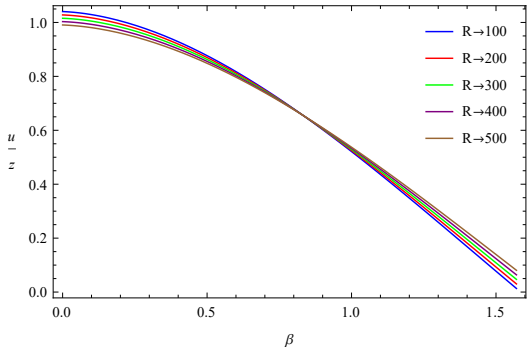

Figure 3.10: Axial-velocity profiles over a range of R at $\alpha = 10$, $G_r = 0.02$, $K = 0.01$ and $P_r = 6$.

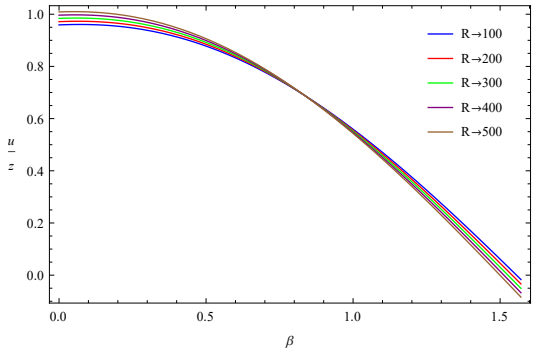

Figure 3.11: Axial-velocity profiles over a range of R at $\alpha = 10$, $G_r = 0.02$, $K = -0.01$ and $P_r = 6$.

Figures 3.10 and 3.11 illustrate the behaviour of self-axial velocity profiles over a range of radiation R for injection $K = 0.01$ and suction $K = -0.01$. The increase in radiation R, leads to low axial-velocity towards the centre and high axial- velocity towards the surface wall during injection and also leads to the increase in axial-velocity towards the centre while decrease the axial-velocity towards the surface wall during suction. This behaviour is due to high Prandtl number ($P_r = 6$) which leads to the domination of momentum diffusivity dominates over thermal diffusivity, thus as fluid particles absorb high radiation when fluid is injected into combustion chamber as a result create friction inside the combustion chamber, thus an increase in radiation leads to a decrease in axial-velocity in the case of injection. In the case of sucking fluid out of the combustion chamber fluid with more radiation will be sucked out, thus less friction will be created inside the combustion chamber as a result, the fluid will flow with higher axial-velocity towards the centre and lower axial-velocity towards the surface wall.

Effects of Grashof number on axial-velocity

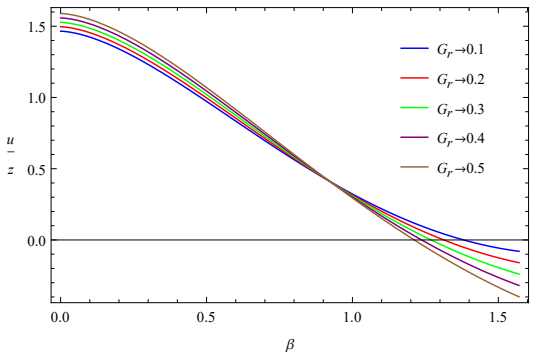

Figure 3.12: Axial-velocity profiles over a range of G_r at $K = 0.01$, $P_r = 2$, $R = 10$ and $\alpha = 50$.

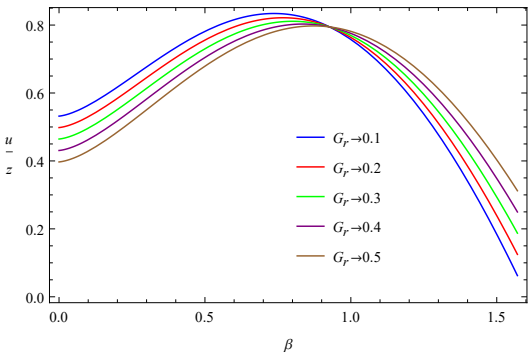

Figure 3.13: Axial-velocity profiles over a range of G_r at $K = -0.01$, $P_r = 2$, $R = 10$ and $\alpha = 50$.

Figures 3.12 and 3.13 illustrate the behaviour of axial-velocity inside the combustion chamber of a solid rocket motor. When injecting propellant ($K > 0$) into combustion chamber, we observe that the increase in Grashof number leads to an increase in the axial-velocity towards the centre and decrease in axial-velocity towards the surface wall of the combustion chamber. This is due to less dense fluid particles moving towards the top of the combustion chamber to occupy the space created by chamber expansion. In the case of ($K < 0$) the higher the Grashof number, the more fluid particles will move toward the surface wall, thus decrease the axial-velocity towards the wall. Also the more dense fluid particles will move towards the bottom of the chamber due to gravity and move less dense fluid particles side ways in the axial direction, thus increase the velocity far from the upper surface (towards the centre). The less dense fluid will move at higher speed towards the centre to occupy the space created by the chamber as it expands. Near the surface wall of the combustion chamber, it is observed that the fluid creates a reverse flow due to the effects of fluid injection. In the case of suction, we observe that the less dense fluid has lower speed at the wall compared to more dense fluid. For suction, the more dense fluid will move towards the centre due to force of gravity and the less dense particles will move towards the upper surface wall, thus for high Grashof number the more dense particles will move faster towards the centre and less dense will move faster towards the surface wall.

3.5.2 Temperature distribution under the influence of dimensionless quantities

In this subsection, effects of various parameter which influence temperature distribution of propellant as it flows inside the combustion of solid rocket motors during operation are studied.

Effects of Prandtl number on temperature distribution

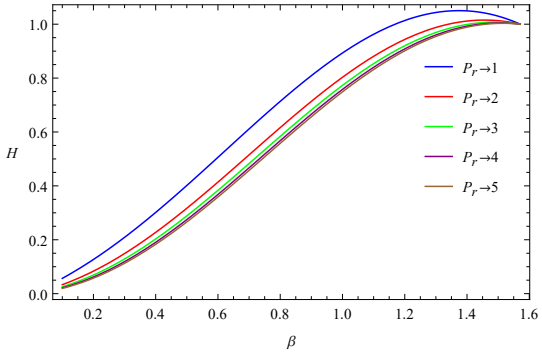

Figure 3.14: Temperature distribution for a range of P_r at $K = 0.002$, $R = 10$, $\alpha = 5$ and $G_r = 0.02$.

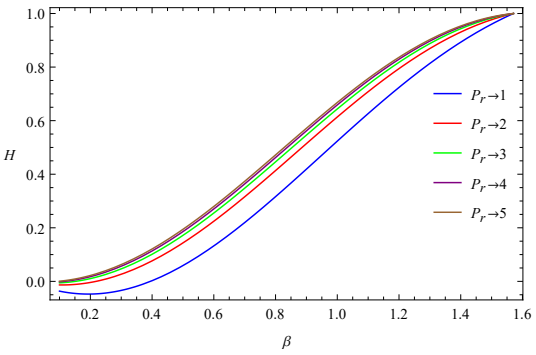

Figure 3.15: Temperature distribution for a range of P_r at $K = -0.002$, $R = 10$, $\alpha = 5$ and $G_r = 0.02$.

Figures 3.14 and 3.15 illustrate that the propellant temperature decreases from the surface wall towards the centre for both injection and suction.

The increase in Prandtl number throughout the rocket chamber leads to a sharp decrease in temperature during injection compared to suction. Since Prandtl number is directly proportional to momentum diffusivity (velocity) and inversely proportional to thermal diffusivity (heat conduction) which implies that the increase in Prandtl number leads to the decrease in heat conduction, thus an increase in Prandtl number result in decrease in temperature. Also fluid injection increases momentum diffusivity which increase Prandtl number. Suction decrease momentum diffusivity and Prandtl number which leads to increase in heat condition, thus temperature decreases more for small Prandtl number during suction. The temperature increases slightly close to the surface wall during injection (addition of energy due work done by additional particles) thereafter decrease towards centre. This slight increase in temperature

close to the surface wall provides the propellant with energy to penetrate deeply towards the centre of the combustion chamber and also contributes to reaction away from the combustion chamber surface wall. The decrease in temperature is due to the fact that the increase in Prandtl number leads to the decrease in temperature difference, thus decrease heat conduction of the propellant. The decrease in temperature towards the centre is caused by the transformation of internal energy to rocket thrust which propels from the centre of mass of the rocket, thus lose the temperature towards the centre in a form of rocket thrust.

Effects of radiation number on temperature distribution

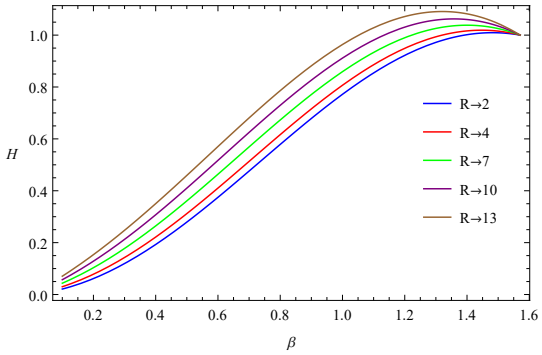

Figure 3.16: Temperature distribution for a range of R at $K = 0.002$, $\alpha = 5$, $P_r = 6$ and $G_r = 0.02$.

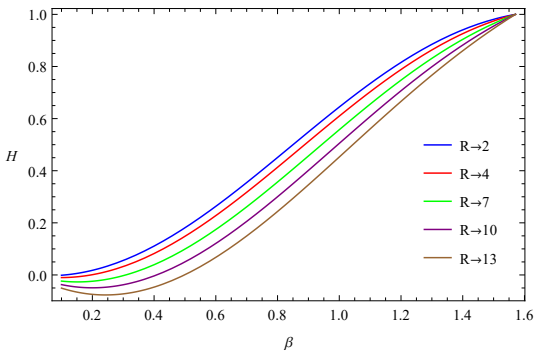

Figure 3.17: Temperature distribution for a range of R at $K = -0.002$, $\alpha = 5$, $P_r = 6$ and $G_r = 0.02$.

Figure 3.16 illustrates the increase radiation leads to the increase in temperature. This observation is due to fact that additional energy in a form of radiation will increase the temperature inside combustion chamber. Similarly the temperature decreases towards the centre since the system loses temperature in a form of rocket thrust at the centre. Figures 3.17 illustrates that the increase in radiation leads to the decrease in temperature. This observation is due to fact that energy in a form of radiation is decreased as particles decreases when sucked out of the system which leads to the decrease in temperature inside combustion chamber.

Effects of Reynolds number on temperature distribution

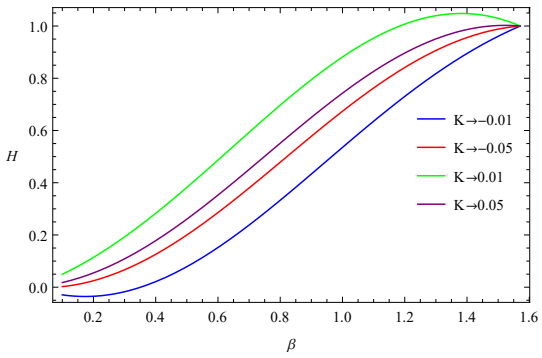

Figure 3.18: Temperature distribution for a range of K at $R = 10$, $\alpha = 5$, $P_r = 6$ and $G_r = 0.02$.

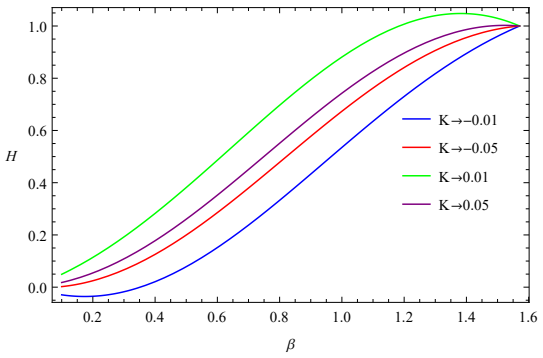

Figure 3.19: Temperature distribution for a range of K at $R = 10$, $\alpha = -5$, $P_r = 6$ and $G_r = 0.02$.

Figures 3.18 and 3.19 illustrate that the temperature of propellant gas for both contracting or expanding chamber increases when there is fluid injection during solid rocket motor operation. The increase in temperature is due to the fact that injection of fluid particles inside the chamber increases momentum as a result the temperature increase (work energy principle which relates the energy to momentum), thus the system temperature will increase. Also, the decrease in fluid particles during operation (suction) decreases momentum, thus decrease temperature. Figure 3.19 indicates that irrespective of contraction or expansion the temperature distribution behaves the same.

Effects of Grashof number on temperature distribution

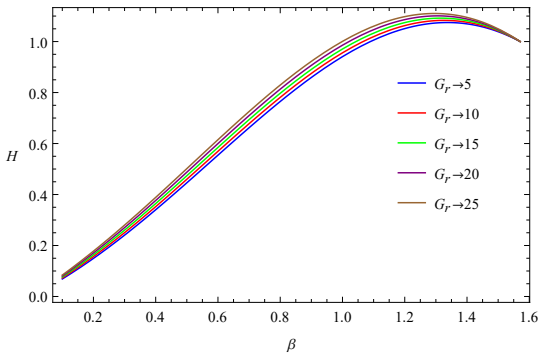

Figure 3.20: Temperature distribution for a range of G_r at $K = 0.002$, $R = 10$, $\alpha = 5$, $P_r = 6$.

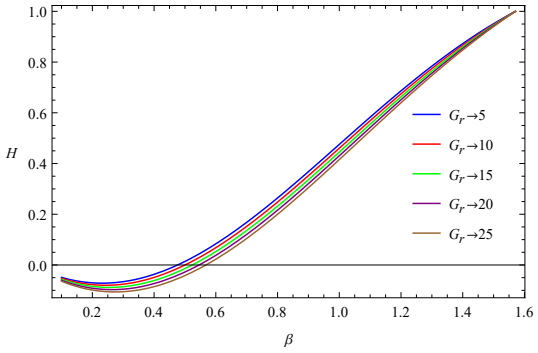

Figure 3.21: Temperature distribution for a range of G_r at $K = -0.002$, $R = 10$, $\alpha = 5$, $P_r = 6$.

Figures 3.20 and 3.21 indicate the effects of Grashof number on temperature distribution of propellant gas for injecting and sucking fluid.

The temperature increases slightly close to the surface wall thereafter decrease towards the centre when injecting propellant into the system, see Figure 3.20. This slight increase in temperature close to the surface wall provides the propellant gas (fuel) with energy to penetrate deeply towards the centre of the combustion chamber and also contribute to chemical reaction, which causes combustion away from the surface wall. This observation is due to high Grashof number (high temperature difference) which leads to high heat diffusion and more heat transfer within the fluid bulk which raises the temperature and decreases the density of the fluid/propellant. The rise in temperature will be more for high Grashof number since more temperature is absorbed from the surface wall. In the case of suction, see Figure 3.21, the system will have more less dense fluid particle towards the surface wall and more dense fluid particles towards the centre since the temperature from the surface wall affects particles close the wall more. Sucking out fluid particles from the chamber decreases the temperature of the system since the less dense particles sucked out of the chamber posses high temperature, hence takes temperature out of system.

3.6 Concluding remarks

In this project, we further studied the problem of viscous incompressible fluid in a cylindrical porous pipe with expanding or contracting surface wall [1]. To further understand the dynamics of solid rocket motor thrust. Lie group technique was employed to find semi-analytical solutions of the problem in conjunction with double perturbation expansions method.

The semi-analytical solutions obtained for both velocity and temperature were analysed to understand the flow behaviour of the propellant gas, thus optimize the rocket thrust and temperature distribution inside the rocket combustion chamber. However the major drawback in finding these semi-analytical solutions was due to the introduction of series expansions of non-integrable functions, which made the solution process to be long and tedious for both momentum and energy equations. The obtained solutions for momentum and energy depend on Prandtl number P_r, Grashof number G_r, radiation number R, Reynolds number R_e and wall dilation rate α, thus allow the investigation of the effects of these parameters on velocity and temperature during solid rocket motor operation. Also the solution of [1] was recovered by taking Grashof number to be zero from the obtained momentum solution, which should be the case since the current work was an extension of [1]. Velocity and temperature profiles obtained were similar to those in the literature. The reputable parabolic velocity profile which can ascribed to no slip condition [30, 31] and the slightly S shaped temperature profile which can be ascribed to strong convective action which bring hot combustion products closer to the centre in a circular pipe [32–34] were obtained.

The following findings are critical:

- **Wall Dilation**: To have optimal solid rocket motor thrust, the volume of the chamber should decrease during operation to increase internal pressure along with injection. The decrease in chamber volume and suction leads to an increase in velocity of the propellant but the overall thrust becomes minimal due to removal of propellant due to sucking.
- **Reynolds number**: Propellant injection is ideal whereas propellant suction is not ideal, reason being to maximize thrust during operation more propellant inside combustion chamber is needed to increase thrust output.

- **Prandtl number**: The increase in temperature which result from the increase in Prandtl number is ideal during operation since the increase in temperature leads to the increase internal energy of the system and the work done to propel increase, thus maximize thrust.
- **Radiation Number:** The increase in radiative effects increases internal energy of the system such that the work done to propel increases, thus maximize thrust.
- **Grashof number:** The increase in Grashof number effects increases internal energy of the system due the work done by buoyancy effect such that the work done to propel increases, thus maximize thrust.
- **Pressure:** Dilation of the chamber must be in such a way that the work done by the surface wall leads to the increase internal pressure, thus increase thrust output.

Chapter 4

Conclusion

In this research project, Lie group method was employed to study propellant flow and heat transfer inside the combustion chamber of solid rocket motors.

In Chapter 1, a brief introduction of Lie group theory for partial differential equations was given.

In Chapter 2, Lie group method was employed to determine the symmetries and integration of the heat equation.

In Chapter 3, the flow analysis of [1] was extended to study internal flow and heat transfer inside a combustion chamber of solid rocket motor. Lie group method along with double perturbation was employed to find semi-analytical solutions of velocity and temperature. Effects of wall dilation α, Prandtl number P_r, Reynolds number R_e, radiation number R and Grashof number G_r were on both axial-velocity and temperature distribution were shown graphically.

In future, effects of concentration which arise for the non-homogenous propellant will be studied.

Bibliography

[1] Boutros Y., Abd-el-Malek M., Badran N., Hassan H., Lie-Group method for unsteady flows in a semi-infinite expanding or contracting pipe with injection or suction through a porous wall. Journal of Computational and Applied Mathematics 197, 465-494, 2006.

[2] Ovsiannikov, L.V., Group Analysis of Differential Equations, Academic Press, New York, 1982.

[3] Olver, P.J., Applications of Lie Groups to Differential Equations, Springer-Verlag, New York, 1993.

[4] Bluman, G.W., Kumei, S., Symmetries and Differential Equations, Springer, New York, 1989.

[5] Stephani, H., Differential Equations. Thier solutions using symmetries, Cambridge University Press, Cambridge, 1989.

[6] Ibragimov, N.H., Elementary Lie Group Analysis and Ordinary Differential Equations, John Wiley and Sons, Chichester, 1999.

[7] Ibragimov, N.H., Groups of transformation in mathematical physics, Riedel, Dordrecht, 1985.

[8] Ibragimov, N.H., CRC handbook of Lie group analysis of differential equations, vols. 1-3, CRC Press, Boa Raton, Florida, 1994-1996.

[9] Mahomed, F.M., Recent trends in symmetry analysis of differential equations, *Notices of SAMS*, 33, 11-40, 2002.

[10] Currie I.G., Fundamental Mechanics of fluids, 4th Edition, CRC Press, New York.

[11] Flandro, G.A., Majdalalani, J., Aeoroacoustic Instablity in Rockets. AIAA Journal, 41(3), 485-497, 2003.

[12] Flandro, G.A., Effects of vorticity on rocket combustion stability. Journal of Propulsion and Power, 11(4), 607-616, 1995.

[13] Majdalani, J., On steady roational high speed flows:the compressible Taylor-Culick profile. Proceedings of the Royal Society A: Mathematical, Physical and Engineering Sciences, 463(2077), 131-162, 2006.

[14] Berman, A.S Laminar Flow in Channels with Porous Walls. Journal of Applied Physics, 24(9), 1232-1235, 1953.

[15] Terrill, R.M., Thomas, P.W., On Laminar Flow Through a Uniformly Porous pipe. Applied Scientific Research, 21(1), 37-67, 1969.

[16] Chellam, S., Liu, M., Effect of slip on existence,uniqueness and behaviour of similarity solutions for steady incompressible laminar flow in porous tubes and channels. Physics of fluids, 18(8), 2006.

[17] Brandy, J.F., Flow development in a porous channel and tube. Physics of Fluids, 27(5), 1061, 1984.

[18] Quaile, J.P., Leby, E.K., Laminar flow in a porous tube with suction. Journal of Heat Transfer, 97(1), 66-71, 1975.

[19] Galowin, L.S., Desantis, M.J., Theoretical analyis of laminar pipe flow in a porous wall cylinder. Journal of Dynamics Systems, Measurement, and Control,1971, 93(2), 102-108, 1971.

[20] Saad, T., Majdalani, J., Visocus Mean Flow Approximations For Porous Tubes with Radially Regressing Walls. AIAA Journal, 55(11), 3868-3880, 2017.

[21] Zhou, C., Majdalani, J., Improved Mean-Flow Solution for Slab Rocket Motors with Regressing Walls. Journals of Propulsion and Power, 18(3), 703-711, 2002.

[22] Pearce, B.E., Radiative heat transfer within a solid propellant rocket motor, Journal of Spacecraft and Rockets , 15(2), 125-128, 1978.

[23] Xia, X.L., Ren, D.P., and Tan, H.P., Thermal radiation effects of a high temperature developing laminar flow in a tube, Heat Transfer Asian Research, 33(5), 299-309, 2004.

[24] Viskanda, R., Interaction of Heat Transfer by Conduction, Convection, and Radiation in a Radiating Fluid, Journal of Heat Transfer, 85(4), 318-328, 1963.

[25] Huang, J.M., and Lin, J.D., Combined radiative and forced convective in a thermally developing laminar flow through a circular pipe. Chemical Engineering Communications, 101(1), 147-164, 1991.

[26] Hariprasad, V., Sankar, P., Shivahari, P., Sanal Kumar VR, Studies on gravity influence on solid Propellant Burn Rate, Applied Mechanics and Materials, 232, 342-347, 2012.

[27] Ishigaki, H., The effect of Buoyancy on Laminar Flow and Heat Transfer in Pipes, JSME International Journal Series B, 40(2), 273-280, 1997.

[28] Azimi M., Hedesh A. M., Karimian S., Flow Modeling in a Porous Cylinder with Regressing Walls Using Semi Analytical Approach. Mechanics and Mechanical Engineering 18(2), 77-84, 2014.

[29] Matebese B., Adem A., Khalique M., Hayat T., Two-dimensional flow in a deformable channel with porous medium and variable magnetic field, Mathematical and Computational applications, 31, 674-684, 2010.

[30] Boutros Y.Z., Abd-el-Malek M.B., Badran N.A., Hassan H.S., Lie-group method solution for two-dimensional viscous flow between slowly expanding or contracting walls with weak permeability. Applied Mathematical Modelling, 31(6), 1092-1108, 2007.

[31] Kandasamy R., Muhaimin I., Norsarahaida S. A., Lie group analysis for the effect og temperature-dependent fluid viscosity with thermophoresis on magnetohydrodynamic free convective heat and mass transfer over a porous stretching surface. International Journal of Computational Fluid Dynamics, 24(1-2), 1-11, 2010.

[32] Chu W.W.,Yang V., Majdalani J., Premixed flame response to acoustic waves in a porous-walled chamber with surface mass injection. Combustion and Flame, 133(3), 359-370, 2002.

[33] Vyas A.B., Majdalani J., Yang V. Estimation of the laminar premixed flame temperature and velocity in injection-driven combustion chambers. Combustion and Flame, 133(3), 371-374, 2003.

[34] Song J., An W., Wu Y., Tian W. Neutronics and Thermal Hydraulics Analysis of a Conceptual Ultra-High Temperature MHD Cermet Fuel Core for Nuclear Electric Propulsion. Frontiers in Energy Research, 6, 1-10, 2018.